Figure 1.3: Components of a computer-controlled system. The upper dashed box represents the process dynamics, which include the sensors and actuators in addition to the dynamical system being controlled. Noise and external disturbances can perturb the dynamics of the process. The controller is shown in the lower dashed box. It consists of a filter and analog-to-digital (A/D) and digital-to-analog (D/A) converters, as well as a computer that implements the control algorithm. A system clock controls the operation of the controller, synchronizing the A/D, D/A and computing processes. The operator input is also fed to the computer as an external input.

A modern controller senses the operation of a system, compares it against the desired behavior, computes corrective actions based on a model of the system's response to external inputs and actuates the system to effect the desired change. This basic *feedback loop* of sensing, computation and actuation is the central concept in control. The key issues in designing control logic are ensuring that the dynamics of the closed loop system are stable (bounded disturbances give bounded errors) and that they have additional desired behavior (good disturbance attenuation, fast responsiveness to changes in operating point, etc). These properties are established using a variety of modeling and analysis techniques that capture the essential dynamics of the system and permit the exploration of possible behaviors in the presence of uncertainty, noise and component failure.

A typical example of a control system is shown in Figure 1.3. The basic elements of sensing, computation and actuation are clearly seen. In modern control systems, computation is typically implemented on a digital computer, requiring the use of analog-to-digital (A/D) and digital-to-analog (D/A) converters. Uncertainty enters the system through noise in sensing and actuation subsystems, external disturbances that affect the underlying system operation and uncertain dynamics in the system (parameter errors, unmodeled effects, etc). The algorithm that computes the control action as a function of the sensor values is often called a *control law*. The system can be influenced externally by an operator who introduces *command signals* to the system.
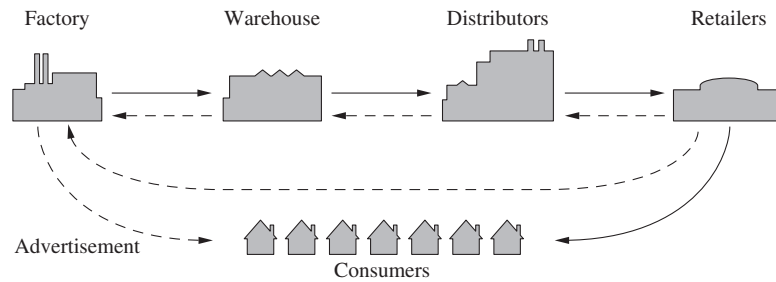
Figure 1.11: Supply chain dynamics (after Forrester [75]). Products flow from the producer to the customer through distributors and retailers as indicated by the solid lines. There are typically many factories and warehouses and even more distributors and retailers. Multiple feedback loops are present as each agent tries to maintain the proper inventory level.

many different products, there may be different factories that are geographically distributed and the factories may require raw material or subassemblies.

Control of supply chains was proposed by Forrester in 1961 [75] and is now growing in importance. Considerable economic benefits can be obtained by using models to minimize inventories. Their use accelerated dramatically when information technology was applied to predict sales, keep track of products and enable just-in-time manufacturing. Supply chain management has contributed significantly to the growing success of global distributors.

Advertising on the Internet is an emerging application of control. With network-based advertising it is easy to measure the effect of different marketing strategies quickly. The response of customers can then be modeled, and feedback strategies can be developed.

Feedback in Nature

Many problems in the natural sciences involve understanding aggregate behavior in complex large-scale systems. This behavior emerges from the interaction of a multitude of simpler systems with intricate patterns of information flow. Representative examples can be found in fields ranging from embryology to seismology. Researchers who specialize in the study of specific complex systems often develop an intuitive emphasis on analyzing the role of feedback (or interconnection) in facilitating and stabilizing aggregate behavior.

While sophisticated theories have been developed by domain experts for the analysis of various complex systems, the development of a rigorous methodology that can discover and exploit common features and essential mathematical structure is just beginning to emerge. Advances in science and technology are creating a new understanding of the underlying dynamics and the importance of feedback in a wide variety of natural and technological systems. We briefly highlight three application areas here.

Biological Systems. A major theme currently of interest to the biology commu-
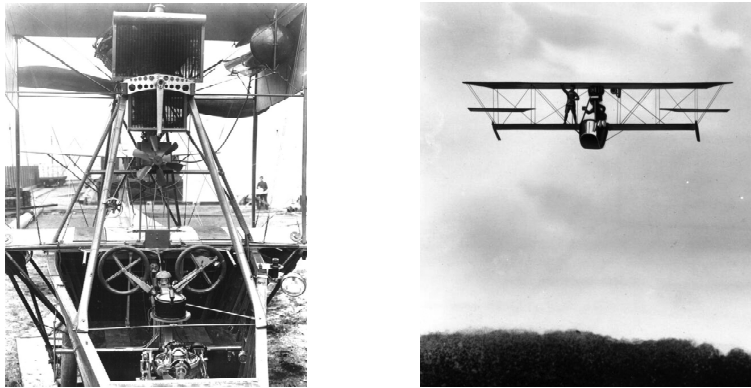
Figure 1.14: Aircraft autopilot system. The Sperry autopilot (left) contained a set of four gyros coupled to a set of air valves that controlled the wing surfaces. The 1912 Curtiss used an autopilot to stabilize the roll, pitch and yaw of the aircraft and was able to maintain level flight as a mechanic walked on the wing (right) [105].

weight of the wings themselves, but also that of the engine, and of the engineer as well. Men also know how to build engines and screws of sufficient lightness and power to drive these planes at sustaining speed ... Inability to balance and steer still confronts students of the flying problem ... When this one feature has been worked out, the age of flying will have arrived, for all other difficulties are of minor importance.

The Wright brothers thus realized that control was a key issue to enable flight. They resolved the compromise between stability and maneuverability by building an airplane, the Wright Flyer, that was unstable but maneuverable. The Flyer had a rudder in the front of the airplane, which made the plane very maneuverable. A disadvantage was the necessity for the pilot to keep adjusting the rudder to fly the plane: if the pilot let go of the stick, the plane would crash. Other early aviators tried to build stable airplanes. These would have been easier to fly, but because of their poor maneuverability they could not be brought up into the air. By using their insight and skillful experiments the Wright brothers made the first successful flight at Kitty Hawk in 1903.

Since it was quite tiresome to fly an unstable aircraft, there was strong motivation to find a mechanism that would stabilize an aircraft. Such a device, invented by Sperry, was based on the concept of feedback. Sperry used a gyro-stabilized pendulum to provide an indication of the vertical. He then arranged a feedback mechanism that would pull the stick to make the plane go up if it was pointing down, and vice versa. The Sperry autopilot was the first use of feedback in aeronautical engineering, and Sperry won a prize in a competition for the safest airplane in Paris in 1914. Figure 1.14 shows the Curtiss seaplane and the Sperry autopilot. The autopilot is a good example of how feedback can be used to stabilize an unstable system and hence "design the dynamics" of the aircraft.
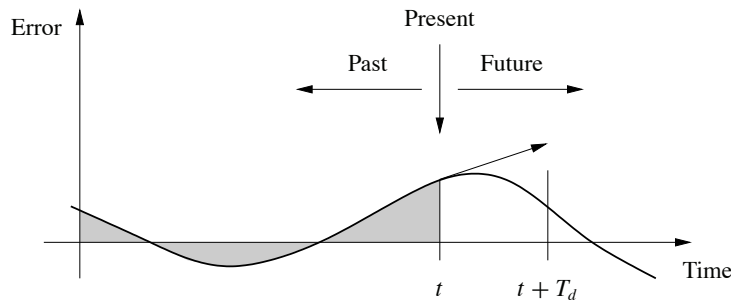
Figure 1.17: Action of a PID controller. At time t, the proportional term depends on the instantaneous value of the error. The integral portion of the feedback is based on the integral of the error up to time t (shaded portion). The derivative term provides an estimate of the growth or decay of the error over time by looking at the rate of change of the error. T_d represents the approximate amount of time in which the error is projected forward (see text).

1.6 Further Reading

The material in this section draws heavily from the report of the Panel on Future Directions on Control, Dynamics and Systems [155]. Several additional papers and reports have highlighted the successes of control [159] and new vistas in control [45, 130, 204]. The early development of control is described by Mayr [148] and in the books by Bennett [28, 29], which cover the period 1800–1955. A fascinating examination of some of the early history of control in the United States has been written by Mindell [152]. A popular book that describes many control concepts across a wide range of disciplines is *Out of Control* by Kelly [121]. There are many textbooks available that describe control systems in the context of specific disciplines. For engineers, the textbooks by Franklin, Powell and Emami-Naeini [79], Dorf and Bishop [61], Kuo and Golnaraghi [133] and Seborg, Edgar and Mellichamp [178] are widely used. More mathematically oriented treatments of control theory include Sontag [182] and Lewis [136]. The book by Hellerstein et al. [97] provides a description of the use of feedback control in computing systems. A number of books look at the role of dynamics and feedback in biological systems, including Milhorn [151] (now out of print), J. D. Murray [154] and Ellner and Guckenheimer [70]. The book by Fradkov [77] and the tutorial article by Bechhoefer [25] cover many specific topics of interest to the physics community.

Exercises

1.1 (Eye motion) Perform the following experiment and explain your results: Holding your head still, move one of your hands left and right in front of your face, following it with your eyes. Record how quickly you can move your hand before you begin to lose track of it. Now hold your hand still and shake your head left to right, once again recording how quickly you can move before losing track of your hand.

dynamics as first-order differential equations, but we will see that this can capture the dynamics of higher-order differential equations by appropriate definition of the state and the maps f and h.

Adding inputs and outputs has increased the richness of the classical problems and led to many new concepts. For example, it is natural to ask if possible states x can be reached with the proper choice of u (reachability) and if the measurement y contains enough information to reconstruct the state (observability). These topics will be addressed in greater detail in Chapters 6 and 7.

A final development in building the control point of view was the emergence of disturbances and model uncertainty as critical elements in the theory. The simple way of modeling disturbances as deterministic signals like steps and sinusoids has the drawback that such signals cannot be predicted precisely. A more realistic approach is to model disturbances as random signals. This viewpoint gives a natural connection between prediction and control. The dual views of input/output representations and state space representations are particularly useful when modeling uncertainty since state models are convenient to describe a nominal model but uncertainties are easier to describe using input/output models (often via a frequency response description). Uncertainty will be a constant theme throughout the text and will be studied in particular detail in Chapter 12.

An interesting observation in the design of control systems is that feedback systems can often be analyzed and designed based on comparatively simple models. The reason for this is the inherent robustness of feedback systems. However, other uses of models may require more complexity and more accuracy. One example is feedforward control strategies, where one uses a model to precompute the inputs that cause the system to respond in a certain way. Another area is system validation, where one wishes to verify that the detailed response of the system performs as it was designed. Because of these different uses of models, it is common to use a hierarchy of models having different complexity and fidelity.

Multidomain Modeling

Modeling is an essential element of many disciplines, but traditions and methods from individual disciplines can differ from each other, as illustrated by the previous discussion of mechanical and electrical engineering. A difficulty in systems engineering is that it is frequently necessary to deal with heterogeneous systems from many different domains, including chemical, electrical, mechanical and information systems.

To model such multidomain systems, we start by partitioning a system into smaller subsystems. Each subsystem is represented by balance equations for mass, energy and momentum, or by appropriate descriptions of information processing in the subsystem. The behavior at the interfaces is captured by describing how the variables of the subsystem behave when the subsystems are interconnected. These interfaces act by constraining variables within the individual subsystems to be equal (such as mass, energy or momentum fluxes). The complete model is then obtained by combining the descriptions of the subsystems and the interfaces.

In this problem, we will explore some of the properties of this discrete-time system as a function of the parameters, the initial conditions and the inputs.

(a) For the case when $a_{12} = 0$ and $u = 0$, give a closed form expression for the output of the system.

(b) A discrete system is in *equilibrium* when $x[k + 1] = x[k]$ for all k. Let $u = r$ be a constant input and compute the resulting equilibrium point for the system. Show that if $|a_{ii}| < 1$ for all i, all initial conditions give solutions that converge to the equilibrium point.

(c) Write a computer program to plot the output of the system in response to a unit step input, $u[k] = 1, k \geq 0$. Plot the response of your system with $x[0] = 0$ and A given by $a_{11} = 0.5, a_{12} = 1$ and $a_{22} = 0.25$.

2.4 (Keynesian economics) Keynes' simple model for an economy is given by

$$Y[k] = C[k] + I[k] + G[k],$$

where Y, C, I and G are gross national product (GNP), consumption, investment and government expenditure for year k. Consumption and investment are modeled by difference equations of the form

$$C[k + 1] = aY[k], \qquad I[k + 1] = b(C[k + 1] - C[k]),$$

where a and b are parameters. The first equation implies that consumption increases with GNP but that the effect is delayed. The second equation implies that investment is proportional to the rate of change of consumption.

Show that the equilibrium value of the GNP is given by

$$Y_e = \frac{1}{1 - a}(I_e + G_e),$$

where the parameter $1/(1 - a)$ is the Keynes multiplier (the gain from I or G to Y). With $a = 0.25$ an increase of government expenditure will result in a fourfold increase of GNP. Also show that the model can be written as the following discrete-time state model:

$$\begin{bmatrix} C[k + 1] \\ I[k + 1] \end{bmatrix} = \begin{bmatrix} a & a \\ ab - b & ab \end{bmatrix} \begin{bmatrix} C[k] \\ I[k] \end{bmatrix} + \begin{bmatrix} a \\ ab \end{bmatrix} G[k],$$

$$Y[k] = C[k] + I[k] + G[k].$$

2.5 (Least squares system identification) Consider a nonlinear differential equation that can be written in the form

$$\frac{dx}{dt} = \sum_{i=1}^{M} \alpha_i f_i(x),$$

where $f_i(x)$ are known nonlinear functions and α_i are unknown, but constant, parameters. Suppose that we have measurements (or estimates) of the full state x

at time instants $t_1, t_2, \ldots, t_N$, with $N > M$. Show that the parameters α_i can be determined by finding the least squares solution to a linear equation of the form

$$H\alpha = b,$$

where $\alpha \in \mathbb{R}^M$ is the vector of all parameters and $H \in \mathbb{R}^{N \times M}$ and $b \in \mathbb{R}^N$ are appropriately defined.

2.6 (Normalized oscillator dynamics) Consider a damped spring–mass system with dynamics

$$m\ddot{q} + c\dot{q} + kq = F.$$

Let $\omega_0 = \sqrt{k/m}$ be the natural frequency and $\zeta = c/(2\sqrt{km})$ be the damping ratio.

(a) Show that by rescaling the equations, we can write the dynamics in the form

$$\ddot{q} + 2\zeta\omega_0\dot{q} + \omega_0^2 q = \omega_0^2 u, \tag{2.35}$$

where $u = F/k$. This form of the dynamics is that of a linear oscillator with natural frequency ω_0 and damping ratio ζ.

(b) Show that the system can be further normalized and written in the form

$$\frac{dz_1}{d\tau} = z_2, \qquad \frac{dz_2}{d\tau} = -z_1 - 2\zeta z_2 + v. \tag{2.36}$$

The essential dynamics of the system are governed by a single damping parameter ζ. The *Q-value* defined as $Q = 1/2\zeta$ is sometimes used instead of ζ.

2.7 (Electric generator) An electric generator connected to a strong power grid can be modeled by a momentum balance for the rotor of the generator:

$$J\frac{d^2\varphi}{dt^2} = P_m - P_e = P_m - \frac{EV}{X}\sin\varphi,$$

where J is the effective moment of inertia of the generator, φ the angle of rotation, P_m the mechanical power that drives the generator, P_e is the active electrical power, E the generator voltage, V the grid voltage and X the reactance of the line. Assuming that the line dynamics are much faster than the rotor dynamics, $P_e = VI = (EV/X)\sin\varphi$, where I is the current component in phase with the voltage E and φ is the phase angle between voltages E and V. Show that the dynamics of the electric generator have a normalized form that is similar to the dynamics of a pendulum with forcing at the pivot.

2.8 (Admission control for a queue) Consider the queuing system described in Example 2.10. The long delays created by temporary overloads can be reduced by rejecting requests when the queue gets large. This allows requests that are accepted to be serviced quickly and requests that cannot be accommodated to receive a rejection quickly so that they can try another server. Consider an admission control system described by

$$\frac{dx}{dt} = \lambda u - \mu_{\max}\frac{x}{x+1}, \qquad u = \text{sat}_{(0,1)}(k(r-x)), \tag{2.37}$$

where the controller is a simple proportional control with saturation ($\mathrm{sat}_{(a,b)}$ defined by equation (3.9)) and r is the desired (reference) queue length. Use a simulation to show that this controller reduces the rush-hour effect and explain how the choice of r affects the system dynamics.

2.9 (Biological switch) A genetic switch can be formed by connecting two repressors together in a cycle as shown below.
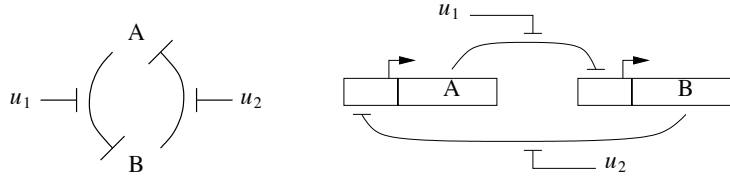
Using the models from Example 2.13—assuming that the parameters are the same for both genes and that the mRNA concentrations reach steady state quickly—show that the dynamics can be written in normalized coordinates as

$$\frac{dz_1}{d\tau} = \frac{\mu}{1 + z_2^n} - z_1 - v_1, \qquad \frac{dz_2}{d\tau} = \frac{\mu}{1 + z_1^n} - z_2 - v_2, \qquad (2.38)$$

where z_1 and z_2 are scaled versions of the protein concentrations and the time scale has also been changed. Show that $\mu \approx 200$ using the parameters in Example 2.13, and use simulations to demonstrate the switch-like behavior of the system.

2.10 (Motor drive) Consider a system consisting of a motor driving two masses that are connected by a torsional spring, as shown in the diagram below.
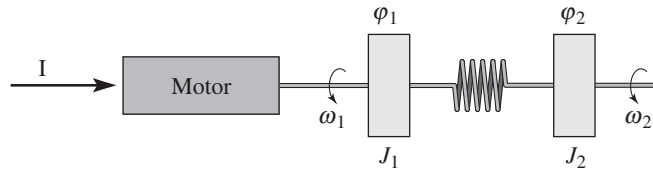
This system can represent a motor with a flexible shaft that drives a load. Assuming that the motor delivers a torque that is proportional to the current, the dynamics of the system can be described by the equations

$$\begin{aligned}
J_1 \frac{d^2\varphi_1}{dt^2} + c\left(\frac{d\varphi_1}{dt} - \frac{d\varphi_2}{dt}\right) + k(\varphi_1 - \varphi_2) &= k_I I, \\
J_2 \frac{d^2\varphi_2}{dt^2} + c\left(\frac{d\varphi_2}{dt} - \frac{d\varphi_1}{dt}\right) + k(\varphi_2 - \varphi_1) &= T_d.
\end{aligned} \qquad (2.39)$$

Similar equations are obtained for a robot with flexible arms and for the arms of DVD and optical disk drives.

Derive a state space model for the system by introducing the (normalized) state variables $x_1 = \varphi_1$, $x_2 = \varphi_2$, $x_3 = \omega_1/\omega_0$, and $x_4 = \omega_2/\omega_0$, where $\omega_0 = \sqrt{k(J_1 + J_2)/(J_1 J_2)}$ is the undamped natural frequency of the system when the control signal is zero.

control dynamics. We can obtain substantial insight by considering a special case in which we have N identical sources and 1 link. In addition, we assume for the moment that the forward and backward time delays can be ignored, in which case the dynamics can be reduced to the form

$$\frac{dw_i}{dt} = \frac{1}{\tau} - \frac{\rho c(2 + w_i^2)}{2}, \qquad \frac{db}{dt} = \sum_{i=1}^{N} \frac{w_i}{\tau} - c, \qquad \tau = \frac{b}{c}, \qquad (3.19)$$

where $w_i \in \mathbb{R}, i = 1, \ldots, N$, are the window sizes for the sources of data, $b \in \mathbb{R}$ is the current buffer size of the router, ρ controls the rate at which packets are dropped and c is the capacity of the link connecting the router to the computers. The variable τ represents the amount of time required for a packet to be processed by a router, based on the size of the buffer and the capacity of the link. Substituting τ into the equations, we write the state space dynamics as

$$\frac{dw_i}{dt} = \frac{c}{b} - \rho c \left(1 + \frac{w_i^2}{2}\right), \qquad \frac{db}{dt} = \sum_{i=1}^{N} \frac{cw_i}{b} - c. \qquad (3.20)$$

More sophisticated models can be found in [101, 137].

The nominal operating point for the system can be found by setting $\dot{w}_i = \dot{b} = 0$:

$$0 = \frac{c}{b} - \rho c \left(1 + \frac{w_i^2}{2}\right), \qquad 0 = \sum_{i=1}^{N} \frac{cw_i}{b} - c.$$

Exploiting the fact that all of the source dynamics are identical, it follows that all of the w_i should be the same, and it can be shown that there is a unique equilibrium satisfying the equations

$$w_{i,e} = \frac{b_e}{N} = \frac{c\tau_e}{N}, \qquad \frac{1}{2\rho^2 N^2}(\rho b_e)^3 + (\rho b_e) - 1 = 0. \qquad (3.21)$$

The solution for the second equation is a bit messy but can easily be determined numerically. A plot of its solution as a function of $1/(2\rho^2 N^2)$ is shown in Figure 3.12b. We also note that at equilibrium we have the following additional equalities:

$$\tau_e = \frac{b_e}{c} = \frac{Nw_e}{c}, \qquad q_e = Np_e = N\rho b_e, \qquad r_e = \frac{w_e}{\tau_e}. \qquad (3.22)$$

Figure 3.13 shows a simulation of 60 sources communicating across a single link, with 20 sources dropping out at $t = 500$ ms and the remaining sources increasing their rates (window sizes) to compensate. Note that the buffer size and window sizes automatically adjust to match the capacity of the link.

A comprehensive treatment of computer networks is given in the textbook by Tannenbaum [189]. A good presentation of the ideas behind the control principles for the Internet is given by one of its designers, Van Jacobson, in [108]. F. Kelly [120] presents an early effort on the analysis of the system. The book by Hellerstein et al. [97] gives many examples of the use of feedback in computer systems.
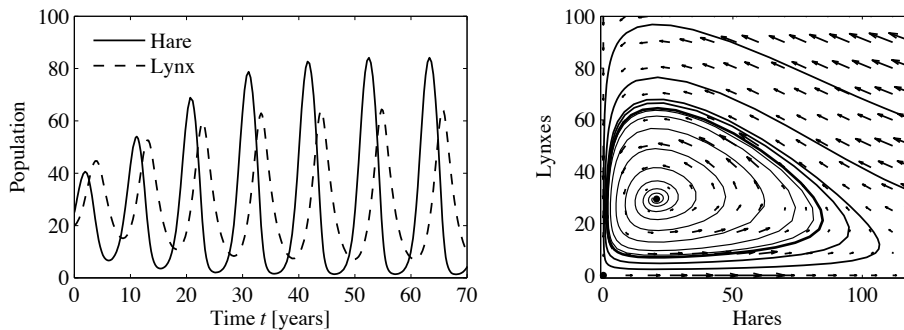
Figure 3.20: Simulation of the predator–prey system. The figure on the left shows a simulation of the two populations as a function of time. The figure on the right shows the populations plotted against each other, starting from different values of the population. The oscillation seen in both figures is an example of a *limit cycle*. The parameter values used for the simulations are $a = 3.2, b = 0.6, c = 50, d = 0.56, k = 125$ and $r = 1.6$.

Figure 3.20 shows a simulation of the dynamics starting from a set of population values near the nonzero equilibrium values. We see that for this choice of parameters, the simulation predicts an oscillatory population count for each species, reminiscent of the data shown in Figure 2.6.

Volume I of the two-volume set by J. D. Murray [154] give a broad coverage of population dynamics.

Exercises

3.1 (Cruise control) Consider the cruise control example described in Section 3.1. Build a simulation that re-creates the response to a hill shown in Figure 3.3b and show the effects of increasing and decreasing the mass of the car by 25%. Redesign the controller (using trial and error is fine) so that it returns to within 1% of the desired speed within 3 s of encountering the beginning of the hill.

3.2 (Bicycle dynamics) Show that the dynamics of a bicycle frame given by equation (3.5) can be approximated in state space form as

$$\frac{d}{dt} \begin{bmatrix} x_1 \\ x_2 \end{bmatrix} = \begin{bmatrix} 0 & 1 \\ mgh/J & 0 \end{bmatrix} \begin{bmatrix} x_1 \\ x_2 \end{bmatrix} + \begin{bmatrix} Dv_0/(bJ) \\ mv_0^2 h/(bJ) \end{bmatrix} u,$$

$$y = \begin{bmatrix} 1 & 0 \end{bmatrix} x,$$

where the input u is the steering angle δ and the output y is the tilt angle φ. What do the states x_1 and x_2 represent?

3.3 (Bicycle steering) Combine the bicycle model given by equation (3.5) and the model for steering kinematics in Example 2.8 to obtain a model that describes the path of the center of mass of the bicycle.

3.4 (Operational amplifier circuit) Consider the op amp circuit shown below.
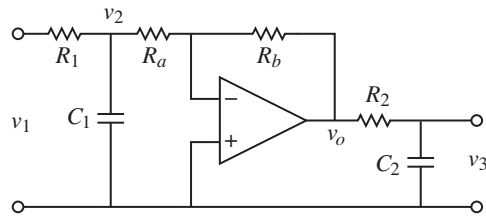
Show that the dynamics can be written in state space form as

$$
\frac{dx}{dt} = \begin{bmatrix} -\dfrac{1}{R_1C_1} - \dfrac{1}{R_aC_1} & 0 \\[2ex] \dfrac{R_b}{R_a}\dfrac{1}{R_2C_2} & -\dfrac{1}{R_2C_2} \end{bmatrix} x + \begin{bmatrix} \dfrac{1}{R_1C_1} \\[2ex] 0 \end{bmatrix} u, \quad y = \begin{bmatrix} 0 & 1 \end{bmatrix} x,
$$

where $u = v_1$ and $y = v_3$. (Hint: Use v_2 and v_3 as your state variables.)

3.5 (Operational amplifier oscillator) The op amp circuit shown below is an implementation of an oscillator.
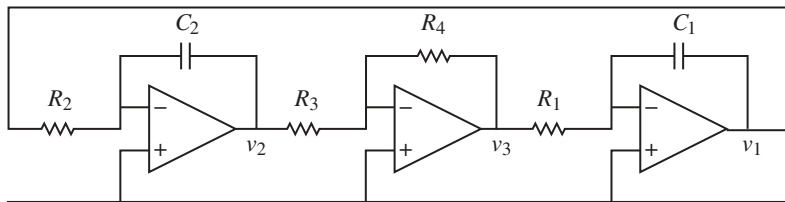
Show that the dynamics can be written in state space form as

$$
\frac{dx}{dt} = \begin{bmatrix} 0 & \dfrac{R_4}{R_1 R_3 C_1} \\[2ex] -\dfrac{1}{R_2 C_2} & 0 \end{bmatrix} x,
$$

where the state variables represent the voltages across the capacitors $x_1 = v_1$ and $x_2 = v_2$.

3.6 (Congestion control using RED [138]) A number of improvements can be made to the model for Internet congestion control presented in Section 3.4. To ensure that the router's buffer size remains positive, we can modify the buffer dynamics to satisfy

$$
\frac{db_l}{dt} = \begin{cases} s_l - c_l & b_l > 0 \\ \text{sat}_{(0,\infty)}(s_l - c_l) & b_l = 0. \end{cases}
$$

In addition, we can model the drop probability of a packet based on how close we

Another simple case is when the dynamics are in the block diagonal form

$$\frac{dx}{dt} = \begin{bmatrix} \sigma_1 & \omega_1 & & 0 & 0 \\ -\omega_1 & \sigma_1 & & 0 & 0 \\ 0 & 0 & \ddots & \vdots & \vdots \\ 0 & 0 & & \sigma_m & \omega_m \\ 0 & 0 & & -\omega_m & \sigma_m \end{bmatrix} x.$$

In this case, the eigenvalues can be shown to be $\lambda_j = \sigma_j \pm i\omega_j$. We once again can separate the state trajectories into independent solutions for each pair of states, and the solutions are of the form

$$x_{2j-1}(t) = e^{\sigma_j t}\big(x_{2j-1}(0)\cos\omega_j t + x_{2j}(0)\sin\omega_j t\big),$$
$$x_{2j}(t) = e^{\sigma_j t}\big(-x_{2j-1}(0)\sin\omega_j t + x_{2j}(0)\cos\omega_j t\big),$$

where $j = 1, 2, \ldots, m$. We see that this system is asymptotically stable if and only if $\sigma_j = \operatorname{Re}\lambda_j < 0$. It is also possible to combine real and complex eigenvalues in (block) diagonal form, resulting in a mixture of solutions of the two types.

Very few systems are in one of the diagonal forms above, but some systems can be transformed into these forms via coordinate transformations. One such class of systems is those for which the dynamics matrix has distinct (nonrepeating) eigenvalues. In this case there is a matrix $T \in \mathbb{R}^{n \times n}$ such that the matrix TAT^{-1} is in (block) diagonal form, with the block diagonal elements corresponding to the eigenvalues of the original matrix A (see Exercise 4.14). If we choose new coordinates $z = Tx$, then

$$\frac{dz}{dt} = T\dot{x} = TAx = TAT^{-1}z$$

and the linear system has a (block) diagonal dynamics matrix. Furthermore, the eigenvalues of the transformed system are the same as the original system since if v is an eigenvector of A, then $w = Tv$ can be shown to be an eigenvector of TAT^{-1}. We can reason about the stability of the original system by noting that $x(t) = T^{-1}z(t)$, and so if the transformed system is stable (or asymptotically stable), then the original system has the same type of stability.

This analysis shows that for linear systems with distinct eigenvalues, the stability of the system can be completely determined by examining the real part of the eigenvalues of the dynamics matrix. For more general systems, we make use of the following theorem, proved in the next chapter:

Theorem 4.1 (Stability of a linear system). *The system*

$$\frac{dx}{dt} = Ax$$

is asymptotically stable if and only if all eigenvalues of A all have a strictly negative real part and is unstable if any eigenvalue of A has a strictly positive real part.

Example 4.6 Compartment model
Consider the two-compartment module for drug delivery introduced in Section 3.6.

Using concentrations as state variables and denoting the state vector by x, the system dynamics are given by

$$\frac{dx}{dt} = \begin{bmatrix} -k_0 - k_1 & k_1 \\ k_2 & -k_2 \end{bmatrix} x + \begin{bmatrix} b_0 \\ 0 \end{bmatrix} u, \qquad y = \begin{bmatrix} 0 & 1 \end{bmatrix} x,$$

where the input u is the rate of injection of a drug into compartment 1 and the concentration of the drug in compartment 2 is the measured output y. We wish to design a feedback control law that maintains a constant output given by $y = y_d$.

We choose an output feedback control law of the form

$$u = -k(y - y_d) + u_d,$$

where u_d is the rate of injection required to maintain the desired concentration and k is a feedback gain that should be chosen such that the closed loop system is stable. Substituting the control law into the system, we obtain

$$\frac{dx}{dt} = \begin{bmatrix} -k_0 - k_1 & k_1 - b_0 k \\ k_2 & -k_2 \end{bmatrix} x + \begin{bmatrix} b_0 \\ 0 \end{bmatrix} u_d =: Ax + Bu_d,$$

$$y = \begin{bmatrix} 0 & 1 \end{bmatrix} x =: Cx.$$

The equilibrium concentration $x_e \in \mathbb{R}^2$ is given by $x_e = -A^{-1} B u_d$ and

$$y_e = -C A^{-1} B u_d = \frac{b_0 k_2}{k_0 k_2 + b_0 k_2 k} u_d.$$

Choosing u_d such that $y_e = y_d$ provides the constant rate of injection required to maintain the desired output. We can now shift coordinates to place the equilibrium point at the origin, which yields

$$\frac{dz}{dt} = \begin{bmatrix} -k_0 - k_1 & k_1 - b_0 k \\ k_2 & -k_2 \end{bmatrix} z,$$

where $z = x - x_e$. We can now apply the results of Theorem 4.1 to determine the stability of the system. The eigenvalues of the system are given by the roots of the characteristic polynomial

$$\lambda(s) = s^2 + (k_0 + k_1 + k_2)s + (k_0 k_2 + b_0 k_2 k).$$

While the specific form of the roots is messy, it can be shown that the roots are positive as long as the linear term and the constant term are both positive (Exercise 4.16). Hence the system is stable for any $k > 0$. ∇

Stability Analysis via Linear Approximation

An important feature of differential equations is that it is often possible to determine the local stability of an equilibrium point by approximating the system by a linear system. The following example illustrates the basic idea.

Example 4.7 Inverted pendulum

Consider again an inverted pendulum whose open loop dynamics are given by

$$\frac{dx}{dt} = \begin{bmatrix} x_2 \\ \sin x_1 - \gamma\, x_2 \end{bmatrix},$$

where we have defined the state as $x = (\theta, \dot{\theta})$. We first consider the equilibrium point at $x = (0, 0)$, corresponding to the straight-up position. If we assume that the angle $\theta = x_1$ remains small, then we can replace $\sin x_1$ with x_1 and $\cos x_1$ with 1, which gives the approximate system

$$\frac{dx}{dt} = \begin{bmatrix} x_2 \\ x_1 - \gamma\, x_2 \end{bmatrix} = \begin{bmatrix} 0 & 1 \\ 1 & -\gamma \end{bmatrix} x. \qquad (4.9)$$

Intuitively, this system should behave similarly to the more complicated model as long as x_1 is small. In particular, it can be verified that the equilibrium point $(0, 0)$ is unstable by plotting the phase portrait or computing the eigenvalues of the dynamics matrix in equation (4.9)

We can also approximate the system around the stable equilibrium point at $x = (\pi, 0)$. In this case we have to expand $\sin x_1$ and $\cos x_1$ around $x_1 = \pi$, according to the expansions

$$\sin(\pi + \theta) = -\sin\theta \approx -\theta, \qquad \cos(\pi + \theta) = -\cos(\theta) \approx -1.$$

If we define $z_1 = x_1 - \pi$ and $z_2 = x_2$, the resulting approximate dynamics are given by

$$\frac{dz}{dt} = \begin{bmatrix} z_2 \\ -z_1 - \gamma\, z_2 \end{bmatrix} = \begin{bmatrix} 0 & 1 \\ -1 & -\gamma \end{bmatrix} z. \qquad (4.10)$$

Note that $z = (0, 0)$ is the equilibrium point for this system and that it has the same basic form as the dynamics shown in Figure 4.8. Figure 4.11 shows the phase portraits for the original system and the approximate system around the corresponding equilibrium points. Note that they are very similar, although not exactly the same. It can be shown that if a linear approximation has either asymptotically stable or unstable equilibrium points, then the local stability of the original system must be the same (Theorem 4.3). ∇

More generally, suppose that we have a nonlinear system

$$\frac{dx}{dt} = F(x)$$

that has an equilibrium point at x_e. Computing the Taylor series expansion of the vector field, we can write

$$\frac{dx}{dt} = F(x_e) + \left.\frac{\partial F}{\partial x}\right|_{x_e} (x - x_e) + \text{higher-order terms in } (x - x_e).$$

Since $F(x_e) = 0$, we can approximate the system by choosing a new state variable

Differentiation gives the following linear equations for $\dot{r}$ and $\dot{\varphi}$:

$$\dot{x}_1 = \dot{r}\cos\varphi - r\dot{\varphi}\sin\varphi, \qquad \dot{x}_2 = \dot{r}\sin\varphi + r\dot{\varphi}\cos\varphi.$$

Solving this linear system for $\dot{r}$ and $\dot{\varphi}$ gives, after some calculation,

$$\frac{dr}{dt} = r(1 - r^2), \qquad \frac{d\varphi}{dt} = -1.$$

Notice that the equations are decoupled; hence we can analyze the stability of each state separately.

The equation for r has three equilibria: $r = 0, r = 1$ and $r = -1$ (not realizable since r must be positive). We can analyze the stability of these equilibria by linearizing the radial dynamics with $F(r) = r(1 - r^2)$. The corresponding linear dynamics are given by

$$\frac{dr}{dt} = \left.\frac{\partial F}{\partial r}\right|_{r_e} r = (1 - 3r_e^2)r, \quad r_e = 0,\ 1,$$

where we have abused notation and used r to represent the deviation from the equilibrium point. It follows from the sign of $(1 - 3r_e^2)$ that the equilibrium $r = 0$ is unstable and the equilibrium $r = 1$ is asymptotically stable. Thus for any initial condition $r > 0$ the solution goes to $r = 1$ as time goes to infinity, but if the system starts with $r = 0$, it will remain at the equilibrium for all times. This implies that all solutions to the original system that do not start at $x_1 = x_2 = 0$ will approach the circle $x_1^2 + x_2^2 = 1$ as time increases.

To show the stability of the full solution (4.12), we must investigate the behavior of neighboring solutions with different initial conditions. We have already shown that the radius r will approach that of the solution (4.12) as long as $r(0) > 0$. The equation for the angle φ can be integrated analytically to give $\varphi(t) = -t + \varphi(0)$, which shows that solutions starting at different angles φ will neither converge nor diverge. Thus, the unit circle is *attracting*, but the solution (4.12) is only stable, not asymptotically stable. The behavior of the system is illustrated by the simulation in Figure 4.12. Notice that the solutions approach the circle rapidly, but that there is a constant phase shift between the solutions. ∇

4.4 Lyapunov Stability Analysis

We now return to the study of the full nonlinear system

$$\frac{dx}{dt} = F(x), \quad x \in \mathbb{R}^n. \tag{4.13}$$

Having defined when a solution for a nonlinear dynamical system is stable, we can now ask how to prove that a given solution is stable, asymptotically stable or unstable. For physical systems, one can often argue about stability based on dissipation of energy. The generalization of that technique to arbitrary dynamical systems is based on the use of Lyapunov functions in place of energy.
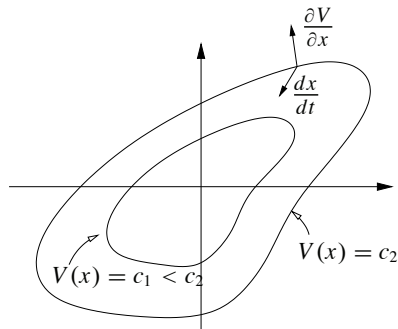
Figure 4.13: Geometric illustration of Lyapunov's stability theorem. The closed contours represent the level sets of the Lyapunov function $V(x) = c$. If dx/dt points inward to these sets at all points along the contour, then the trajectories of the system will always cause $V(x)$ to decrease along the trajectory.

$\mathbb{R}^n$ *and let* $\dot{V}$ *represent the time derivative of* V *along trajectories of the system dynamics* (4.13):

$$\dot{V} = \frac{\partial V}{\partial x}\frac{dx}{dt} = \frac{\partial V}{\partial x}F(x).$$

Let $B_r = B_r(0)$ *be a ball of radius* r *around the origin. If there exists* $r > 0$ *such that* V *is positive definite and* $\dot{V}$ *is negative semidefinite for all* $x \in B_r$, *then* $x = 0$ *is locally stable in the sense of Lyapunov. If* V *is positive definite and* $\dot{V}$ *is negative definite in* B_r, *then* $x = 0$ *is locally asymptotically stable.*

If V satisfies one of the conditions above, we say that V is a (local) *Lyapunov function* for the system. These results have a nice geometric interpretation. The level curves for a positive definite function are the curves defined by $V(x) = c$, $c > 0$, and for each c this gives a closed contour, as shown in Figure 4.13. The condition that $\dot{V}(x)$ is negative simply means that the vector field points toward lower-level contours. This means that the trajectories move to smaller and smaller values of V and if $\dot{V}$ is negative definite then x must approach 0.

Example 4.9 Scalar nonlinear system
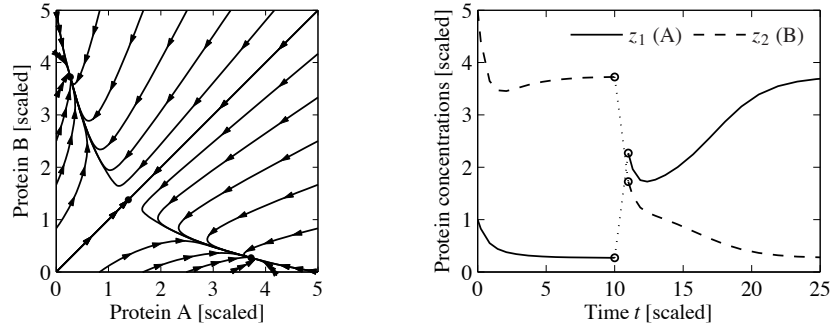Consider the scalar nonlinear system

$$\frac{dx}{dt} = \frac{2}{1+x} - x.$$

This system has equilibrium points at $x = 1$ and $x = -2$. We consider the equilibrium point at $x = 1$ and rewrite the dynamics using $z = x - 1$:

$$\frac{dz}{dt} = \frac{2}{2+z} - z - 1,$$

which has an equilibrium point at $z = 0$. Now consider the candidate Lyapunov function

$$V(z) = \frac{1}{2}z^2,$$

Figure 4.15: Dynamics of a genetic switch. The phase portrait on the left shows that the switch has three equilibrium points, corresponding to protein A having a concentration greater than, equal to or less than protein B. The equilibrium point with equal protein concentrations is unstable, but the other equilibrium points are stable. The simulation on the right shows the time response of the system starting from two different initial conditions. The initial portion of the curve corresponds to initial concentrations $z(0) = (1, 5)$ and converges to the equilibrium where $z_{1e} < z_{2e}$. At time $t = 10$, the concentrations are perturbed by $+2$ in z_1 and -2 in z_2, moving the state into the region of the state space whose solutions converge to the equilibrium point where $z_{2e} < z_{1e}$.

point. By construction,

$$\dot{V} = w^T(PA + A^TP)w + \tilde{F}^T(w)Pw + w^TP\tilde{F}(w)$$
$$= -w^Tw + \tilde{F}^T(w)Pw + w^TP\tilde{F}(w).$$

Since all terms in $\tilde{F}$ are quadratic or higher order in w, it follows that $\tilde{F}^T(w)Pw$ and $w^TP\tilde{F}(w)$ consist of terms that are at least third order in w. Therefore if w is sufficiently close to zero, then the cubic and higher-order terms will be smaller than the quadratic terms. Hence, sufficiently close to $w = 0$, $\dot{V}$ is negative definite, allowing us to conclude that these equilibrium points are both stable.

Figure 4.15 shows the phase portrait and time traces for a system with $\mu = 4$, illustrating the bistable nature of the system. When the initial condition starts with a concentration of protein B greater than that of A, the solution converges to the equilibrium point at (approximately) $(1/\mu^{n-1}, \mu)$. If A is greater than B, then it goes to $(\mu, 1/\mu^{n-1})$. The equilibrium point with $z_{1e} = z_{2e}$ is unstable. ∇

More generally, we can investigate what the linear approximation tells about the stability of a solution to a nonlinear equation. The following theorem gives a partial answer for the case of stability of an equilibrium point.

Theorem 4.3. *Consider the dynamical system* (4.15) *with* $F(0) = 0$ *and* $\tilde{F}$ *such that* $\lim \|\tilde{F}(x)\|/\|x\| \to 0$ *as* $\|x\| \to 0$. *If the real parts of all eigenvalues of A are strictly less than zero, then* $x_e = 0$ *is a locally asymptotically stable equilibrium point of equation* (4.15).

This theorem implies that asymptotic stability of the linear approximation implies *local* asymptotic stability of the original nonlinear system. The theorem is very
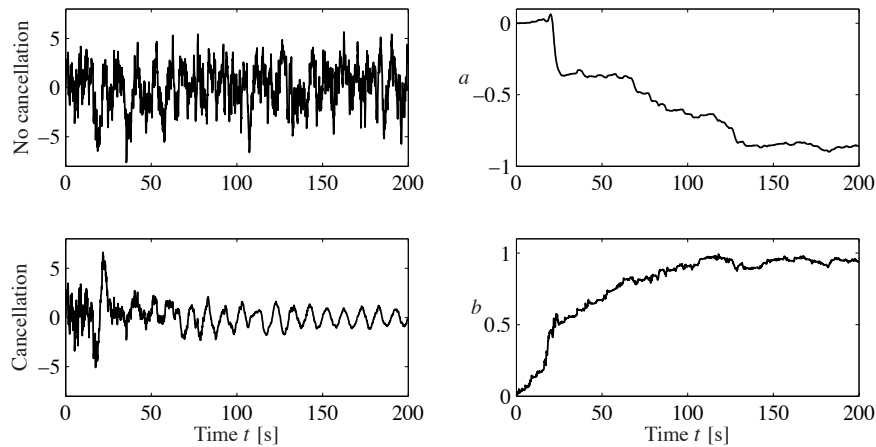
Figure 4.20: Simulation of noise cancellation. The top left figure shows the headphone signal without noise cancellation, and the bottom left figure shows the signal with noise cancellation. The right figures show the parameters a and b of the filter.

4.6 Further Reading

The field of dynamical systems has a rich literature that characterizes the possible features of dynamical systems and describes how parametric changes in the dynamics can lead to topological changes in behavior. Readable introductions to dynamical systems are given by Strogatz [188] and the highly illustrated text by Abraham and Shaw [2]. More technical treatments include Andronov, Vitt and Khaikin [8], Guckenheimer and Holmes [91] and Wiggins [201]. For students with a strong interest in mechanics, the texts by Arnold [13] and Marsden and Ratiu [147] provide an elegant approach using tools from differential geometry. Finally, good treatments of dynamical systems methods in biology are given by Wilson [203] and Ellner and Guckenheimer [70]. There is a large literature on Lyapunov stability theory, including the classic texts by Malkin [144], Hahn [94] and Krasovski [128]. We highly recommend the comprehensive treatment by Khalil [123].

Exercises

4.1 (Time-invariant systems) Show that if we have a solution of the differential equation (4.1) given by $x(t)$ with initial condition $x(t_0) = x_0$, then $\tilde{x}(\tau) = x(t - t_0)$ is a solution of the differential equation

$$\frac{d\tilde{x}}{d\tau} = F(\tilde{x})$$

with initial condition $\tilde{x}(0) = x_0$, where $\tau = t - t_0$.

4.2 (Flow in a tank) A cylindrical tank has cross section A m^2, effective outlet area a m^2 and inflow q_{in} m^3/s. An energy balance shows that the outlet velocity is

$v = \sqrt{2gh}$ m/s, where g m/s^2 is the acceleration of gravity and h is the distance between the outlet and the water level in the tank (in meters). Show that the system can be modeled by

$$\frac{dh}{dt} = -\frac{a}{A}\sqrt{2gh} - \frac{1}{A}q_{in}, \qquad q_{out} = a\sqrt{2gh}.$$

Use the parameters $A = 0.2, a = 0.01$. Simulate the system when the inflow is zero and the initial level is $h = 0.2$. Do you expect any difficulties in the simulation?

4.3 (Cruise control) Consider the cruise control system described in Section 3.1. Generate a phase portrait for the closed loop system on flat ground ($\theta = 0$), in third gear, using a PI controller (with $k_p = 0.5$ and $k_i = 0.1$), $m = 1000$ kg and desired speed 20 m/s. Your system model should include the effects of saturating the input between 0 and 1.

4.4 (Lyapunov functions) Consider the second-order system

$$\frac{dx_1}{dt} = -ax_1, \qquad \frac{dx_2}{dt} = -bx_1 - cx_2,$$

where $a, b, c > 0$. Investigate whether the functions

$$V_1(x) = \frac{1}{2}x_1^2 + \frac{1}{2}x_2^2, \qquad V_2(x) = \frac{1}{2}x_1^2 + \frac{1}{2}(x_2 + \frac{b}{c-a}x_1)^2$$

are Lyapunov functions for the system and give any conditions that must hold.

4.5 (Damped spring–mass system) Consider a damped spring–mass system with dynamics

$$m\ddot{q} + c\dot{q} + kq = 0.$$

A natural candidate for a Lyapunov function is the total energy of the system, given by

$$V = \frac{1}{2}m\dot{q}^2 + \frac{1}{2}kq^2.$$

Use the Krasovski–Lasalle theorem to show that the system is asymptotically stable.

4.6 (Electric generator) The following simple model for an electric generator connected to a strong power grid was given in Exercise 2.7:

$$J\frac{d^2\varphi}{dt^2} = P_m - P_e = P_m - \frac{EV}{X}\sin\varphi.$$

The parameter

$$a = \frac{P_{max}}{P_m} = \frac{EV}{XP_m} \tag{4.25}$$

is the ratio between the maximum deliverable power $P_{max} = EV/X$ and the mechanical power P_m.

(a) Consider a as a bifurcation parameter and discuss how the equilibria depend on a.

(b) For $a > 1$, show that there is a center at $\varphi_0 = \arcsin(1/a)$ and a saddle at $\varphi = \pi - \varphi_0$.

(c) Show that if $P_m/J = 1$ there is a solution through the saddle that satisfies

$$\frac{1}{2}\left(\frac{d\varphi}{dt}\right)^2 - \varphi + \varphi_0 - a\cos\varphi - \sqrt{a^2 - 1} = 0. \qquad (4.26)$$

Use simulation to show that the stability region is the interior of the area enclosed by this solution. Investigate what happens if the system is in equilibrium with a value of a that is slightly larger than 1 and a suddenly decreases, corresponding to the reactance of the line suddenly increasing.

4.7 (Lyapunov equation) Show that Lyapunov equation (4.14) always has a solution if all of the eigenvalues of A are in the left half-plane. (Hint: Use the fact that the Lyapunov equation is linear in P and start with the case where A has distinct eigenvalues.)

4.8 (Congestion control) Consider the congestion control problem described in Section 3.4. Confirm that the equilibrium point for the system is given by equation (3.21) and compute the stability of this equilibrium point using a linear approximation.

4.9 (Swinging up a pendulum) Consider the inverted pendulum, discussed in Example 4.4, that is described by

$$\ddot{\theta} = \sin\theta + u\cos\theta,$$

where θ is the angle between the pendulum and the vertical and the control signal u is the acceleration of the pivot. Using the energy function

$$V(\theta, \dot{\theta}) = \cos\theta - 1 + \frac{1}{2}\dot{\theta}^2,$$

show that the state feedback $u = k(V_0 - V)\dot{\theta}\cos\theta$ causes the pendulum to "swing up" to the upright position.

4.10 (Root locus diagram) Consider the linear system

$$\frac{dx}{dt} = \begin{bmatrix} 0 & 1 \\ 0 & -3 \end{bmatrix} x + \begin{bmatrix} -1 \\ 4 \end{bmatrix} u, \qquad y = \begin{bmatrix} 1 & 0 \end{bmatrix} x,$$

with the feedback $u = -ky$. Plot the location of the eigenvalues as a function the parameter k.

4.11 (Discrete-time Lyapunov function) Consider a nonlinear discrete-time system with dynamics $x[k+1] = f(x[k])$ and equilibrium point $x_e = 0$. Suppose there exists a smooth, positive definite function $V : \mathbb{R}^n \to \mathbb{R}$ such that $V(f(x)) - V(x) < 0$ for $x \neq 0$ and $V(0) = 0$. Show that $x_e = 0$ is (locally) asymptotically stable.

4.12 (Operational amplifier oscillator) An op amp circuit for an oscillator was shown in Exercise 3.5. The oscillatory solution for that linear circuit was stable but not asymptotically stable. A schematic of a modified circuit that has nonlinear elements is shown in the figure below.
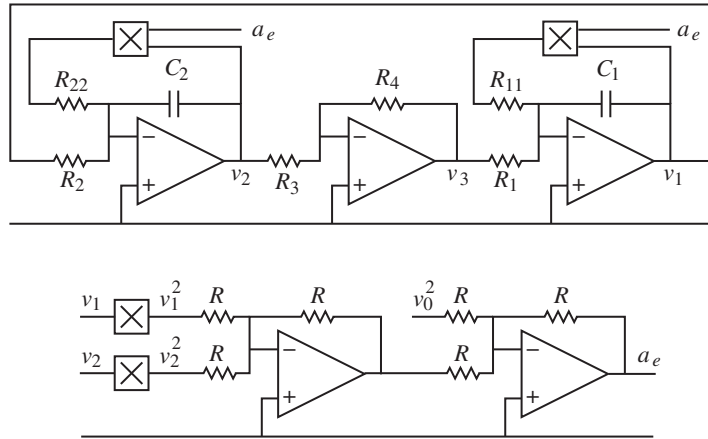
The modification is obtained by making a feedback around each operational amplifier that has capacitors using multipliers. The signal $a_e = v_1^2 + v_2^2 - v_0^2$ is the amplitude error. Show that the system is modeled by

$$\frac{dv_1}{dt} = \frac{R_4}{R_1 R_3 C_1} v_2 + \frac{1}{R_{11} C_1} v_1 (v_0^2 - v_1^2 - v_2^2),$$

$$\frac{dv_2}{dt} = -\frac{1}{R_2 C_2} v_1 + \frac{1}{R_{22} C_2} v_2 (v_0^2 - v_1^2 - v_2^2).$$

Show that the circuit gives an oscillation with a stable limit cycle with amplitude v_0. (Hint: Use the results of Example 4.8.)

4.13 (Self-activating genetic circuit) Consider the dynamics of a genetic circuit that implements *self-activation*: the protein produced by the gene is an activator for the protein, thus stimulating its own production through positive feedback. Using the models presented in Example 2.13, the dynamics for the system can be written as

$$\frac{dm}{dt} = \frac{\alpha p^2}{1 + k p^2} + \alpha_0 - \gamma m, \qquad \frac{dp}{dt} = \beta m - \delta p, \qquad (4.27)$$

for $p, m \geq 0$. Find the equilibrium points for the system and analyze the local stability of each using Lyapunov analysis.

4.14 (Diagonal systems) Let $A \in \mathbb{R}^{n \times n}$ be a square matrix with real eigenvalues $\lambda_1, \ldots, \lambda_n$ and corresponding eigenvectors $v_1, \ldots, v_n$.

(a) Show that if the eigenvalues are distinct ($\lambda_i \neq \lambda_j$ for $i \neq j$), then $v_i \neq v_j$ for $i \neq j$.

(b) Show that the eigenvectors form a basis for $\mathbb{R}^n$ so that any vector x can be written as $x = \sum \alpha_i v_i$ for $\alpha_i \in \mathbb{R}$.

(c) Let $T = \begin{bmatrix} v_1 & v_2 & \ldots & v_n \end{bmatrix}$ and show that $T^{-1} A T$ is a diagonal matrix of the form (4.8).

Chapter Five
Linear Systems

Few physical elements display truly linear characteristics. For example the relation between force on a spring and displacement of the spring is always nonlinear to some degree. The relation between current through a resistor and voltage drop across it also deviates from a straight-line relation. However, if in each case the relation is reasonably *linear, then it will be found that the system behavior will be very close to that obtained by assuming an ideal, linear physical element, and the analytical simplification is so enormous that we make linear assumptions wherever we can possibly do so in good conscience.*

Robert H. Cannon, *Dynamics of Physical Systems*, 1967 [49].

In Chapters 2–4 we considered the construction and analysis of differential equation models for dynamical systems. In this chapter we specialize our results to the case of linear, time-invariant input/output systems. Two central concepts are the matrix exponential and the convolution equation, through which we can completely characterize the behavior of a linear system. We also describe some properties of the input/output response and show how to approximate a nonlinear system by a linear one.

5.1 Basic Definitions

We have seen several instances of linear differential equations in the examples in the previous chapters, including the spring–mass system (damped oscillator) and the operational amplifier in the presence of small (nonsaturating) input signals. More generally, many dynamical systems can be modeled accurately by linear differential equations. Electrical circuits are one example of a broad class of systems for which linear models can be used effectively. Linear models are also broadly applicable in mechanical engineering, for example, as models of small deviations from equilibria in solid and fluid mechanics. Signal-processing systems, including digital filters of the sort used in CD and MP3 players, are another source of good examples, although these are often best modeled in discrete time (as described in more detail in the exercises).

In many cases, we *create* systems with a linear input/output response through the use of feedback. Indeed, it was the desire for linear behavior that led Harold S. Black to the invention of the negative feedback amplifier. Almost all modern signal processing systems, whether analog or digital, use feedback to produce linear or near-linear input/output characteristics. For these systems, it is often useful to represent the input/output characteristics as linear, ignoring the internal details required to get that linear response.

(a) Piecewise constant input   (b) Output response
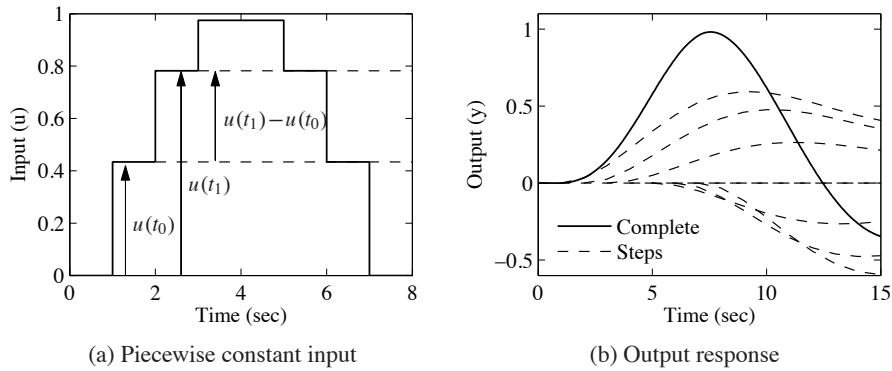
Figure 5.2: Response to piecewise constant inputs. A piecewise constant signal can be represented as a sum of step signals (a), and the resulting output is the sum of the individual outputs (b).

posing the responses to a combination of step inputs. Let $H(t)$ be the response to a unit step applied at time 0. The response to the first step is then $H(t - t_0)u(t_0)$, the response to the second step is $H(t - t_1)\big(u(t_1) - u(t_0)\big)$, and we find that the complete response is given by

$$
\begin{aligned}
y(t) &= H(t - t_0)u(t_0) + H(t - t_1)\big(u(t_1) - u(t_0)\big) + \cdots \\
&= \big(H(t - t_0) - H(t - t_1)\big)u(t_0) + \big(H(t - t_1) - H(t - t_2)\big)u(t_1) + \cdots \\
&= \sum_{n=0}^{\substack{t_n < t \\ \infty}} \big(H(t - t_n) - H(t - t_{n+1})\big)u(t_n) \\
&= \sum_{n=0}^{t_n < t} \frac{H(t - t_n) - H(t - t_{n+1})}{t_{n+1} - t_n} u(t_n)\big(t_{n+1} - t_n\big).
\end{aligned}
$$

An example of this computation is shown in Figure 5.2b.

The response to a continuous input signal is obtained by taking the limit as $t_{n+1} - t_n \to 0$, which gives

$$
y(t) = \int_0^t H'(t - \tau)u(\tau)d\tau, \tag{5.5}
$$

where H' is the derivative of the step response, also called the *impulse response*. The response of a linear time-invariant system to any input can thus be computed from the step response. Notice that the output depends only on the input since we assumed the system was initially at rest, $x(0) = 0$. We will derive equation (5.5) in a slightly different way in the Section 5.3.

$\lambda = \sigma \pm i\omega$ and $v = u \pm iw$, which implies that

$$u = \frac{v + v^*}{2}, \qquad w = \frac{v - v^*}{2i}.$$

Making use of the matrix exponential, we have

$$e^{At}v = e^{\lambda t}(u + iw) = e^{\sigma t}\big((u\cos\omega t - w\sin\omega t) + i(u\sin\omega t + w\cos\omega t)\big),$$

from which it follows that

$$e^{At}u = \frac{1}{2}\big(e^{At}v + e^{At}v^*\big) = ue^{\sigma t}\cos\omega t - we^{\sigma t}\sin\omega t,$$

$$e^{At}w = \frac{1}{2i}\big(e^{At}v - e^{At}v^*\big) = ue^{\sigma t}\sin\omega t + we^{\sigma t}\cos\omega t.$$

A solution with initial conditions in the subspace spanned by the real part u and imaginary part w of the eigenvector will thus remain in that subspace. The solution will be a logarithmic spiral characterized by σ and ω. We again call the solution corresponding to λ a mode of the system, and v the mode shape.

If a matrix A has n distinct eigenvalues $\lambda_1, \ldots, \lambda_n$, then the initial condition response can be written as a linear combination of the modes. To see this, suppose for simplicity that we have all real eigenvalues with corresponding unit eigenvectors $v_1, \ldots, v_n$. From linear algebra, these eigenvectors are linearly independent, and we can write the initial condition $x(0)$ as

$$x(0) = \alpha_1 v_1 + \alpha_2 v_2 + \cdots + \alpha_n v_n.$$

Using linearity, the initial condition response can be written as

$$x(t) = \alpha_1 e^{\lambda_1 t} v_1 + \alpha_2 e^{\lambda_2 t} v_2 + \cdots + \alpha_n e^{\lambda_n t} v_n.$$

Thus, the response is a linear combination of the modes of the system, with the amplitude of the individual modes growing or decaying as $e^{\lambda_i t}$. The case for distinct complex eigenvalues follows similarly (the case for nondistinct eigenvalues is more subtle and requires making use of the Jordan form discussed in the previous section).

Example 5.5 Coupled spring–mass system
Consider the spring–mass system shown in Figure 5.4, but with the addition of dampers on each mass. The equations of motion of the system are

$$m_1\ddot{q}_1 = -2kq_1 - c\dot{q}_1 + kq_2, \qquad m_2\ddot{q}_2 = kq_1 - 2kq_2 - c\dot{q}_2.$$

In state space form, we define the state to be $x = (q_1, q_2, \dot{q}_1, \dot{q}_2)$, and we can rewrite the equations as

$$\frac{dx}{dt} = \begin{bmatrix} 0 & 0 & 1 & 0 \\ 0 & 0 & 0 & 1 \\ -\dfrac{2k}{m} & \dfrac{k}{m} & -\dfrac{c}{m} & 0 \\ \dfrac{k}{m} & -\dfrac{2k}{m} & 0 & -\dfrac{c}{m} \end{bmatrix} x.$$

We now define a transformation $z = Tx$ that puts this system into a simpler form. Let $z_1 = \frac{1}{2}(q_1 + q_2), z_2 = \dot{z}_1, z_3 = \frac{1}{2}(q_1 - q_2)$ and $z_4 = \dot{z}_3$, so that

$$z = Tx = \frac{1}{2}\begin{bmatrix} 1 & 1 & 0 & 0 \\ 0 & 0 & 1 & 1 \\ 1 & -1 & 0 & 0 \\ 0 & 0 & 1 & -1 \end{bmatrix} x.$$

In the new coordinates, the dynamics become

$$\frac{dz}{dt} = \begin{bmatrix} 0 & 1 & 0 & 0 \\ -\dfrac{k}{m} & -\dfrac{c}{m} & 0 & 0 \\ 0 & 0 & 0 & 1 \\ 0 & 0 & -\dfrac{3k}{m} & -\dfrac{c}{m} \end{bmatrix} z,$$

and we see that the system is in block diagonal (or *modal*) form.

In the z coordinates, the states z_1 and z_2 parameterize one mode with eigenvalues $\lambda \approx c/(2\sqrt{km}) \pm i\sqrt{k/m}$, and the states z_3 and z_4 another mode with $\lambda \approx c/(2\sqrt{3km}) \pm i\sqrt{3k/m}$. From the form of the transformation T we see that these modes correspond exactly to the modes in Figure 5.4, in which q_1 and q_2 move either toward or against each other. The real and imaginary parts of the eigenvalues give the decay rates σ and frequencies ω for each mode. ∇

5.3 Input/Output Response

In the previous section we saw how to compute the initial condition response using the matrix exponential. In this section we derive the convolution equation, which includes the inputs and outputs as well.

The Convolution Equation

We return to the general input/output case in equation (5.3), repeated here:

$$\frac{dx}{dt} = Ax + Bu, \qquad y = Cx + Du. \tag{5.13}$$

Using the matrix exponential, the solution to equation (5.13) can be written as follows.

Theorem 5.4. *The solution to the linear differential equation* (5.13) *is given by*

$$x(t) = e^{At}x(0) + \int_0^t e^{A(t-\tau)}Bu(\tau)d\tau. \tag{5.14}$$

Proof. To prove this, we differentiate both sides and use the property (5.8) of the matrix exponential. This gives

$$\frac{dx}{dt} = Ae^{At}x(0) + \int_0^t Ae^{A(t-\tau)}Bu(\tau)d\tau + Bu(t) = Ax + Bu,$$

(a) Pulse and impulse functions   (b) Pulse and impulse responses
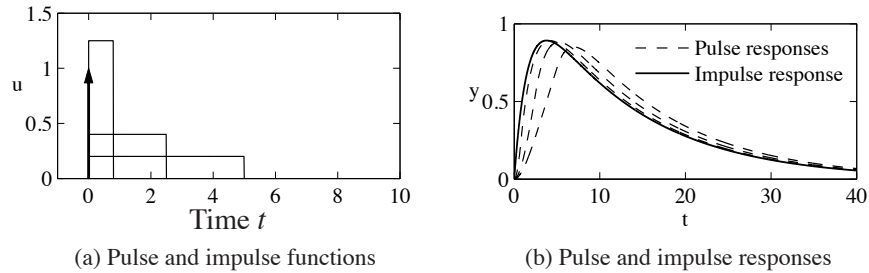
Figure 5.6: Pulse response and impulse response. (a) The rectangles show pulses of width 5, 2.5 and 0.8, each with total area equal to 1. The arrow denotes an impulse $\delta(t)$ defined by equation (5.17). The corresponding pulse responses for a linear system with eigenvalues $\lambda = \{-0.08, -0.62\}$ are shown in (b) as dashed lines. The solid line is the true impulse response, which is well approximated by a pulse of duration 0.8.

which proves the result. Notice that the calculation is essentially the same as for proving the result for a first-order equation. □

It follows from equations (5.13) and (5.14) that the input/output relation for a linear system is given by

$$y(t) = Ce^{At}x(0) + \int_0^t Ce^{A(t-\tau)}Bu(\tau)d\tau + Du(t). \tag{5.15}$$

It is easy to see from this equation that the output is jointly linear in both the initial conditions and the input, which follows from the linearity of matrix/vector multiplication and integration.

Equation (5.15) is called the *convolution equation*, and it represents the general form of the solution of a system of coupled linear differential equations. We see immediately that the dynamics of the system, as characterized by the matrix A, play a critical role in both the stability and performance of the system. Indeed, the matrix exponential describes *both* what happens when we perturb the initial condition and how the system responds to inputs.

Another interpretation of the convolution equation can be given using the concept of the *impulse response* of a system. Consider the application of an input signal $u(t)$ given by the following equation:

$$u(t) = p_\epsilon(t) = \begin{cases} 0 & t < 0 \\ 1/\epsilon & 0 \leq t < \epsilon \\ 0 & t \geq \epsilon. \end{cases} \tag{5.16}$$

This signal is a *pulse* of duration ϵ and amplitude $1/\epsilon$, as illustrated in Figure 5.6a. We define an *impulse* $\delta(t)$ to be the limit of this signal as $\epsilon \to 0$:

$$\delta(t) = \lim_{\epsilon \to 0} p_\epsilon(t). \tag{5.17}$$

In state space form, we define the state to be $x = (q_1, q_2, \dot{q}_1, \dot{q}_2)$, and we can rewrite the equations as

$$\frac{dx}{dt} = \begin{bmatrix} 0 & 0 & 1 & 0 \\ 0 & 0 & 0 & 1 \\ -\dfrac{2k}{m} & \dfrac{k}{m} & -\dfrac{c}{m} & 0 \\ \dfrac{k}{m} & -\dfrac{2k}{m} & 0 & -\dfrac{c}{m} \end{bmatrix} x + \begin{bmatrix} 0 \\ 0 \\ 0 \\ \dfrac{k}{m} \end{bmatrix} u.$$

This is a coupled set of four differential equations and is quite complicated to solve in analytical form.

The dynamics matrix is the same as in Example 5.5, and we can use the coordinate transformation defined there to put the system in modal form:

$$\frac{dz}{dt} = \begin{bmatrix} 0 & 1 & 0 & 0 \\ -\dfrac{k}{m} & -\dfrac{c}{m} & 0 & 0 \\ 0 & 0 & 0 & 1 \\ 0 & 0 & -\dfrac{3k}{m} & -\dfrac{c}{m} \end{bmatrix} z + \begin{bmatrix} 0 \\ \dfrac{k}{2m} \\ 0 \\ -\dfrac{k}{2m} \end{bmatrix} u.$$

Note that the resulting matrix equations are block diagonal and hence decoupled. We can solve for the solutions by computing the solutions of two sets of second-order systems represented by the states (z_1, z_2) and (z_3, z_4). Indeed, the functional form of each set of equations is identical to that of a single spring–mass system. (The explicit solution is derived in Section 6.3.)

Once we have solved the two sets of independent second-order equations, we can recover the dynamics in the original coordinates by inverting the state transformation and writing $x = T^{-1}z$. We can also determine the stability of the system by looking at the stability of the independent second-order systems. ∇

Steady-State Response

Given a linear input/output system

$$\frac{dx}{dt} = Ax + Bu, \qquad y = Cx + Du, \tag{5.21}$$

the general form of the solution to equation (5.21) is given by the convolution equation:

$$y(t) = Ce^{At}x(0) + \int_0^t Ce^{A(t-\tau)}Bu(\tau)d\tau + Du(t).$$

We see from the form of this equation that the solution consists of an initial condition response and an input response.

The input response, corresponding to the last two terms in the equation above, itself consists of two components—the *transient response* and the *steady-state*

(a) Input/output response   (b) Frequency response
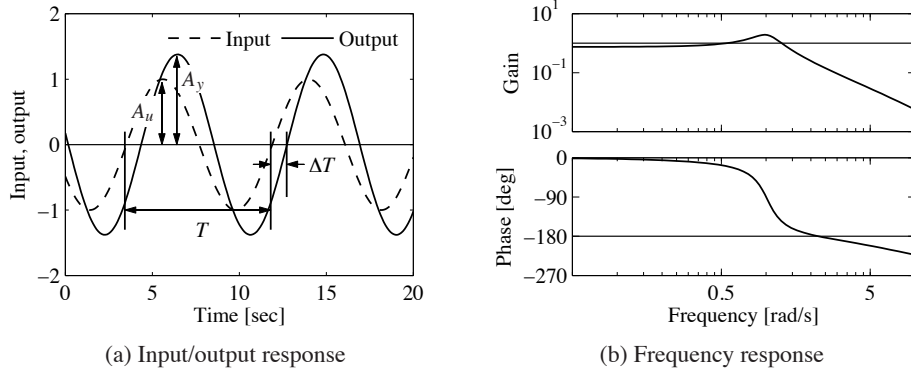
Figure 5.11: Response of a linear system to a sinusoid. (a) A sinusoidal input of magnitude A_u (dashed) gives a sinusoidal output of magnitude A_y (solid), delayed by ΔT seconds. (b) Frequency response, showing gain and phase. The gain is given by the ratio of the output amplitude to the input amplitude, $M = A_y/A_u$. The phase lag is given by $\theta = -2\pi \, \Delta T/T$; it is negative for the case shown because the output lags the input.

A convenient way to view the frequency response is to plot how the gain and phase in equation (5.24) depend on ω (through $s = i\omega$). Figure 5.11b shows an example of this type of representation.

Example 5.8 Active band-pass filter

Consider the op amp circuit shown in Figure 5.12a. We can derive the dynamics of the system by writing the *nodal equations*, which state that the sum of the currents at any node must be zero. Assuming that $v_- = v_+ = 0$, as we did in Section 3.3, we have

$$0 = \frac{v_1 - v_2}{R_1} - C_1 \frac{dv_2}{dt}, \qquad 0 = C_1 \frac{dv_2}{dt} + \frac{v_3}{R_2} + C_2 \frac{dv_3}{dt}.$$

Choosing v_2 and v_3 as our states and using these equations, we obtain

$$\frac{dv_2}{dt} = \frac{v_1 - v_2}{R_1 C_1}, \qquad \frac{dv_3}{dt} = \frac{-v_3}{R_2 C_2} - \frac{v_1 - v_2}{R_1 C_2}.$$

Rewriting these in linear state space form, we obtain

$$\frac{dx}{dt} = \begin{bmatrix} -\dfrac{1}{R_1 C_1} & 0 \\[2mm] \dfrac{1}{R_1 C_2} & -\dfrac{1}{R_2 C_2} \end{bmatrix} x + \begin{bmatrix} \dfrac{1}{R_1 C_1} \\[2mm] \dfrac{-1}{R_1 C_2} \end{bmatrix} u, \qquad y = \begin{bmatrix} 0 & 1 \end{bmatrix} x, \qquad (5.25)$$

where $x = (v_2, v_3)$, $u = v_1$ and $y = v_3$.

The frequency response for the system can be computed using equation (5.24):

$$Me^{j\theta} = C(sI - A)^{-1}B + D = -\frac{R_2}{R_1} \frac{R_1 C_1 s}{(1 + R_1 C_1 s)(1 + R_2 C_2 s)}, \qquad s = i\omega.$$

The magnitude and phase are plotted in Figure 5.12b for $R_1 = 100 \ \Omega$, $R_2 = 5 \ \text{k}\Omega$ and $C_1 = C_2 = 100 \ \mu\text{F}$. We see that the circuit passes through signals with

(a) Circuit diagram   (b) Frequency response
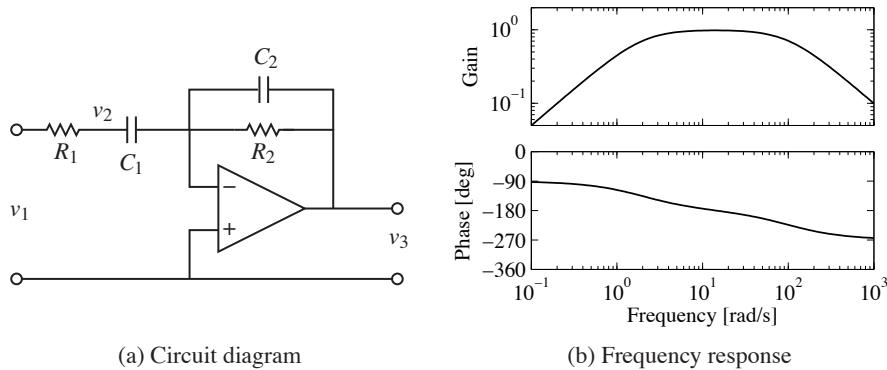
Figure 5.12: Active band-pass filter. The circuit diagram (a) shows an op amp with two *RC* filters arranged to provide a band-pass filter. The plot in (b) shows the gain and phase of the filter as a function of frequency. Note that the phase starts at -90° due to the negative gain of the operational amplifier.

frequencies at about 10 rad/s, but attenuates frequencies below 5 rad/s and above 50 rad/s. At 0.1 rad/s the input signal is attenuated by $20\times$ (0.05). This type of circuit is called a *band-pass filter* since it passes through signals in the band of frequencies between 5 and 50 rad/s. ∇

As in the case of the step response, a number of standard properties are defined for frequency responses. The gain of a system at $\omega = 0$ is called the *zero frequency gain* and corresponds to the ratio between a constant input and the steady output:

$$M_0 = -CA^{-1}B + D.$$

The zero frequency gain is well defined only if A is invertible (and, in particular, if it does not have eigenvalues at 0). It is also important to note that the zero frequency gain is a relevant quantity only when a system is stable about the corresponding equilibrium point. So, if we apply a constant input $u = r$, then the corresponding equilibrium point $x_e = -A^{-1}Br$ must be stable in order to talk about the zero frequency gain. (In electrical engineering, the zero frequency gain is often called the *DC gain*. DC stands for direct current and reflects the common separation of signals in electrical engineering into a direct current (zero frequency) term and an alternating current (AC) term.)

The *bandwidth* ω_b of a system is the frequency range over which the gain has decreased by no more than a factor of $1/\sqrt{2}$ from its reference value. For systems with nonzero, finite zero frequency gain, the bandwidth is the frequency where the gain has decreased by $1/\sqrt{2}$ from the zero frequency gain. For systems that attenuate low frequencies but pass through high frequencies, the reference gain is taken as the high-frequency gain. For a system such as the band-pass filter in Example 5.8, bandwidth is defined as the range of frequencies where the gain is larger than $1/\sqrt{2}$ of the gain at the center of the band. (For Example 5.8 this would give a bandwidth of approximately 50 rad/s.)

(a) AFM block diagram   (b) Frequency response
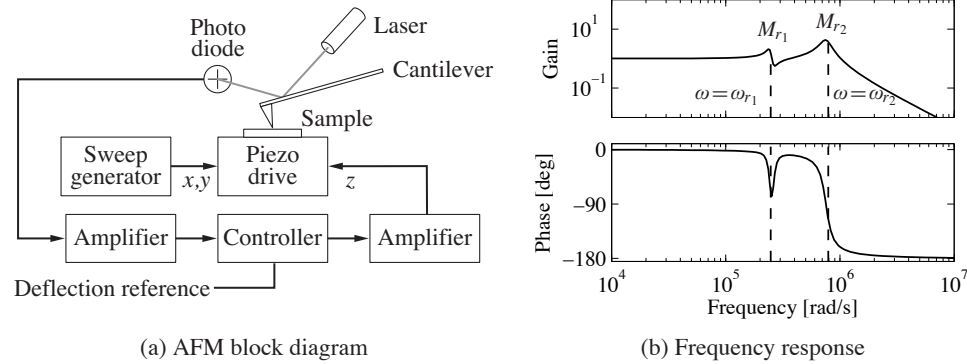
Figure 5.13: AFM frequency response. (a) A block diagram for the vertical dynamics of an atomic force microscope in contact mode. The plot in (b) shows the gain and phase for the piezo stack. The response contains two frequency peaks at resonances of the system, along with an antiresonance at $\omega = 268$ krad/s. The combination of a resonant peak followed by an antiresonance is common for systems with multiple lightly damped modes.

Another important property of the frequency response is the *resonant peak* M_r, the largest value of the frequency response, and the *peak frequency* ω_{mr}, the frequency where the maximum occurs. These two properties describe the frequency of the sinusoidal input that produces the largest possible output and the gain at the frequency.

Example 5.9 Atomic force microscope in contact mode

Consider the model for the vertical dynamics of the atomic force microscope in contact mode, discussed in Section 3.5. The basic dynamics are given by equation (3.23). The piezo stack can be modeled by a second-order system with undamped natural frequency ω_3 and damping ratio ζ_3. The dynamics are then described by the linear system

$$
\frac{dx}{dt} = \begin{bmatrix} 0 & 1 & 0 & 0 \\ -k_2/(m_1+m_2) & -c_2/(m_1+m_2) & 1/m_2 & 0 \\ 0 & 0 & 0 & \omega_3 \\ 0 & 0 & -\omega_3 & -2\zeta_3\omega_3 \end{bmatrix} x + \begin{bmatrix} 0 \\ 0 \\ 0 \\ \omega_3 \end{bmatrix} u,
$$

$$
y = \frac{m_2}{m_1+m_2} \begin{bmatrix} \dfrac{m_1 k_2}{m_1+m_2} & \dfrac{m_1 c_2}{m_1+m_2} & 1 & 0 \end{bmatrix} x,
$$

where the input signal is the drive signal to the amplifier and the output is the elongation of the piezo. The frequency response of the system is shown in Figure 5.13b. The zero frequency gain of the system is $M_0 = 1$. There are two resonant poles with peaks $M_{r1} = 2.12$ at $\omega_{mr1} = 238$ krad/s and $M_{r2} = 4.29$ at $\omega_{mr2} = 746$ krad/s. The bandwidth of the system, defined as the lowest frequency where the gain is $\sqrt{2}$ less than the zero frequency gain, is $\omega_b = 292$ krad/s. There is also a dip in the gain $M_d = 0.556$ for $\omega_{md} = 268$ krad/s. This dip, called an *antiresonance*, is associated with a dip in the phase and limits the performance when the system is controlled by simple controllers, as we will see in Chapter 10. ∇

Sampling

It is often convenient to use both differential and difference equations in modeling and control. For linear systems it is straightforward to transform from one to the other. Consider the general linear system described by equation (5.13) and assume that the control signal is constant over a sampling interval of constant length h. It follows from equation (5.14) of Theorem 5.4 that

$$x(t+h) = e^{Ah}x(t) + \int_t^{t+h} e^{A(t+h-\tau)}Bu(k)\,d\tau = \Phi x(t) + \Gamma u(t), \qquad (5.26)$$

where we have assumed that the discontinuous control signal is continuous from the right. The behavior of the system at the sampling times $t = kh$ is described by the difference equation

$$x[k+1] = \Phi x[k] + \Gamma u[k], \qquad y[k] = Cx[k] + Du[k]. \qquad (5.27)$$

Notice that the difference equation (5.27) is an exact representation of the behavior of the system at the sampling instants. Similar expressions can also be obtained if the control signal is linear over the sampling interval.

The transformation from (5.26) to (5.27) is called *sampling*. The relations between the system matrices in the continuous and sampled representations are as follows:

$$\Phi = e^{Ah}, \quad \Gamma = \left(\int_0^h e^{As}\,ds\right)B; \qquad A = \frac{1}{h}\log\Phi, \quad B = \left(\int_0^h e^{At}\,dt\right)^{-1}\Gamma. \qquad (5.28)$$

Notice that if A is invertible, we have

$$\Gamma = A^{-1}\left(e^{Ah} - I\right).$$

All continuous-time systems can be sampled to obtain a discrete-time version, but there are discrete-time systems that do not have a continuous-time equivalent. The precise condition is that the matrix Φ cannot have real eigenvalues on the negative real axis.

Example 5.10 IBM Lotus server
In Example 2.4 we described how the dynamics of an IBM Lotus server were obtained as the discrete-time system

$$y[k+1] = ay[k] + bu[k],$$

where $a = 0.43$, $b = 0.47$ and the sampling period is $h = 60$ s. A differential equation model is needed if we would like to design control systems based on continuous-time theory. Such a model is obtained by applying equation (5.28); hence

$$A = \frac{\log a}{h} = -0.0141, \qquad B = \left(\int_0^h e^{At}\,dt\right)^{-1}b = 0.0116,$$

and we find that the difference equation can be interpreted as a sampled version of

described in Gardner and Barnes [81]. Use of the matrix exponential started with developments of control theory in the 1960s, strongly stimulated by a textbook by Zadeh and Desoer [207]. Use of matrix techniques expanded rapidly when the powerful methods of numeric linear algebra were packaged in programs like LabVIEW, MATLAB and Mathematica.

Exercises

5.1 (Response to the derivative of a signal) Show that if $y(t)$ is the output of a linear system corresponding to input $u(t)$, then the output corresponding to an input $\dot{u}(t)$ is given by $\dot{y}(t)$. (Hint: Use the definition of the derivative: $\dot{y}(t) = \lim_{\epsilon \to 0}\big(y(t + \epsilon) - y(t)\big)/\epsilon$.)

5.2 (Impulse response and convolution) Show that a signal $u(t)$ can be decomposed in terms of the impulse function $\delta(t)$ as

$$u(t) = \int_0^t \delta(t - \tau)u(\tau)\,d\tau$$

and use this decomposition plus the principle of superposition to show that the response of a linear system to an input $u(t)$ (assuming a zero initial condition) can be written as

$$y(t) = \int_0^t h(t - \tau)u(\tau)\,d\tau,$$

where $h(t)$ is the impulse response of the system.

5.3 (Pulse response for a compartment model) Consider the compartment model given in Example 5.7. Compute the step response for the system and compare it with Figure 5.10b. Use the principle of superposition to compute the response to the 5 s pulse input shown in Figure 5.10c. Use the parameter values $k_0 = 0.1$, $k_1 = 0.1, k_2 = 0.5$ and $b_0 = 1.5$.

5.4 (Matrix exponential for second-order system) Assume that $\zeta < 1$ and let $\omega_d = \omega_0\sqrt{1 - \zeta^2}$. Show that

$$\exp\begin{bmatrix} -\zeta\omega_0 & \omega_d \\ -\omega_d & -\zeta\omega_0 \end{bmatrix} t = \begin{bmatrix} e^{-\zeta\omega_0 t}\cos\omega_d t & e^{-\zeta\omega_0 t}\sin\omega_d t \\ -e^{-\zeta\omega_0 t}\sin\omega_d t & e^{-\zeta\omega_0 t}\cos\omega_d t \end{bmatrix}.$$

5.5 (Lyapunov function for a linear system) Consider a linear system $\dot{x} = Ax$ with $\mathrm{Re}\,\lambda_j < 0$ for all eigenvalues λ_j of the matrix A. Show that the matrix

$$P = \int_0^\infty e^{A^T\tau}Qe^{A\tau}\,d\tau$$

defines a Lyapunov function of the form $V(x) = x^T P x$.

5.6 (Nondiagonal Jordan form) Consider a linear system with a Jordan form that is non-diagonal.

(a) Prove Proposition 5.3 by showing that if the system contains a real eigenvalue $\lambda = 0$ with a nontrivial Jordan block, then there exists an initial condition with a solution that grows in time.

(b) Extend this argument to the case of complex eigenvalues with $\mathrm{Re}\,\lambda = 0$ by using the block Jordan form

$$
J_i = \begin{bmatrix} 0 & \omega & 1 & 0 \\ -\omega & 0 & 0 & 1 \\ 0 & 0 & 0 & \omega \\ 0 & 0 & -\omega & 0 \end{bmatrix}.
$$

5.7 (Rise time for a first-order system) Consider a first-order system of the form

$$
\tau \frac{dx}{dt} = -x + u, \qquad y = x.
$$

We say that the parameter τ is the *time constant* for the system since the zero input system approaches the origin as $e^{-t/\tau}$. For a first-order system of this form, show that the rise time for a step response of the system is approximately 2τ, and that $1\%, 2\%$, and 5% settling times approximately corresponds to $4.6\tau, 4\tau$ and 3τ.

5.8 (Discrete-time systems) Consider a linear discrete-time system of the form

$$
x[k+1] = Ax[k] + Bu[k], \qquad y[k] = Cx[k] + Du[k].
$$

(a) Show that the general form of the output of a discrete-time linear system is given by the discrete-time convolution equation:

$$
y[k] = C A^k x[0] + \sum_{j=0}^{k-1} C A^{k-j-1} Bu[j] + Du[k].
$$

(b) Show that a discrete-time linear system is asymptotically stable if and only if all the eigenvalues of A have a magnitude strictly less than 1.

(c) Let $u[k] = \sin(\omega k)$ represent an oscillatory input with frequency $\omega < \pi$ (to avoid "aliasing"). Show that the steady-state component of the response has gain M and phase θ, where

$$
Me^{i\theta} = C(e^{i\omega}I - A)^{-1}B + D.
$$

(d) Show that if we have a nonlinear discrete-time system

$$
\begin{aligned}
x[k] &= f(x[k], u[k]), & x[k] \in \mathbb{R}^n, \ u \in \mathbb{R}, \\
y[k] &= h(x[k], u[k]), & y \in \mathbb{R},
\end{aligned}
$$

then we can linearize the system around an equilibrium point (x_e, u_e) by defining the matrices A, B, C and D as in equation (5.34).

5.9 (Keynesian economics) Consider the following simple Keynesian macroeco-nomic model in the form of a linear discrete-time system discussed in Exercise 5.8:

$$\begin{bmatrix} C[t+1] \\ I[t+1] \end{bmatrix} = \begin{bmatrix} a & a \\ ab-b & ab \end{bmatrix} \begin{bmatrix} C[t] \\ I[t] \end{bmatrix} + \begin{bmatrix} a \\ ab \end{bmatrix} G[t],$$

$$Y[t] = C[t] + I[t] + G[t].$$

Determine the eigenvalues of the dynamics matrix. When are the magnitudes of the eigenvalues less than 1? Assume that the system is in equilibrium with constant values capital spending C, investment I and government expenditure G. Explore what happens when government expenditure increases by 10%. Use the values $a = 0.25$ and $b = 0.5$.

5.10 Consider a scalar system

$$\frac{dx}{dt} = 1 - x^3 + u.$$

Compute the equilibrium points for the unforced system ($u = 0$) and use a Taylor series expansion around the equilibrium point to compute the linearization. Verify that this agrees with the linearization in equation (5.33).

5.11 (Transcriptional regulation) Consider the dynamics of a genetic circuit that im-plements *self-repression*: the protein produced by a gene is a repressor for that gene, thus restricting its own production. Using the models presented in Example 2.13, the dynamics for the system can be written as

$$\frac{dm}{dt} = \frac{\alpha}{1 + kp^2} + \alpha_0 - \gamma m - u, \qquad \frac{dp}{dt} = \beta m - \delta p, \qquad (5.40)$$

where u is a disturbance term that affects RNA transcription and $m, p \geq 0$. Find the equilibrium points for the system and use the linearized dynamics around each equilibrium point to determine the local stability of the equilibrium point and the step response of the system to a disturbance.

Figure 6.1b shows a sample trajectory bringing the system to the origin. Note that if we steer the system to an equilibrium point, it is possible to remain there indefinitely (since $\dot{x}_1 = 0$ when $x_2 = 0$), but if we go to any other point in the state space, we can pass through the point only in a transient fashion. ∇

To find general conditions under which a linear system is reachable, we will first give a heuristic argument based on formal calculations with impulse functions. We note that if we can reach all points in the state space through some choice of input, then we can also reach all equilibrium points.

Testing for Reachability

When the initial state is zero, the response of the system to an input $u(t)$ is given by

$$x(t) = \int_0^t e^{A(t-\tau)} Bu(\tau) \, d\tau. \tag{6.2}$$

If we choose the input to be a impulse function $\delta(t)$ as defined in Section 5.3, the state becomes

$$x_\delta = \int_0^t e^{A(t-\tau)} B\delta(\tau) \, d\tau = \frac{dx_S}{dt} = e^{At} B.$$

(Note that the state changes instantaneously in response to the impulse.) We can find the response to the derivative of an impulse function by taking the derivative of the impulse response (Exercise 5.1):

$$x_{\dot{\delta}} = \frac{dx_\delta}{dt} = Ae^{At} B.$$

Continuing this process and using the linearity of the system, the input

$$u(t) = \alpha_1 \delta(t) + \alpha_2 \dot{\delta}(t) + \alpha_3 \ddot{\delta}(t) + \cdots + \alpha_n \delta^{(n-1)}(t)$$

gives the state

$$x(t) = \alpha_1 e^{At} B + \alpha_2 A e^{At} B + \alpha_3 A^2 e^{At} B + \cdots + \alpha_n A^{n-1} e^{At} B.$$

Taking the limit as t goes to zero through positive values, we get

$$\lim_{t \to 0+} x(t) = \alpha_1 B + \alpha_2 AB + \alpha_3 A^2 B + \cdots + \alpha_n A^{n-1} B.$$

On the right is a linear combination of the columns of the matrix

$$W_r = \begin{bmatrix} B & AB & \cdots & A^{n-1}B \end{bmatrix}. \tag{6.3}$$

To reach an arbitrary point in the state space, we thus require that there are n linear independent columns of the matrix W_r. The matrix W_r is called the *reachability matrix*.

An input consisting of a sum of impulse functions and their derivatives is a very violent signal. To see that an arbitrary point can be reached with smoother signals

(a) Step response for varying ω_c

(b) Step response for varying ζ_c
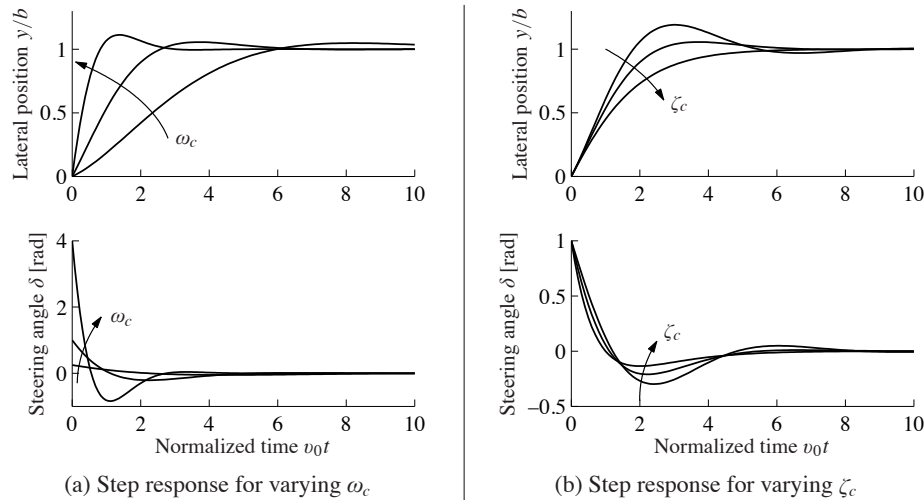
Figure 6.6: State feedback control of a steering system. Step responses obtained with controllers designed with $\zeta_c = 0.7$ and $\omega_c = 0.5, 1$ and 2 [rad/s] are shown in (a). Notice that response speed increases with increasing ω_c, but that large ω_c also give large initial control actions. Step responses obtained with a controller designed with $\omega_c = 1$ and $\zeta_c = 0.5, 0.7$ and 1 are shown in (b).

The step responses for the closed loop system for different values of the design parameters are shown in Figure 6.6. The effect of ω_c is shown in Figure 6.6a, which shows that the response speed increases with increasing ω_c. The responses for $\omega_c = 0.5$ and 1 have reasonable overshoot. The settling time is about 15 car lengths for $\omega_c = 0.5$ (beyond the end of the plot) and decreases to about 6 car lengths for $\omega_c = 1$. The control signal δ is large initially and goes to zero as time increases because the closed loop dynamics have an integrator. The initial value of the control signal is $u(0) = k_r = \omega_c^2 r$, and thus the achievable response time is limited by the available actuator signal. Notice in particular the dramatic increase in control signal when ω_c changes from 1 to 2. The effect of ζ_c is shown in Figure 6.6b. The response speed and the overshoot increase with decreasing damping. Using these plots, we conclude that reasonable values of the design parameters are to have ω_c in the range of 0.5 to 1 and $\zeta_c \approx 0.7$.   ▽

The example of the vehicle steering system illustrates how state feedback can be used to set the eigenvalues of a closed loop system to arbitrary values.

State Feedback for Systems in Reachable Canonical Form

The reachable canonical form has the property that the parameters of the system are the coefficients of the characteristic polynomial. It is therefore natural to consider systems in this form when solving the eigenvalue assignment problem.

To have zero frequency gain equal to unity, the parameter k_r should be chosen as

$$k_r = \frac{a_n + \tilde{k}_n}{b_n} = \frac{p_n}{b_n}.$$ (6.19)

Notice that it is essential to know the precise values of parameters a_n and b_n in order to obtain the correct zero frequency gain. The zero frequency gain is thus obtained by precise calibration. This is very different from obtaining the correct steady-state value by integral action, which we shall see in later sections.

Eigenvalue Assignment

We have seen through the examples how feedback can be used to design the dynamics of a system through assignment of its eigenvalues. To solve the problem in the general case, we simply change coordinates so that the system is in reachable canonical form. Consider the system

$$\frac{dx}{dt} = Ax + Bu, \qquad y = Cx + Du.$$ (6.20)

We can change the coordinates by a linear transformation $z = Tx$ so that the transformed system is in reachable canonical form (6.15). For such a system the feedback is given by equation (6.16), where the coefficients are given by equation (6.18). Transforming back to the original coordinates gives the feedback

$$u = -\tilde{K}z + k_r r = -\tilde{K}Tx + k_r r.$$

The results obtained can be summarized as follows.

Theorem 6.3 (Eigenvalue assignment by state feedback)**.** *Consider the system given by equation (6.20), with one input and one output. Let $\lambda(s) = s^n + a_1 s^{n-1} + \cdots + a_{n-1}s + a_n$ be the characteristic polynomial of A. If the system is reachable, then there exists a feedback*

$$u = -Kx + k_r r$$

that gives a closed loop system with the characteristic polynomial

$$p(s) = s^n + p_1 s^{n-1} + \cdots + p_{n-1}s + p_n$$

and unity zero frequency gain between r and y. The feedback gain is given by

$$K = \tilde{K}T = \begin{bmatrix} p_1 - a_1 & p_2 - a_2 & \cdots & p_n - a_n \end{bmatrix} \tilde{W}_r W_r^{-1},$$ (6.21)

where a_i are the coefficients of the characteristic polynomial of the matrix A and the matrices W_r and $\tilde{W}_r$ are given by

$$W_r = \begin{bmatrix} B & AB & \cdots & A^{n-1}B \end{bmatrix}, \qquad \tilde{W}_r = \begin{bmatrix} 1 & a_1 & a_2 & \cdots & a_{n-1} \\ 0 & 1 & a_1 & \cdots & a_{n-2} \\ \vdots & & \ddots & \ddots & \vdots \\ 0 & 0 & \cdots & 1 & a_1 \\ 0 & 0 & 0 & \cdots & 1 \end{bmatrix}^{-1}.$$

The reference gain is given by

$$k_r = -1/\big(C(A - BK)^{-1}B\big).$$

For simple problems, the eigenvalue assignment problem can be solved by introducing the elements k_i of K as unknown variables. We then compute the characteristic polynomial

$$\lambda(s) = \det(sI - A + BK)$$

and equate coefficients of equal powers of s to the coefficients of the desired characteristic polynomial

$$p(s) = s^n + p_1 s^{n-1} + \cdots + p_{n-1}s + p_n.$$

This gives a system of linear equations to determine k_i. The equations can always be solved if the system is reachable, exactly as we did in Example 6.4.

Equation (6.21), which is called Ackermann's formula [3, 4], can be used for numeric computations. It is implemented in the MATLAB function `acker`. The MATLAB function `place` is preferable for systems of high order because it is better conditioned numerically.

Example 6.5 Predator–prey
Consider the problem of regulating the population of an ecosystem by modulating the food supply. We use the predator–prey model introduced in Section 3.7. The dynamics for the system are given by

$$\frac{dH}{dt} = (r + u)H\left(1 - \frac{H}{k}\right) - \frac{aHL}{c + H}, \quad H \geq 0,$$

$$\frac{dL}{dt} = b\frac{aHL}{c + H} - dL, \quad L \geq 0.$$

We choose the following nominal parameters for the system, which correspond to the values used in previous simulations:

$$a = 3.2, \qquad b = 0.6, \qquad c = 50,$$
$$d = 0.56, \qquad k = 125 \qquad r = 1.6.$$

We take the parameter r, corresponding to the growth rate for hares, as the input to the system, which we might modulate by controlling a food source for the hares. This is reflected in our model by the term $(r + u)$ in the first equation. We choose the number of lynxes as the output of our system.

To control this system, we first linearize the system around the equilibrium point of the system (H_e, L_e), which can be determined numerically to be $x_e \approx$

(a) Initial condition response   (b) Phase portrait
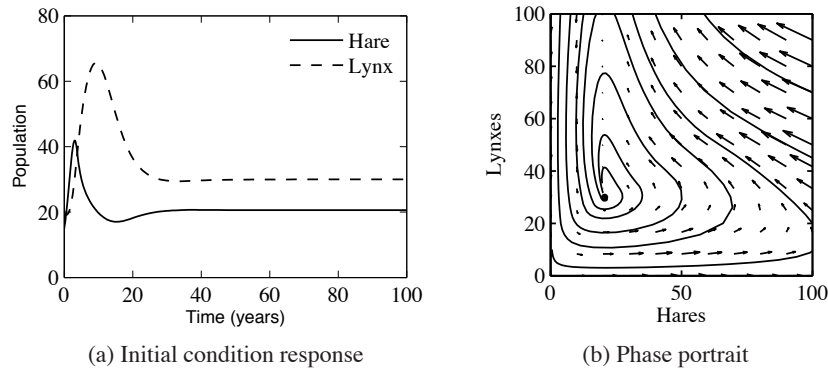
Figure 6.7: Simulation results for the controlled predator–prey system. The population of lynxes and hares as a function of time is shown in (a), and a phase portrait for the controlled system is shown in (b). Feedback is used to make the population stable at $H_e = 20.6$ and $L_e = 20$.

6.3 State Feedback Design

The location of the eigenvalues determines the behavior of the closed loop dynamics, and hence where we place the eigenvalues is the main design decision to be made. As with all other feedback design problems, there are trade-offs among the magnitude of the control inputs, the robustness of the system to perturbations and the closed loop performance of the system. In this section we examine some of these trade-offs starting with the special case of second-order systems.

Second-Order Systems

One class of systems that occurs frequently in the analysis and design of feedback systems is second-order linear differential equations. Because of their ubiquitous nature, it is useful to apply the concepts of this chapter to that specific class of systems and build more intuition about the relationship between stability and performance.

The canonical second-order system is a differential equation of the form

$$\ddot{q} + 2\zeta\omega_0\dot{q} + \omega_0^2 q = k\omega_0^2 u, \qquad y = q. \tag{6.22}$$

In state space form, this system can be represented as

$$\frac{dx}{dt} = \begin{bmatrix} 0 & \omega_0 \\ -\omega_0 & -2\zeta\omega_0 \end{bmatrix} x + \begin{bmatrix} 0 \\ k\omega_0 \end{bmatrix} u, \qquad y = \begin{bmatrix} 1 & 0 \end{bmatrix} x. \tag{6.23}$$

The eigenvalues of this system are given by

$$\lambda = -\zeta\omega_0 \pm \sqrt{\omega_0^2(\zeta^2 - 1)},$$

and we see that the origin is a stable equilibrium point if $\omega_0 > 0$ and $\zeta > 0$. Note that the eigenvalues are complex if $\zeta < 1$ and real otherwise. Equations (6.22)

and (6.23) can be used to describe many second-order systems, including damped oscillators, active filters and flexible structures, as shown in the examples below.

The form of the solution depends on the value of ζ, which is referred to as the *damping ratio* for the system. If $\zeta > 1$, we say that the system is *overdamped*, and the natural response ($u = 0$) of the system is given by

$$y(t) = \frac{\beta x_{10} + x_{20}}{\beta - \alpha} e^{-\alpha t} - \frac{\alpha x_{10} + x_{20}}{\beta - \alpha} e^{-\beta t},$$

where $\alpha = \omega_0(\zeta + \sqrt{\zeta^2 - 1})$ and $\beta = \omega_0(\zeta - \sqrt{\zeta^2 - 1})$. We see that the response consists of the sum of two exponentially decaying signals. If $\zeta = 1$, then the system is *critically damped* and solution becomes

$$y(t) = e^{-\zeta \omega_0 t}\big(x_{10} + (x_{20} + \zeta \omega_0 x_{10})t\big).$$

Note that this is still asymptotically stable as long as $\omega_0 > 0$, although the second term in the solution is increasing with time (but more slowly than the decaying exponential that is multiplying it).

Finally, if $0 < \zeta < 1$, then the solution is oscillatory and equation (6.22) is said to be *underdamped*. The parameter ω_0 is referred to as the *natural frequency* of the system, stemming from the fact that for small ζ, the eigenvalues of the system are approximately $\lambda = -\zeta \omega_0 \pm j\omega_0$. The natural response of the system is given by

$$y(t) = e^{-\zeta \omega_0 t}\left(x_{10}\cos \omega_d t + \Big(\frac{\zeta \omega_0}{\omega_d}x_{10} + \frac{1}{\omega_d}x_{20}\Big)\sin \omega_d t\right),$$

where $\omega_d = \omega_0\sqrt{1 - \zeta^2}$ is called the *damped frequency*. For $\zeta \ll 1$, $\omega_d \approx \omega_0$ defines the oscillation frequency of the solution and ζ gives the damping rate relative to ω_0.

Because of the simple form of a second-order system, it is possible to solve for the step and frequency responses in analytical form. The solution for the step response depends on the magnitude of ζ:

$$
\begin{aligned}
y(t) &= k\left(1 - e^{-\zeta \omega_0 t}\cos \omega_d t - \frac{\zeta}{\sqrt{1-\zeta^2}}e^{-\zeta \omega_0 t}\sin \omega_d t\right), \quad \zeta < 1; \\
y(t) &= k\left(1 - e^{-\omega_0 t}(1 + \omega_0 t)\right), \quad \zeta = 1; \\
y(t) &= k\left(1 - \frac{1}{2}\Big(\frac{\zeta}{\sqrt{\zeta^2-1}} + 1\Big)e^{-\omega_0 t(\zeta - \sqrt{\zeta^2-1})}\right. \\
&\qquad \left. + \frac{1}{2}\Big(\frac{\zeta}{\sqrt{\zeta^2-1}} - 1\Big)e^{-\omega_0 t(\zeta + \sqrt{\zeta^2-1})}\right), \quad \zeta > 1,
\end{aligned}
\tag{6.24}
$$

where we have taken $x(0) = 0$. Note that for the lightly damped case ($\zeta < 1$) we have an oscillatory solution at frequency ω_d.

Step responses of systems with $k = 1$ and different values of ζ are shown in Figure 6.8. The shape of the response is determined by ζ, and the speed of the response is determined by ω_0 (included in the time axis scaling): the response is faster if ω_0 is larger.

(a) Eigenvalues   (b) Step responses
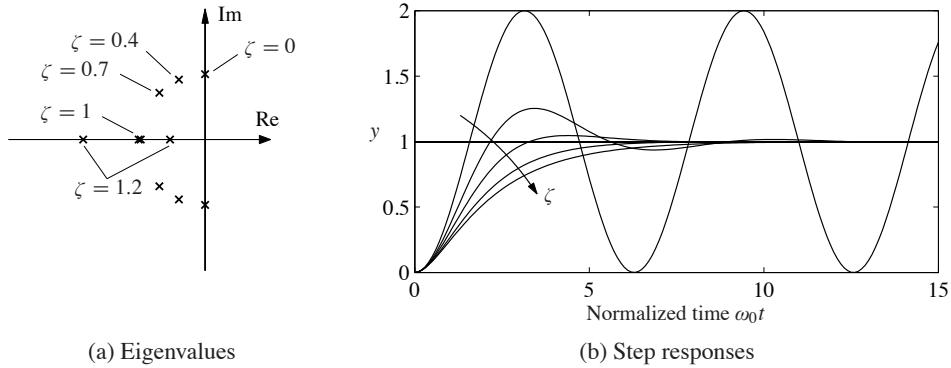
Figure 6.8: Step response for a second-order system. Normalized step responses h for the system (6.23) for $\zeta = 0, 0.4, 0.7, 1$ and 1.2. As the damping ratio is increased, the rise time of the system gets longer, but there is less overshoot. The horizontal axis is in scaled units $\omega_0 t$; higher values of ω_0 result in a faster response (rise time and settling time).

In addition to the explicit form of the solution, we can also compute the properties of the step response that were defined in Section 5.3. For example, to compute the maximum overshoot for an underdamped system, we rewrite the output as

$$y(t) = k\left(1 - \frac{1}{\sqrt{1-\zeta^2}} e^{-\zeta \omega_0 t} \sin(\omega_d t + \varphi)\right), \qquad (6.25)$$

where $\varphi = \arccos \zeta$. The maximum overshoot will occur at the first time in which the derivative of y is zero, which can be shown to be

$$M_p = e^{-\pi \zeta / \sqrt{1-\zeta^2}}.$$

Similar computations can be done for the other characteristics of a step response. Table 6.1 summarizes the calculations.

The frequency response for a second-order system can also be computed ex-

Table 6.1: Properties of the step response for a second-order system with $0 < \zeta < 1$.

Property	Value	$\zeta = 0.5$	$\zeta = 1/\sqrt{2}$	$\zeta = 1$
Steady-state value	k	k	k	k
Rise time	$T_r = 1/\omega_0 \cdot e^{\varphi/\tan\varphi}$	$1.8/\omega_0$	$2.2/\omega_0$	$2.7/\omega_0$
Overshoot	$M_p = e^{-\pi\zeta/\sqrt{1-\zeta^2}}$	16%	4%	0%
Settling time (2%)	$T_s \approx 4/\zeta\omega_0$	$8.0/\omega_0$	$5.9/\omega_0$	$5.8/\omega_0$

for a complex eigenvalue λ to be

$$\zeta = \frac{-\operatorname{Re}\lambda}{|\lambda|}.$$

We say that a complex conjugate pair of eigenvalues λ, λ^* is a *dominant pair* if it has the lowest damping ratio compared with all other eigenvalues of the system.

Assuming that a system is stable, the dominant pair of eigenvalues tends to be the most important element of the response. To see this, assume that we have a system in Jordan form with a simple Jordan block corresponding to the dominant pair of eigenvalues:

$$\frac{dz}{dt} = \begin{bmatrix} \lambda & & & & \\ & \lambda^* & & & \\ & & J_2 & & \\ & & & \ddots & \\ & & & & J_k \end{bmatrix} z + Bu, \qquad y = Cz.$$

(Note that the state z may be complex because of the Jordan transformation.) The response of the system will be a linear combination of the responses from each of the individual Jordan subsystems. As we see from Figure 6.8, for $\zeta < 1$ the subsystem with the slowest response is precisely the one with the smallest damping ratio. Hence, when we add the responses from each of the individual subsystems, it is the dominant pair of eigenvalues that will be the primary factor after the initial transients due to the other terms in the solution die out. While this simple analysis does not always hold (e.g., if some nondominant terms have larger coefficients because of the particular form of the system), it is often the case that the dominant eigenvalues determine the (step) response of the system.

The only formal requirement for eigenvalue assignment is that the system be reachable. In practice there are many other constraints because the selection of eigenvalues has a strong effect on the magnitude and rate of change of the control signal. Large eigenvalues will in general require large control signals as well as fast changes of the signals. The capability of the actuators will therefore impose constraints on the possible location of closed loop eigenvalues. These issues will be discussed in depth in Chapters 11 and 12.

We illustrate some of the main ideas using the balance system as an example.

Example 6.7 Balance system
Consider the problem of stabilizing a balance system, whose dynamics were given in Example 6.2. The dynamics are given by

$$A = \begin{bmatrix} 0 & 0 & 1 & 0 \\ 0 & 0 & 0 & 1 \\ 0 & m^2 l^2 g/\mu & -cJ_t/\mu & -\gamma J_t lm/\mu \\ 0 & M_t mgl/\mu & -clm/\mu & -\gamma M_t/\mu \end{bmatrix}, \qquad B = \begin{bmatrix} 0 \\ 0 \\ J_t/\mu \\ lm/\mu \end{bmatrix},$$

where $M_t = M + m$, $J_t = J + ml^2$, $\mu = M_t J_t - m^2 l^2$ and we have left c and γ

nonzero. We use the following parameters for the system (corresponding roughly to a human being balanced on a stabilizing cart):

$$M = 10 \text{ kg}, \qquad m = 80 \text{ kg}, \qquad c = 0.1 \text{ N s/m},$$
$$J = 100 \text{ kg m}^2/\text{s}^2, \qquad l = 1 \text{ m}, \qquad \gamma = 0.01 \text{ N m s}, \qquad g = 9.8 \text{ m/s}^2.$$

The eigenvalues of the open loop dynamics are given by $\lambda \approx 0, 4.7, -1.9 \pm 2.7i$. We have verified already in Example 6.2 that the system is reachable, and hence we can use state feedback to stabilize the system and provide a desired level of performance.

To decide where to place the closed loop eigenvalues, we note that the closed loop dynamics will roughly consist of two components: a set of fast dynamics that stabilize the pendulum in the inverted position and a set of slower dynamics that control the position of the cart. For the fast dynamics, we look to the natural period of the pendulum (in the hanging-down position), which is given by $\omega_0 = \sqrt{mgl/(J + ml^2)} \approx 2.1$ rad/s. To provide a fast response we choose a damping ratio of $\zeta = 0.5$ and try to place the first pair of eigenvalues at $\lambda_{1,2} \approx -\zeta\omega_0 \pm \omega_0 \approx -1 \pm 2i$, where we have used the approximation that $\sqrt{1 - \zeta^2} \approx 1$. For the slow dynamics, we choose the damping ratio to be 0.7 to provide a small overshoot and choose the natural frequency to be 0.5 to give a rise time of approximately 5 s. This gives eigenvalues $\lambda_{3,4} = -0.35 \pm 0.35i$.

The controller consists of a feedback on the state and a feedforward gain for the reference input. The feedback gain is given by

$$K = \begin{bmatrix} -15.6 & 1730 & -50.1 & 443 \end{bmatrix},$$

which can be computed using Theorem 6.3 or using the MATLAB `place` command. The feedforward gain is $k_r = -1/(C(A - BK)^{-1}B) = -15.5$. The step response for the resulting controller (applied to the linearized system) is given in Figure 6.11a. While the step response gives the desired characteristics, the input required (bottom left) is excessively large, almost three times the force of gravity at its peak.

To provide a more realistic response, we can redesign the controller to have slower dynamics. We see that the peak of the input force occurs on the fast time scale, and hence we choose to slow this down by a factor of 3, leaving the damping ratio unchanged. We also slow down the second set of eigenvalues, with the intuition that we should move the position of the cart more slowly than we stabilize the pendulum dynamics. Leaving the damping ratio for the slow dynamics unchanged at 0.7 and changing the frequency to 1 (corresponding to a rise time of approximately 10 s), the desired eigenvalues become

$$\lambda = \{-0.33 \pm 0.66i, \ -0.18 \pm 0.18i\}.$$

The performance of the resulting controller is shown in Figure 6.11b. ∇

As we see from this example, it can be difficult to determine where to place the eigenvalues using state feedback. This is one of the principal limitations of this

6.2 (Reachability from nonzero initial state) Extend the argument in Section 6.1 to show that if a system is reachable from an initial state of zero, it is reachable from a nonzero initial state.

6.3 (Unreachable systems) Consider the system shown in Figure 6.3. Write the dynamics of the two systems as

$$\frac{dx}{dt} = Ax + Bu, \qquad \frac{dz}{dt} = Az + Bu.$$

If x and z have the same initial condition, they will always have the same state regardless of the input that is applied. Show that this violates the definition of reachability and further show that the reachability matrix W_r is not full rank.

6.4 (Integral feedback for rejecting constant disturbances) Consider a linear system of the form

$$\frac{dx}{dt} = Ax + Bu + Fd, \qquad y = Cx$$

where u is a scalar and d is a disturbance that enters the system through a disturbance vector $F \in \mathbb{R}^n$. Assume that the matrix A is invertible and the zero frequency gain $CA^{-1}B$ is nonzero. Show that integral feedback can be used to compensate for a constant disturbance by giving zero steady-state output error even when $d \neq 0$.

6.5 (Rear-steered bicycle) A simple model for a bicycle was given by equation (3.5) in Section 3.2. A model for a bicycle with rear-wheel steering is obtained by reversing the sign of the velocity in the model. Determine the conditions under which this systems is reachable and explain any situations in which the system is not reachable.

6.6 (Characteristic polynomial for reachable canonical form) Show that the characteristic polynomial for a system in reachable canonical form is given by equation (6.7) and that

$$\frac{d^n z_k}{dt^n} + a_1 \frac{d^{n-1} z_k}{dt^{n-1}} + \cdots + a_{n-1} \frac{dz_k}{dt} + a_n z_k = \frac{d^{n-k} u}{dt^{n-k}},$$

where z_k is the kth state.

6.7 (Reachability matrix for reachable canonical form) Consider a system in reachable canonical form. Show that the inverse of the reachability matrix is given by

$$\tilde{W}_r^{-1} = \begin{bmatrix} 1 & a_1 & a_2 & \cdots & a_n \\ 0 & 1 & a_1 & \cdots & a_{n-1} \\ 0 & 0 & 1 & \ddots & \vdots \\ \vdots & & & \ddots & a_1 \\ 0 & 0 & 0 & \cdots & 1 \end{bmatrix}.$$

6.8 (Non-maintainable equilibria) Consider the normalized model of a pendulum on a cart

$$\frac{d^2x}{dt^2} = u, \qquad \frac{d^2\theta}{dt^2} = -\theta + u,$$

where x is cart position and θ is pendulum angle. Can the angle $\theta = \theta_0$ for $\theta_0 \neq 0$ be maintained?

6.9 (Eigenvalue assignment for unreachable system) Consider the system

$$\frac{dx}{dt} = \begin{bmatrix} 0 & 1 \\ 0 & 0 \end{bmatrix} x + \begin{bmatrix} 1 \\ 0 \end{bmatrix} u, \qquad y = \begin{bmatrix} 1 & 0 \end{bmatrix} x,$$

with the control law

$$u = -k_1 x_1 - k_2 x_2 + k_r r.$$

Show that eigenvalues of the system cannot be assigned to arbitrary values.

6.10 (Cayley–Hamilton theorem) Let $A \in \mathbb{R}^{n \times n}$ be a matrix with characteristic polynomial $\lambda(s) = \det(sI - A) = s^n + a_1 s^{n-1} + \cdots + a_{n-1}s + a_n$. Assume that the matrix A can be diagonalized and show that it satisfies

$$\lambda(A) = A^n + a_1 A^{n-1} + \cdots + a_{n-1}A + a_n I = 0,$$

Use the result to show that A^k, $k \geq n$, can be rewritten in terms of powers of A of order less than n.

6.11 (Motor drive) Consider the normalized model of the motor drive in Exercise 2.10. Using the following normalized parameters,

$$J_1 = 10/9, \qquad J_2 = 10, \qquad c = 0.1, \qquad k = 1, \qquad k_I = 1,$$

verify that the eigenvalues of the open loop system are $0, 0, -0.05 \pm i$. Design a state feedback that gives a closed loop system with eigenvalues $-2, -1$ and $-1 \pm i$. This choice implies that the oscillatory eigenvalues will be well damped and that the eigenvalues at the origin are replaced by eigenvalues on the negative real axis. Simulate the responses of the closed loop system to step changes in the command signal for θ_2 and a step change in a disturbance torque on the second rotor.

6.12 (Whipple bicycle model) Consider the Whipple bicycle model given by equation (3.7) in Section 3.2. Using the parameters from the companion web site, the model is unstable at the velocity $v = 5$ m/s and the open loop eigenvalues are -1.84, -14.29 and $1.30 \pm 4.60i$. Find the gains of a controller that stabilizes the bicycle and gives closed loop eigenvalues at -2, -10 and $-1 \pm i$. Simulate the response of the system to a step change in the steering reference of 0.002 rad.

6.13 (Atomic force microscope) Consider the model of an AFM in contact mode

given in Example 5.9:

$$
\frac{dx}{dt} = \begin{bmatrix} 0 & 1 & 0 & 0 \\ -k_2/(m_1+m_2) & -c_2/(m_1+m_2) & 1/m_2 & 0 \\ 0 & 0 & 0 & \omega_3 \\ 0 & 0 & -\omega_3 & -2\zeta_3\omega_3 \end{bmatrix} x + \begin{bmatrix} 0 \\ 0 \\ 0 \\ \omega_3 \end{bmatrix} u,
$$

$$
y = \frac{m_2}{m_1+m_2} \begin{bmatrix} \frac{m_1 k_2}{m_1+m_2} & \frac{m_1 c_2}{m_1+m_2} & 1 & 0 \end{bmatrix} x.
$$

Use the MATLAB script `afm_data.m` from the companion web site to generate the system matrices.

(a) Compute the reachability matrix of the system and numerically determine its rank. Scale the model by using milliseconds instead of seconds as time units. Repeat the calculation of the reachability matrix and its rank.

(b) Find a state feedback controller that gives a closed loop system with complex poles having damping ratio 0.707. Use the scaled model for the computations.

(c) Compute state feedback gains using linear quadratic control. Experiment by using different weights. Compute the gains for $q_1 = q_2 = 0, q_3 = q_4 = 1$ and $\rho_1 = 0.1$ and explain the result. Choose $q_1 = q_2 = q_3 = q_4 = 1$ and explore what happens to the feedback gains and closed loop eigenvalues when you change ρ_1. Use the scaled system for this computation.

6.14 Consider the second-order system

$$
\frac{d^2 y}{dt^2} + 0.5\frac{dy}{dt} + y = a\frac{du}{dt} + u.
$$

Let the initial conditions be zero.

(a) Show that the initial slope of the unit step response is a. Discuss what it means when $a < 0$.

(b) Show that there are points on the unit step response that are invariant with a. Discuss qualitatively the effect of the parameter a on the solution.

(c) Simulate the system and explore the effect of a on the rise time and overshoot.

6.15 (Bryson's rule) Bryson and Ho [47] have suggested the following method for choosing the matrices Q_x and Q_u in equation (6.26). Start by choosing Q_x and Q_u as diagonal matrices whose elements are the inverses of the squares of the maxima of the corresponding variables. Then modify the elements to obtain a compromise among response time, damping and control effort. Apply this method to the motor drive in Exercise 6.11. Assume that the largest values of the φ_1 and φ_2 are 1, the largest values of $\dot{\varphi}_1$ and $\dot{\varphi}_2$ are 2 and the largest control signal is 10. Simulate the closed loop system for $\varphi_2(0) = 1$ and all other states are initialized to 0. Explore the effects of different values of the diagonal elements for Q_x and Q_u.

a system in observable canonical form, which is given by

$$
W_o = \begin{bmatrix}
1 & 0 & 0 & \cdots & 0 \\
-a_1 & 1 & 0 & \cdots & 0 \\
-a_1^2 - a_1 a_2 & -a_1 & 1 & & 0 \\
\vdots & \vdots & & \ddots & \vdots \\
* & * & & \cdots & 1
\end{bmatrix},
$$

where * represents an entry whose exact value is not important. The rows of this matrix are linearly independent (since it is lower triangular), and hence W_o is full rank. A straightforward but tedious calculation shows that the inverse of the observability matrix has a simple form given by

$$
W_o^{-1} = \begin{bmatrix}
1 & 0 & 0 & \cdots & 0 \\
a_1 & 1 & 0 & \cdots & 0 \\
a_2 & a_1 & 1 & \cdots & 0 \\
\vdots & \vdots & & \ddots & \vdots \\
a_{n-1} & a_{n-2} & a_{n-3} & \cdots & 1
\end{bmatrix}.
$$

As in the case of reachability, it turns out that if a system is observable then there always exists a transformation T that converts the system into observable canonical form. This is useful for proofs since it lets us assume that a system is in observable canonical form without any loss of generality. The observable canonical form may be poorly conditioned numerically.

7.2 State Estimation

Having defined the concept of observability, we now return to the question of how to construct an observer for a system. We will look for observers that can be represented as a linear dynamical system that takes the inputs and outputs of the system we are observing and produces an estimate of the system's state. That is, we wish to construct a dynamical system of the form

$$
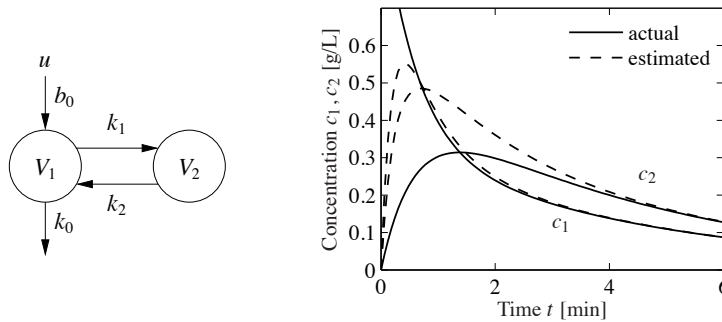\frac{d\hat{x}}{dt} = F\hat{x} + Gu + Hy,
$$

where u and y are the input and output of the original system and $\hat{x} \in \mathbb{R}^n$ is an estimate of the state with the property that $\hat{x}(t) \to x(t)$ as $t \to \infty$.

The Observer

We consider the system in equation (7.1) with D set to zero to simplify the exposition:

$$
\frac{dx}{dt} = Ax + Bu, \qquad y = Cx. \tag{7.6}
$$

Figure 7.4: Observer for a two compartment system. A two compartment model is shown on the left. The observer measures the input concentration u and output concentration $y = c_1$ to determine the compartment concentrations, shown on the right. The true concentrations are shown by solid lines and the estimates generated by the observer by dashed lines.

Let the desired characteristic polynomial of the observer be $s^2 + p_1 s + p_2$, and equation (7.11) gives the observer gain

$$
L = \begin{bmatrix} 1 & 0 \\ -k_0 - k_1 & k_1 \end{bmatrix}^{-1} \begin{bmatrix} 1 & 0 \\ k_0 + k_1 + k_2 & 1 \end{bmatrix}^{-1} \begin{bmatrix} p_1 - k_0 - k_1 - k_2 \\ p_2 - k_0 k_2 \end{bmatrix}
$$

$$
= \begin{bmatrix} p_1 - k_0 - k_1 - k_2 \\ (p_2 - p_1 k_2 + k_1 k_2 + k_2^2)/k_1 \end{bmatrix}.
$$

Notice that the observability condition $k_1 \neq 0$ is essential. The behavior of the observer is illustrated by the simulation in Figure 7.4b. Notice how the observed concentrations approach the true concentrations. ∇

The observer is a dynamical system whose inputs are the process input u and the process output y. The rate of change of the estimate is composed of two terms. One term, $A\hat{x} + Bu$, is the rate of change computed from the model with $\hat{x}$ substituted for x. The other term, $L(y - \hat{y})$, is proportional to the difference $e = y - \hat{y}$ between measured output y and its estimate $\hat{y} = C\hat{x}$. The observer gain L is a matrix that tells how the error e is weighted and distributed among the states. The observer thus combines measurements with a dynamical model of the system. A block diagram of the observer is shown in Figure 7.5.

Computing the Observer Gain

For simple low-order problems it is convenient to introduce the elements of the observer gain L as unknown parameters and solve for the values required to give the desired characteristic polynomial, as illustrated in the following example.

Example 7.3 Vehicle steering
The normalized linear model for vehicle steering derived in Examples 5.12 and 6.4 gives the following state space model dynamics relating lateral path deviation y to

to command signals and disturbances are decoupled. Disturbance responses are governed by the observer and the state feedback, while the response to command signals is governed by the trajectory generator (feedforward).

For an analytic description we start with the full nonlinear dynamics of the process

$$\frac{dx}{dt} = f(x, u), \qquad y = h(x, u). \tag{7.23}$$

Assume that the trajectory generator is able to compute a desired trajectory (x_d, u_{ff}) that satisfies the dynamics (7.23) and satisfies $r = h(x_d, u_{\text{ff}})$. To design the controller, we construct the error system. Let $z = x - x_d$ and $v = u - u_{\text{ff}}$ and compute the dynamics for the error:

$$\dot{z} = \dot{x} - \dot{x}_d = f(x, u) - f(x_d, u_{\text{ff}})$$
$$= f(z + x_d, v + u_{\text{ff}}) - f(x_d, u_{\text{ff}}) =: F(z, v, x_d(t), u_{\text{ff}}(t)).$$

In general, this system is time-varying. Note that $z = -e$ in Figure 7.10 due to the convention of using negative feedback in the block diagram.

For trajectory tracking, we can assume that e is small (if our controller is doing a good job), and so we can linearize around $z = 0$:

$$\frac{dz}{dt} \approx A(t)z + B(t)v, \quad A(t) = \left.\frac{\partial F}{\partial z}\right|_{(x_d(t), u_{\text{ff}}(t))}, \quad B(t) = \left.\frac{\partial F}{\partial v}\right|_{(x_d(t), u_{\text{ff}}(t))}.$$

It is often the case that $A(t)$ and $B(t)$ depend only on x_d, in which case it is convenient to write $A(t) = A(x_d)$ and $B(t) = B(x_d)$.

Assume now that x_d and u_{ff} are either constant or slowly varying (with respect to the performance criterion). This allows us to consider just the (constant) linear system given by $(A(x_d), B(x_d))$. If we design a state feedback controller $K(x_d)$ for each x_d, then we can regulate the system using the feedback

$$v = -K(x_d)z.$$

Substituting back the definitions of e and v, our controller becomes

$$u = -K(x_d)(x - x_d) + u_{\text{ff}}.$$

This form of controller is called a *gain scheduled* linear controller with *feedforward* u_{ff}.

Finally, we consider the observer. The full nonlinear dynamics can be used for the prediction portion of the observer and the linearized system for the correction term:

$$\frac{d\hat{x}}{dt} = f(\hat{x}, u) + L(\hat{x})(y - h(\hat{x}, u)),$$

where $L(\hat{x})$ is the observer gain obtained by linearizing the system around the currently estimated state. This form of the observer is known as an *extended Kalman filter* and has proved to be a very effective means of estimating the state of a nonlinear system.

Theorem 7.3:

$$\frac{d\hat{x}}{dt} = A\hat{x} + Bu + L(y - C\hat{x}), \qquad u = -K\hat{x} + k_r r.$$

Introducing the states x and $\tilde{x} = x - \hat{x}$, the closed loop system can be written as

$$\frac{d}{dt} \begin{bmatrix} x \\ \tilde{x} \end{bmatrix} = \begin{bmatrix} A - BK & BK \\ 0 & A - LC \end{bmatrix} \begin{bmatrix} x \\ \tilde{x} \end{bmatrix} + \begin{bmatrix} Bk_r \\ 0 \end{bmatrix} r, \qquad y = \begin{bmatrix} C & 0 \end{bmatrix} x,$$

which is a Kalman decomposition like the one shown in Figure 7.12b with only two subsystems Σ_{ro} and $\Sigma_{\bar{r}o}$. The subsystem Σ_{ro}, with state x, is reachable and observable, and the subsystem $\Sigma_{\bar{r}o}$, with state $\tilde{x}$, is not reachable but observable. It is natural that the state $\tilde{x}$ is not reachable from the reference signal r because it would not make sense to design a system where changes in the command signal could generate observer errors. The relationship between the reference r and the output y is given by

$$\frac{dx}{dt} = (A - BK)x + Bk_r r, \qquad y = Cx,$$

which is the same relationship as for a system with full state feedback. ∇

Computer Implementation

The controllers obtained so far have been described by ordinary differential equations. They can be implemented directly using analog components, whether electronic circuits, hydraulic valves or other physical devices. Since in modern engineering applications most controllers are implemented using computers, we will briefly discuss how this can be done.

A computer-controlled system typically operates periodically: every cycle, signals from the sensors are sampled and converted to digital form by the A/D converter, the control signal is computed and the resulting output is converted to analog form for the actuators, as shown in Figure 7.13. To illustrate the main principles of how to implement feedback in this environment, we consider the controller described by equations (7.14) and (7.15), i.e.,

$$\frac{d\hat{x}}{dt} = A\hat{x} + Bu + L(y - C\hat{x}), \qquad u = -K\hat{x} + k_r r.$$

The second equation consists only of additions and multiplications and can thus be implemented directly on a computer. The first equation can be implemented by approximating the derivative by a difference

$$\frac{d\hat{x}}{dt} \approx \frac{\hat{x}(t_{k+1}) - \hat{x}(t_k)}{h} = A\hat{x}(t_k) + Bu(t_k) + L\big(y(t_k) - C\hat{x}(t_k)\big),$$

where t_k are the sampling instants and $h = t_{k+1} - t_k$ is the sampling period. Rewriting the equation to isolate $\hat{x}(t_{k+1})$, we get the difference equation

$$\hat{x}(t_{k+1}) = \hat{x}(t_k) + h\big(A\hat{x}(t_k) + Bu(t_k) + L\big(y(t_k) - C\hat{x}(t_k)\big)\big). \qquad (7.29)$$
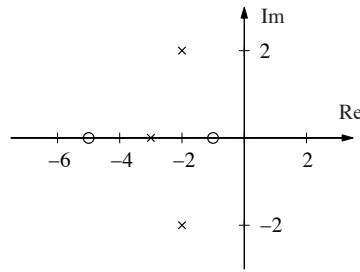
Figure 8.4: A pole zero diagram for a transfer function with zeros at -5 and -1 and poles at -3 and $-2\pm2j$. The circles represent the locations of the zeros, and the crosses the locations of the poles. A complete characterization requires we also specify the gain of the system.

model. One easy way to see this is to notice that the value of $G(s)$ is unbounded when s is an eigenvalue of a system since this is precisely the set of points where the characteristic polynomial $\lambda(s) = \det(sI - A) = 0$ (and hence $sI - A$ is noninvertible). It follows that the poles of a state space system depend only on the matrix A, which represents the intrinsic dynamics of the system. We say that a transfer function is stable if all of its poles have negative real part.

To find the zeros of a state space system, we observe that the zeros are complex numbers s such that the input $u(t) = u_0 e^{st}$ gives zero output. Inserting the pure exponential response $x(t) = x_0 e^{st}$ and $y(t) = 0$ in equation (8.2) gives

$$se^{st}x_0 = Ax_0e^{st} + Bu_0e^{st} \qquad 0 = Ce^{st}x_0 + De^{st}u_0,$$

which can be written as

$$\begin{bmatrix} A - sI & B \\ C & D \end{bmatrix} \begin{bmatrix} x_0 \\ u_0 \end{bmatrix} e^{st} = 0.$$

This equation has a solution with nonzero x_0, u_0 only if the matrix on the left does not have full rank. The zeros are thus the values s such that the matrix

$$\begin{bmatrix} A - sI & B \\ C & D \end{bmatrix} \tag{8.17}$$

looses rank.

Since the zeros depend on A, B, C and D, they therefore depend on how the inputs and outputs are coupled to the states. Notice in particular that if the matrix B has full row rank, then the matrix in equation (8.17) has n linearly independent rows for all values of s. Similarly there are n linearly independent columns if the matrix C has full column rank. This implies that systems where the matrix B or C is square and full rank do not have zeros. In particular it means that a system has no zeros if it is fully actuated (each state can be controlled independently) or if the full state is measured.

A convenient way to view the poles and zeros of a transfer function is through a *pole zero diagram*, as shown in Figure 8.4. In this diagram, each pole is marked with a cross, and each zero with a circle. If there are multiple poles or zeros at a

(a) Cart–pendulum system

(b) Pole zero diagram for $H_{\theta F}$

(c) Pole zero diagram for H_{pF}
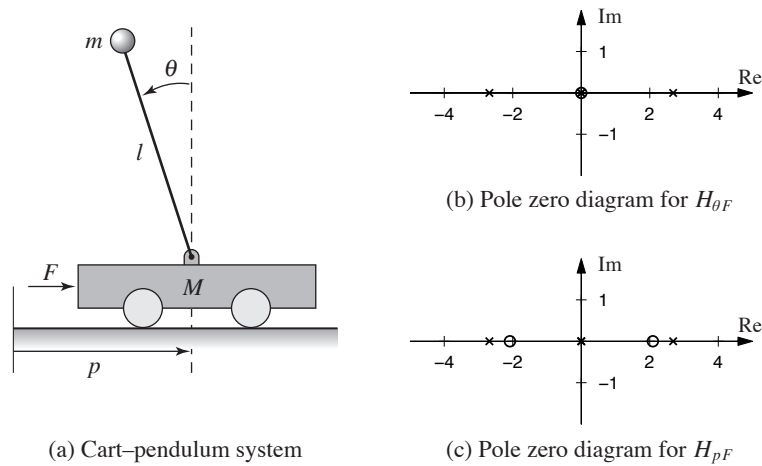
Figure 8.5: Poles and zeros for a balance system. The balance system (a) can be modeled around its vertical equilibrium point by a fourth order linear system. The poles and zeros for the transfer functions $H_{\theta F}$ and H_{pF} are shown in (b) and (c), respectively.

fixed location, these are often indicated with overlapping crosses or circles (or other annotations). Poles in the left half-plane correspond to stable modes of the system, and poles in the right half-plane correspond to unstable modes. We thus call a pole in the left-half plane a *stable pole* and a pole in the right-half plane an *unstable pole*. A similar terminology is used for zeros, even though the zeros do not directly related to stability or instability of the system. Notice that the gain must also be given to have a complete description of the transfer function.

Example 8.5 Balance system
Consider the dynamics for a balance system, shown in Figure 8.5. The transfer function for a balance system can be derived directly from the second-order equations, given in Example 2.1:

$$M_t \frac{d^2 p}{dt^2} - ml \frac{d^2\theta}{dt^2} \cos\theta + c\frac{dp}{dt} + ml \sin\theta \left(\frac{d\theta}{dt}\right)^2 = F,$$

$$-ml \cos\theta \frac{d^2 p}{dt^2} + J_t \frac{d^2\theta}{dt^2} - mgl \sin\theta + \gamma\dot\theta = 0.$$

If we assume that θ and $\dot\theta$ are small, we can approximate this nonlinear system by a set of linear second-order differential equations,

$$M_t \frac{d^2 p}{dt^2} - ml \frac{d^2\theta}{dt^2} + c\frac{dp}{dt} = F,$$

$$-ml \frac{d^2 p}{dt^2} + J_t \frac{d^2\theta}{dt^2} + \gamma\frac{d\theta}{dt} - mgl\theta = 0.$$

and

$$G_{ur}(s) = \frac{k_r}{1 + K G_{\hat{x}u}(s)} = \frac{k_1(s^2 + l_1 s + l_2)}{s^2 + s(\gamma k_1 + k_2 + l_1) + k_1 + l_2 + k_2 l_1 - \gamma k_2 l_2},$$

where k_1 and k_2 are the controller gains.

Finally, we compute the full closed loop dynamics. We begin by deriving the transfer function for the process $P(s)$. We can compute this directly from the state space description of the dynamics, which was given in Example 5.12. Using that description, we have

$$P(s) = G_{yu}(s) = C(sI - A)^{-1}B + D = \begin{bmatrix} 1 & 0 \end{bmatrix} \begin{bmatrix} s & -1 \\ 0 & s \end{bmatrix}^{-1} \begin{bmatrix} \gamma \\ 1 \end{bmatrix} = \frac{\gamma s + 1}{s^2}.$$

The transfer function for the full closed loop system between the input r and the output y is then given by

$$G_{yr} = \frac{k_r P(s)}{1 + P(s)G_{uy}(s)} = \frac{k_1(\gamma s + 1)}{s^2 + (k_1 \gamma + k_2)s + k_1}.$$

Note that the observer gains l_1 and l_2 do not appear in this equation. This is because we are considering steady-state analysis and, in steady state, the estimated state exactly tracks the state of the system assuming perfect models. We will return to this example in Chapter 12 to study the robustness of this particular approach.   ∇

Pole/Zero Cancellations

Because transfer functions are often polynomials in s, it can sometimes happen that the numerator and denominator have a common factor, which can be canceled. Sometimes these cancellations are simply algebraic simplifications, but in other situations they can mask potential fragilities in the model. In particular, if a pole/zero cancellation occurs because terms in separate blocks that just happen to coincide, the cancellation may not occur if one of the systems is slightly perturbed. In some situations this can result in severe differences between the expected behavior and the actual behavior.

To illustrate when we can have pole/zero cancellations, consider the block diagram in Figure 8.7 with $F = 1$ (no feedforward compensation) and C and P given by

$$C(s) = \frac{n_c(s)}{d_c(s)}, \qquad P(s) = \frac{n_p(s)}{d_p(s)}.$$

The transfer function from r to e is then given by

$$G_{er}(s) = \frac{1}{1 + PC} = \frac{d_c(s)d_p(s)}{d_c(s)d_p(s) + n_c(s)n_p(s)}.$$

If there are common factors in the numerator and denominator polynomials, then these terms can be factored out and eliminated from both the numerator and denominator. For example, if the controller has a zero at $s = -a$ and the process has

a pole at $s = -a$, then we will have

$$G_{er}(s) = \frac{(s+a)d_c'(s)d_p(s)}{(s+a)d_c(s)d_p'(s) + (s+a)n_c'(s)n_p(s)} = \frac{d_c'(s)d_p(s)}{d_c(s)d_p'(s) + n_c'(s)n_p(s)},$$

where $n_c'(s)$ and $d_p'(s)$ represent the relevant polynomials with the term $s + a$ factored out. In the case when $a < 0$ (so that the zero or pole is in the right half-plane), we see that there is no impact on the transfer function G_{er}.

Suppose instead that we compute the transfer function from d to e, which represents the effect of a disturbance on the error between the reference and the output. This transfer function is given by

$$G_{ed}(s) = \frac{d_c'(s)n_p(s)}{(s+a)d_c(s)d_p'(s) + (s+a)n_c'(s)n_p(s)}.$$

Notice that if $a < 0$, then the pole is in the right half-plane and the transfer function G_{ed} is *unstable*. Hence, even though the transfer function from r to e appears to be okay (assuming a perfect pole/zero cancellation), the transfer function from d to e can exhibit unbounded behavior. This unwanted behavior is typical of an *unstable pole/zero cancellation*.

It turns out that the cancellation of a pole with a zero can also be understood in terms of the state space representation of the systems. Reachability or observability is lost when there are cancellations of poles and zeros (Exercise 8.11). A consequence is that the transfer function represents the dynamics only in the reachable and observable subspace of a system (see Section 7.5).

Example 8.7 Cruise control
The input/output response from throttle to velocity for the linearized model for a car has the transfer function $G(s) = b/(s-a), a < 0$. A simple (but not necessarily good) way to design a PI controller is to choose the parameters of the PI controller so that the controller zero at $s = -k_i/k_p$ cancels the process pole at $s = a$. The transfer function from reference to velocity is $G_{vr}(s) = bk_p/(s+bk_p)$, and control design is simply a matter of choosing the gain k_p. The closed loop system dynamics are of first order with the time constant $1/bk_p$.

Figure 8.10 shows the velocity error when the car encounters an increase in the road slope. A comparison with the controller used in Figure 3.3b (reproduced in dashed curves) shows that the controller based on pole/zero cancellation has very poor performance. The velocity error is larger, and it takes a long time to settle.

Notice that the control signal remains practically constant after $t = 15$ even if the error is large after that time. To understand what happens we will analyze the system. The parameters of the system are $a = -0.0101$ and $b = 1.32$, and the controller parameters are $k_p = 0.5$ and $k_i = 0.0051$. The closed loop time constant is $1/(bk_p) = 2.5$ s, and we would expect that the error would settle in about 10 s (4 time constants). The transfer functions from road slope to velocity and control
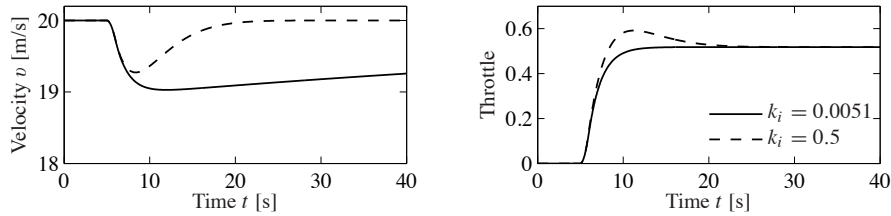
Figure 8.10: Car with PI cruise control encountering a sloping road. The velocity error is shown on the left and the throttle is shown on the right. Results with a PI controller with $k_p = 0.5$ and $k_i = 0.0051$, where the process pole $s = -0.0101$, is shown by solid lines, and a controller with $k_p = 0.5$ and $k_i = 0.5$ is shown by dashed lines. Compare with Figure 3.3b.

signals are

$$G_{v\theta}(s) = \frac{b_g k_p s}{(s-a)(s+bk_p)}, \qquad G_{u\theta}(s) = \frac{bk_p}{s+bk_p}.$$

Notice that the canceled mode $s = a = -0.0101$ appears in $G_{v\theta}$ but not in $G_{u\theta}$. The reason why the control signal remains constant is that the controller has a zero at $s = -0.0101$, which cancels the slowly decaying process mode. Notice that the error would diverge if the canceled pole was unstable.   ∇

The lesson we can learn from this example is that it is a bad idea to try to cancel unstable or slow process poles. A more detailed discussion of pole/zero cancellations is given in Section 12.4.

Algebraic Loops

When analyzing or simulating a system described by a block diagram, it is necessary to form the differential equations that describe the complete system. In many cases the equations can be obtained by combining the differential equations that describe each subsystem and substituting variables. This simple procedure cannot be used when there are closed loops of subsystems that all have a direct connection between inputs and outputs, known as an *algebraic loop*.

To see what can happen, consider a system with two blocks, a first-order nonlinear system,

$$\frac{dx}{dt} = f(x, u), \qquad y = h(x), \tag{8.21}$$

and a proportional controller described by $u = -ky$. There is no direct term since the function h does not depend on u. In that case we can obtain the equation for the closed loop system simply by replacing u by $-ky$ in (8.21) to give

$$\frac{dx}{dt} = f(x, -ky), \qquad y = h(x).$$

Such a procedure can easily be automated using simple formula manipulation.

The situation is more complicated if there is a direct term. If $y = h(x, u)$, then replacing u by $-ky$ gives

$$\frac{dx}{dt} = f(x, -ky), \qquad y = h(x, -ky).$$

To obtain a differential equation for x, the algebraic equation $y = h(x, -ky)$ must be solved to give $y = \alpha(x)$, which in general is a complicated task.

When algebraic loops are present, it is necessary to solve algebraic equations to obtain the differential equations for the complete system. Resolving algebraic loops is a nontrivial problem because it requires the symbolic solution of algebraic equations. Most block diagram-oriented modeling languages cannot handle algebraic loops, and they simply give a diagnosis that such loops are present. In the era of analog computing, algebraic loops were eliminated by introducing fast dynamics between the loops. This created differential equations with fast and slow modes that are difficult to solve numerically. Advanced modeling languages like Modelica use several sophisticated methods to resolve algebraic loops.

8.4 The Bode Plot

The frequency response of a linear system can be computed from its transfer function by setting $s = i\omega$, corresponding to a complex exponential

$$u(t) = e^{i\omega t} = \cos(\omega t) + i\sin(\omega t).$$

The resulting output has the form

$$y(t) = G(i\omega)e^{i\omega t} = Me^{i(\omega t + \varphi)} = M\cos(\omega t + \varphi) + iM\sin(\omega t + \varphi),$$

where M and φ are the gain and phase of G:

$$M = |G(i\omega)|, \qquad \varphi = \arctan\frac{\operatorname{Im} G(i\omega)}{\operatorname{Re} G(i\omega)}.$$

The phase of G is also called the *argument* of G, a term that comes from the theory of complex variables.

It follows from linearity that the response to a single sinusoid (sin or cos) is amplified by M and phase-shifted by φ. Note that $-\pi < \varphi \leq \pi$, so the arctangent must be taken respecting the signs of the numerator and denominator. It will often be convenient to represent the phase in degrees rather than radians. We will use the notation $\angle G(i\omega)$ for the phase in degrees and $\arg G(i\omega)$ for the phase in radians. In addition, while we always take $\arg G(i\omega)$ to be in the range $(-\pi, \pi]$, we will take $\angle G(i\omega)$ to be continuous, so that it can take on values outside the range of $-180°$ to $180°$.

The frequency response $G(i\omega)$ can thus be represented by two curves: the gain curve and the phase curve. The *gain curve* gives $|G(i\omega)|$ as a function of frequency ω, and the *phase curve* gives $\angle G(i\omega)$. One particularly useful way of drawing these
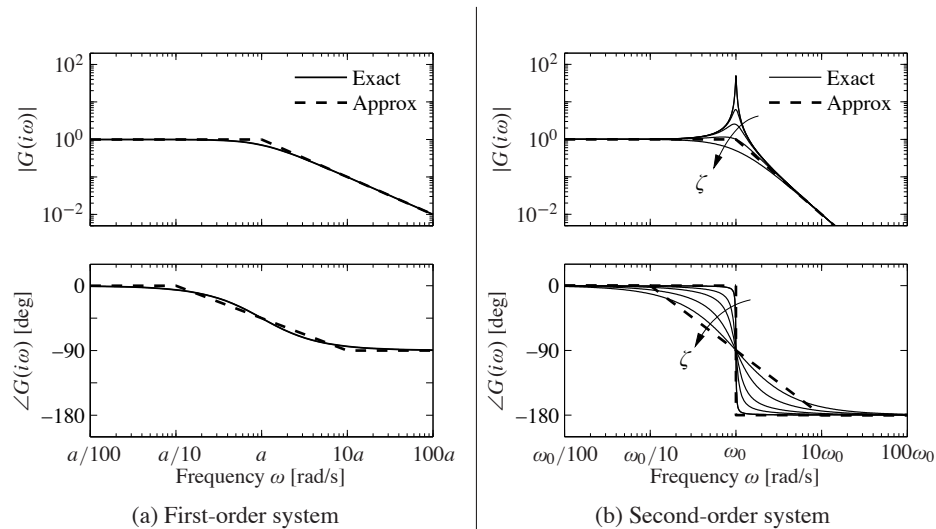
Figure 8.13: Bode plots for first- and second-order systems. (a) The first-order system $G(s) = a/(s + a)$ can be approximated by asymptotic curves (dashed) in both the gain and the frequency, with the breakpoint in the gain curve at $\omega = a$ and the phase decreasing by 90° over a factor of 100 in frequency. (b) The second-order system $G(s) = \omega_0^2/(s^2 + 2\zeta\omega_0 s + \omega_0^2)$ has a peak at frequency a and then a slope of -2 beyond the peak; the phase decreases from 0° to -180°. The height of the peak and the rate of change of phase depending on the damping ratio ζ ($\zeta = 0.02, 0.1, 0.2, 0.5$ and 1.0 shown).

the following straight lines

$$\log |G(i\omega)| \approx \begin{cases} 0 & \text{if } \omega < a \\ \log a - \log \omega & \text{if } \omega > a, \end{cases}$$

$$\angle G(i\omega) \approx \begin{cases} 0 & \text{if } \omega < a/10 \\ -45 - 45(\log \omega - \log a) & a/10 < \omega < 10a \\ -90 & \text{if } \omega > 10a. \end{cases}$$

The approximate gain curve consists of a horizontal line up to frequency $\omega = a$, called the *breakpoint* or *corner frequency*, after which the curve is a line of slope -1 (on a log-log scale). The phase curve is zero up to frequency $a/10$ and then decreases linearly by 45°/decade up to frequency $10a$, at which point it remains constant at 90°. Notice that a first-order system behaves like a constant for low frequencies and like an integrator for high frequencies; compare with the Bode plot in Figure 8.12.

Finally, consider the transfer function for a second-order system,

$$G(s) = \frac{\omega_0^2}{s^2 + 2\omega_0\zeta s + \omega_0^2},$$

for which we have

$$\log |G(i\omega)| = 2 \log \omega_0 - \frac{1}{2} \log \left(\omega^4 + 2\omega_0^2 \omega^2 (2\zeta^2 - 1) + \omega_0^4 \right),$$

$$\angle G(i\omega) = -\frac{180}{\pi} \arctan \frac{2\zeta \omega_0 \omega}{\omega_0^2 - \omega^2}.$$

The gain curve has an asymptote with zero slope for $\omega \ll \omega_0$. For large values of ω the gain curve has an asymptote with slope -2. The largest gain $Q = \max_\omega |G(i\omega)| \approx 1/(2\zeta)$, called the *Q-value*, is obtained for $\omega \approx \omega_0$. The phase is zero for low frequencies and approaches $180°$ for large frequencies. The curves can be approximated with the following piecewise linear expressions

$$\log |G(i\omega)| \approx \begin{cases} 0 & \text{if } \omega \ll \omega_0 \\ 2 \log \omega_0 - 2 \log \omega & \text{if } \omega \gg \omega_0, \end{cases}$$

$$\angle G(i\omega) \approx \begin{cases} 0 & \text{if } \omega \ll \omega_0 \\ -180 & \text{if } \omega \gg \omega_0. \end{cases}$$

The Bode plot is shown in Figure 8.13b. Note that the asymptotic approximation is poor near $\omega = \omega_0$ and that the Bode plot depends strongly on ζ near this frequency.

Given the Bode plots of the basic functions, we can now sketch the frequency response for a more general system. The following example illustrates the basic idea.

Example 8.8 Asymptotic approximation for a transfer function
Consider the transfer function given by

$$G(s) = \frac{k(s + b)}{(s + a)(s^2 + 2\zeta\omega_0 s + \omega_0^2)}, \qquad a \ll b \ll \omega_0.$$
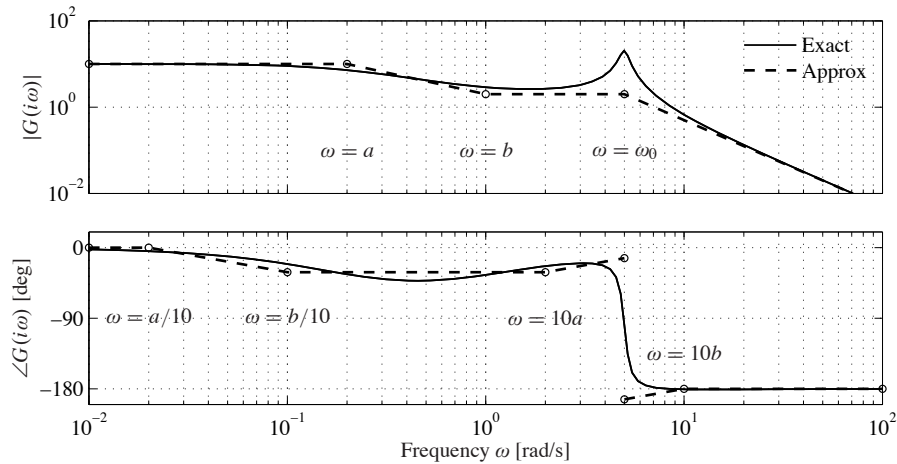
The Bode plot for this transfer function appears in Figure 8.14, with the complete transfer function shown as a solid line and the asymptotic approximation shown as a dashed line.

We begin with the gain curve. At low frequency, the magnitude is given by

$$G(0) = \frac{kb}{a\omega_0^2}.$$

When we reach $\omega = a$, the effect of the pole begins and the gain decreases with slope -1. At $\omega = b$, the zero comes into play and we increase the slope by 1, leaving the asymptote with net slope 0. This slope is used until the effect of the second-order pole is seen at $\omega = \omega_c$, at which point the asymptote changes to slope -2. We see that the gain curve is fairly accurate except in the region of the peak due to the second-order pole (since for this case ζ is reasonably small).

The phase curve is more complicated since the effect of the phase stretches out much further. The effect of the pole begins at $\omega = a/10$, at which point we change from phase 0 to a slope of $-45°$/decade. The zero begins to affect the phase at $\omega = b/10$, producing a flat section in the phase. At $\omega = 10a$ the phase
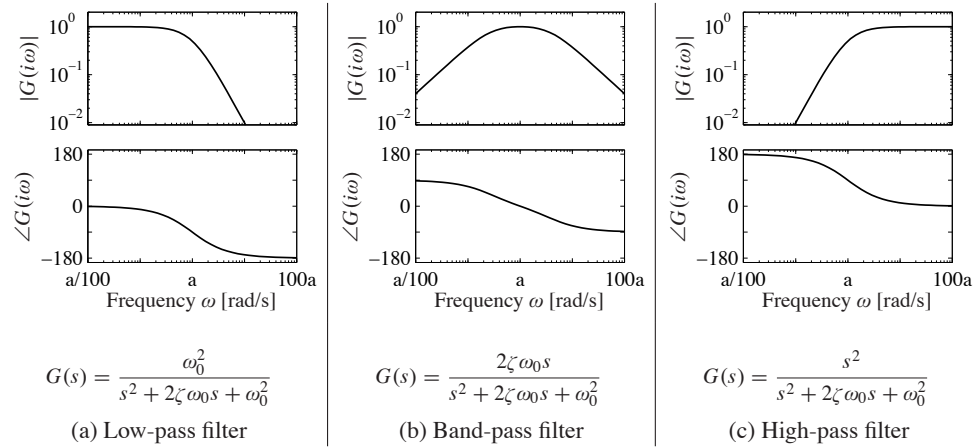
Figure 8.14: Asymptotic approximation to a Bode plot. The thin line is the Bode plot for the transfer function $G(s) = k(s + b)/(s + a)(s^2 + 2\zeta\omega_0 s + \omega_0^2)$, where $a \ll b \ll \omega_0$. Each segment in the gain and phase curves represents a separate portion of the approximation, where either a pole or a zero begins to have effect. Each segment of the approximation is a straight line between these points at a slope given by the rules for computing the effects of poles and zeros.

contributions from the pole end, and we are left with a slope of $+45°$/decade (from the zero). At the location of the second-order pole, $s \approx i\omega_c$, we get a jump in phase of $-180°$. Finally, at $\omega = 10b$ the phase contributions of the zero end, and we are left with a phase of -180 degrees. We see that the straight-line approximation for the phase is not as accurate as it was for the gain curve, but it does capture the basic features of the phase changes as a function of frequency. ∇

The Bode plot gives a quick overview of a system. Since any signal can be decomposed into a sum of sinusoids, it is possible to visualize the behavior of a system for different frequency ranges. The system can be viewed as a filter that can change the amplitude (and phase) of the input signals according to the frequency response. For example, if there are frequency ranges where the gain curve has constant slope and the phase is close to zero, the action of the system for signals with these frequencies can be interpreted as a pure gain. Similarly, for frequencies where the slope is $+1$ and the phase close to $90°$, the action of the system can be interpreted as a differentiator, as shown in Figure 8.12.

Three common types of frequency responses are shown in Figure 8.15. The system in Figure 8.15a is called a *low-pass filter* because the gain is constant for low frequencies and drops for high frequencies. Notice that the phase is zero for low frequencies and $-180°$ for high frequencies. The systems in Figure 8.15b and c are called a *band-pass filter* and *high-pass filter* for similar reasons.

To illustrate how different system behaviors can be read from the Bode plots we consider the band-pass filter in Figure 8.15b. For frequencies around $\omega = \omega_0$, the signal is passed through with no change in gain. However, for frequencies well

$$G(s) = \frac{\omega_0^2}{s^2 + 2\zeta\omega_0 s + \omega_0^2}$$

(a) Low-pass filter

$$G(s) = \frac{2\zeta\omega_0 s}{s^2 + 2\zeta\omega_0 s + \omega_0^2}$$

(b) Band-pass filter

$$G(s) = \frac{s^2}{s^2 + 2\zeta\omega_0 s + \omega_0^2}$$

(c) High-pass filter

Figure 8.15: Bode plots for low-pass, band-pass and high-pass filters. The top plots are the gain curves and the bottom plots are the phase curves. Each system passes frequencies in a different range and attenuates frequencies outside of that range.

below or well above ω_0, the signal is attenuated. The phase of the signal is also affected by the filter, as shown in the phase curve. For frequencies below $a/100$ there is a phase lead of $90°$, and for frequencies above $100a$ there is a phase lag of $90°$. These actions correspond to differentiation and integration of the signal in these frequency ranges.

Example 8.9 Transcriptional regulation

Consider a genetic circuit consisting of a single gene. We wish to study the response of the protein concentration to fluctuations in the mRNA dynamics. We consider two cases: a *constitutive promoter* (no regulation) and self-repression (negative feedback), illustrated in Figure 8.16. The dynamics of the system are given by

$$\frac{dm}{dt} = \alpha(p) - \gamma m - u, \qquad \frac{dp}{dt} = \beta m - \delta p,$$

where u is a disturbance term that affects mRNA transcription.

For the case of no feedback we have $\alpha(p) = \alpha_0$, and the system has an equilibrium point at $m_e = \alpha_0/\gamma$, $p_e = \beta\alpha_0/(\delta\gamma)$. The transfer function from v to p is given by
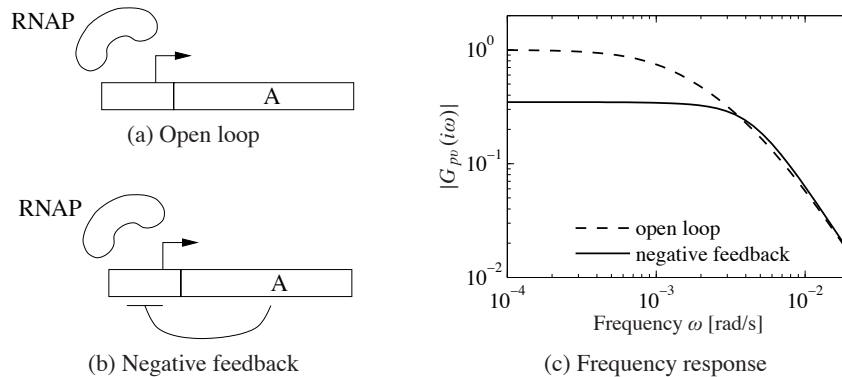
$$G_{pv}^{\text{ol}}(s) = \frac{-\beta}{(s + \gamma)(s + \delta)}.$$

For the case of negative regulation, we have

$$\alpha(p) = \frac{\alpha_1}{1 + kp^n} + \alpha_0,$$

and the equilibrium points satisfy

$$m_e = \frac{\delta}{\beta}p_e, \qquad \frac{\alpha}{1 + kp_e^n} + \alpha_0 = \gamma m_e = \frac{\gamma\delta}{\beta}p_e.$$

(a) Open loop

(b) Negative feedback

(c) Frequency response

Figure 8.16: Noise attenuation in a genetic circuit. The open loop system (a) consists of a constitutive promoter, while the closed loop circuit (b) is self-regulated with negative feedback (repressor). The frequency response for each circuit is shown in (c).

The resulting transfer function is given by

$$G_{pv}^{\text{cl}}(s) = \frac{\beta}{(s+\gamma)(s+\delta)+\beta\sigma}, \qquad \sigma = \frac{n\alpha_1 k p_e^{n-1}}{(1+k p_e^n)^2}.$$

Figure 8.16c shows the frequency response for the two circuits. We see that the feedback circuit attenuates the response of the system to disturbances with low-frequency content but slightly amplifies disturbances at high frequency (compared to the open loop system). Notice that these curves are very similar to the frequency response curves for the op amp shown in Figure 8.3b.   ∇

Transfer Functions from Experiments

The transfer function of a system provides a summary of the input/output response and is very useful for analysis and design. However, modeling from first principles can be difficult and time-consuming. Fortunately, we can often build an input/output model for a given application by directly measuring the frequency response and fitting a transfer function to it. To do so, we perturb the input to the system using a sinusoidal signal at a fixed frequency. When steady state is reached, the amplitude ratio and the phase lag give the frequency response for the excitation frequency. The complete frequency response is obtained by sweeping over a range of frequencies.

By using correlation techniques it is possible to determine the frequency response very accurately, and an analytic transfer function can be obtained from the frequency response by curve fitting. The success of this approach has led to instruments and software that automate this process, called *spectrum analyzers*. We illustrate the basic concept through two examples.

Example 8.10 Atomic force microscope
To illustrate the utility of spectrum analysis, we consider the dynamics of the atomic force microscope, introduced in Section 3.5. Experimental determination of the
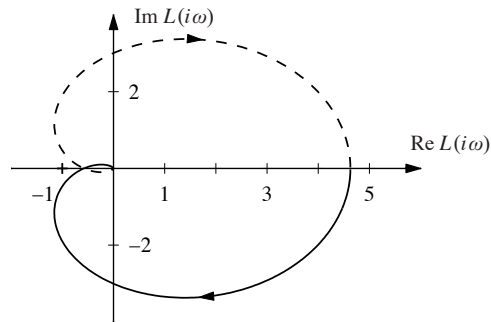
Figure 9.4: Nyquist plot for a third-order transfer function. The Nyquist plot consists of a trace of the loop transfer function $L(s) = 1/(s + a)^3$. The solid line represents the portion of the transfer function along the positive imaginary axis, and the dashed line the negative imaginary axis. The outer arc of the D contour maps to the origin.

Nyquist D contour. This arc has the form $s = Re^{i\theta}$ for $R \to \infty$. This gives

$$L(Re^{i\theta}) = \frac{1}{(Re^{i\theta} + a)^3} \to 0 \quad \text{as} \quad R \to \infty.$$

Thus the outer arc of the D contour maps to the origin on the Nyquist plot.   ∇

An alternative to computing the Nyquist plot explicitly is to determine the plot from the frequency response (Bode plot), which gives the Nyquist curve for $s = i\omega$, $\omega > 0$. We start by plotting $G(i\omega)$ from $\omega = 0$ to $\omega = \infty$, which can be read off from the magnitude and phase of the transfer function. We then plot $G(Re^{i\theta})$ with $\theta \in [-\pi/2, \pi/2]$ and $R \to \infty$, which almost always maps to zero. The remaining parts of the plot can be determined by taking the mirror image of the curve thus far (normally plotted using a dashed line). The plot can then be labeled with arrows corresponding to a clockwise traversal around the D contour (the same direction in which the first portion of the curve was plotted).

Example 9.3 Third-order system with a pole at the origin
Consider the transfer function

$$L(s) = \frac{k}{s(s + 1)^2},$$

where the gain has the nominal value $k = 1$. The Bode plot is shown in Figure 9.5a. The system has a single pole at $s = 0$ and a double pole at $s = -1$. The gain curve of the Bode plot thus has the slope -1 for low frequencies, and at the double pole $s = 1$ the slope changes to -3. For small s we have $L \approx k/s$, which means that the low-frequency asymptote intersects the unit gain line at $\omega = k$. The phase curve starts at $-90°$ for low frequencies, it is $-180°$ at the breakpoint $\omega = 1$ and it is $-270°$ at high frequencies.

Having obtained the Bode plot, we can now sketch the Nyquist plot, shown in Figure 9.5b. It starts with a phase of $-90°$ for low frequencies, intersects the negative real axis at the breakpoint $\omega = 1$ where $L(i) = 0.5$ and goes to zero along

(a) Inverted pendulum   (b) Nyquist plot
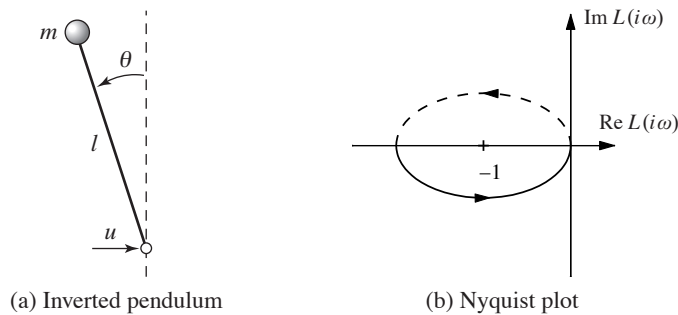
Figure 9.8: PD control of an inverted pendulum. (a) The system consists of a mass that is balanced by applying a force at the pivot point. A proportional-derivative controller with transfer function $C(s) = k(s + 2)$ is used to command u based on θ. (b) A Nyquist plot of the loop transfer function for gain $k = 2$. There is one counterclockwise encirclement of the critical point, giving $N = -1$ clockwise encirclements.

Derivation of Nyquist's Stability Theorem

We will now prove the Nyquist stability theorem for a general loop transfer function $L(s)$. This requires some results from the theory of complex variables, for which the reader can consult Ahlfors [6]. Since some precision is needed in stating Nyquist's criterion properly, we will use a more mathematical style of presentation. We also follow the mathematical convention of counting encirclements in the counterclockwise direction for the remainder of this section. The key result is the following theorem about functions of complex variables.

Theorem 9.3 (Principle of variation of the argument). *Let D be a closed region in the complex plane and let Γ be the boundary of the region. Assume the function $f : \mathbb{C} \to \mathbb{C}$ is analytic in D and on Γ, except at a finite number of poles and zeros. Then the* winding number w_n *is given by*

$$w_n = \frac{1}{2\pi} \Delta_\Gamma \arg f(z) = \frac{1}{2\pi i} \int_\Gamma \frac{f'(z)}{f(z)} dz = Z - P,$$

where Δ_Γ is the net variation in the angle when z traverses the contour Γ in the counterclockwise direction, Z is the number of zeros in D and P is the number of poles in D. Poles and zeros of multiplicity m are counted m times.

Proof. Assume that $z = a$ is a zero of multiplicity m. In the neighborhood of $z = a$ we have

$$f(z) = (z - a)^m g(z),$$

where the function g is analytic and different from zero. The ratio of the derivative of f to itself is then given by

$$\frac{f'(z)}{f(z)} = \frac{m}{z - a} + \frac{g'(z)}{g(z)},$$

and the second term is analytic at $z = a$. The function f'/f thus has a single pole

at $z = a$ with the residue m. The sum of the residues at the zeros of the function is Z. Similarly, we find that the sum of the residues of the poles of is $-P$, and hence

$$Z - P = \frac{1}{2\pi i} \int_{\Gamma} \frac{f'(z)}{f(z)} \, dz = \frac{1}{2\pi i} \int_{\Gamma} \frac{d}{dz} \log f(z) \, dz = \frac{1}{2\pi i} \Delta_{\Gamma} \log f(z),$$

where Δ_{Γ} again denotes the variation along the contour Γ. We have

$$\log f(z) = \log |f(z)| + i \arg f(z),$$

and since the variation of $|f(z)|$ around a closed contour is zero it follows that

$$\Delta_{\Gamma} \log f(z) = i \Delta_{\Gamma} \arg f(z),$$

and the theorem is proved.   □

This theorem is useful in determining the number of poles and zeros of a function of complex variables in a given region. By choosing an appropriate closed region D with boundary Γ, we can determine the difference between the number of poles and zeros through computation of the winding number.

Theorem 9.3 can be used to prove Nyquist's stability theorem by choosing Γ as the Nyquist contour shown in Figure 9.3a, which encloses the right half-plane. To construct the contour, we start with part of the imaginary axis $-jR \leq s \leq jR$ and a semicircle to the right with radius R. If the function f has poles on the imaginary axis, we introduce small semicircles with radii r to the right of the poles as shown in the figure. The Nyquist contour is obtained by letting $R \rightarrow \infty$ and $r \rightarrow 0$. Note that Γ has orientation *opposite* that shown in Figure 9.3a. (The convention in engineering is to traverse the Nyquist contour in the clockwise direction since this corresponds to moving upwards along the imaginary axis, which makes it easy to sketch the Nyquist contour from a Bode plot.)

To see how we use the principle of variation of the argument to compute stability, consider a closed loop system with the loop transfer function $L(s)$. The closed loop poles of the system are the zeros of the function $f(s) = 1 + L(s)$. To find the number of zeros in the right half-plane, we investigate the winding number of the function $f(s) = 1 + L(s)$ as s moves along the Nyquist contour Γ in the *counterclockwise* direction. The winding number can conveniently be determined from the Nyquist plot. A direct application of Theorem 9.3 gives the Nyquist criterion, taking care to flip the orientation. Since the image of $1 + L(s)$ is a shifted version of $L(s)$, we usually state the Nyquist criterion as net encirclements of the -1 point by the image of $L(s)$.

9.3 Stability Margins

In practice it is not enough that a system is stable. There must also be some margins of stability that describe how stable the system is and its robustness to perturbations. There are many ways to express this, but one of the most common is the use of gain and phase margins, inspired by Nyquist's stability criterion. The key idea is that it

(a) Block diagram   (b) Nyquist plot
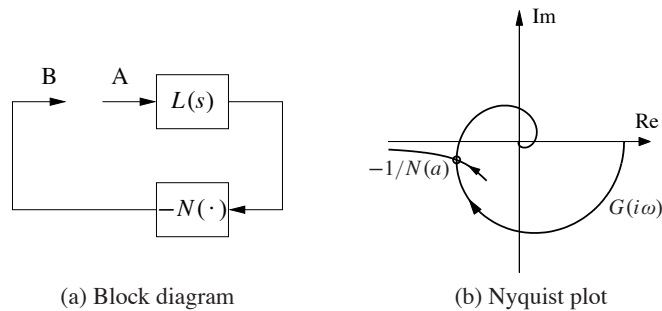
Figure 9.16: Describing function analysis. A feedback connection between a static nonlinearity and a linear system is shown in (a). The linear system is characterized by its transfer function $L(s)$, which depends on frequency, and the nonlinearity by its describing function $N(a)$, which depends on the amplitude a of its input. The Nyquist plot of $L(i\omega)$ and the plot of the $-1/N(a)$ are shown in (b). The intersection of the curves represents a possible limit cycle.

Systems where the phase between inputs and outputs is $90°$ or less for all inputs are called *passive systems*. It follows from the Nyquist stability theorem that a closed loop linear system is stable if the phase of the loop transfer function is between $-\pi$ and π. This result can be extended to nonlinear systems as well. It is called the *passivity theorem* and is closely related to the small gain theorem. See Khalil [123] for a more detailed description.

Additional applications of the small gain theorem and its application to robust stability are given in Chapter 12.

Describing Functions

For special nonlinear systems like the one shown in Figure 9.16a, which consists of a feedback connection between a linear system and a static nonlinearity, it is possible to obtain a generalization of Nyquist's stability criterion based on the idea of *describing functions*. Following the approach of the Nyquist stability condition, we will investigate the conditions for maintaining an oscillation in the system. If the linear subsystem has low-pass character, its output is approximately sinusoidal even if its input is highly irregular. The condition for oscillation can then be found by exploring the propagation of a sinusoid that corresponds to the first harmonic.

To carry out this analysis, we have to analyze how a sinusoidal signal propagates through a static nonlinear system. In particular we investigate how the first harmonic of the output of the nonlinearity is related to its (sinusoidal) input. Letting F represent the nonlinear function, we expand $F(e^{i\omega t})$ in terms of its harmonics:

$$F(ae^{i\omega t}) = \sum_{n=0}^{\infty} M_n(a)e^{i(n\omega t+\varphi_n(a))},$$

where $M_n(a)$ and $\varphi_n(a)$ represent the gain and phase of the nth harmonic, which depend on the input amplitude since the function F is nonlinear. We define the

transfer function $C(s) = k_d s + k_p$, where the gains are $k_d = 2\zeta\omega_0$ and $k_p = \omega_0^2$. Calculate and plot the gain, phase and stability margins as a function ζ.

9.7 (Congestion control in overload conditions) A strongly simplified flow model of a TCP loop under overload conditions is given by the loop transfer function

$$L(s) = \frac{k}{s}e^{-s\tau},$$

where the queuing dynamics are modeled by an integrator, the TCP window control is a time delay τ and the controller is simply a proportional controller. A major difficulty is that the time delay may change significantly during the operation of the system. Show that if we can measure the time delay, it is possible to choose a gain that gives a stability margin of $s_n \geq 0.6$ for all time delays τ.

9.8 (Bode's formula) Consider Bode's formula (9.8) for the relation between gain and phase for a transfer function that has all its singularities in the left half-plane. Plot the weighting function and make an assessment of the frequencies where the approximation $\arg G \approx (\pi/2)d \log |G|/d \log \omega$ is valid.

9.9 (Padé approximation to a time delay) Consider the transfer functions

$$G_1(s) = e^{-s\tau}, \qquad G_2(s) = e^{-s\tau} \approx \frac{1 - s\tau/2}{1 + s\tau/2}. \tag{9.16}$$

Show that the minimum phase properties of the transfer functions are similar for frequencies $\omega < 1/\tau$. A long time delay τ is thus equivalent to a small right half-plane zero. The approximation (9.16) is called a first-order *Padé approximation*.

9.10 (Inverse response) Consider a system whose input/output response is modeled by $G(s) = 6(-s + 1)/(s^2 + 5s + 6)$, which has a zero in the right half-plane. Compute the step response for the system, and show that the output goes in the wrong direction initially, which is also referred to as an *inverse response*. Compare the response to a minimum phase system by replacing the zero at $s = 1$ with a zero at $s = -1$.

9.11 (Describing function analysis) . Consider the system with the block diagram shown on the left below.
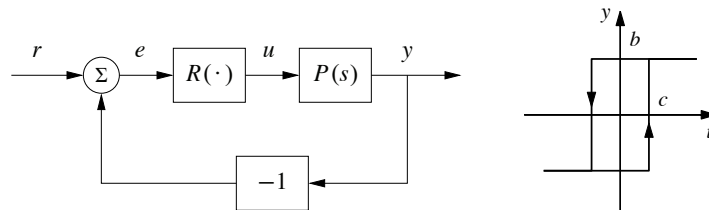
The block R is a relay with hysteresis whose input/output response is shown on the right and the process transfer function is $P(s) = e^{-s\tau}/s$. Use describing function analysis to determine frequency and amplitude of possible limit cycles. Simulate the system and compare with the results of the describing function analysis.
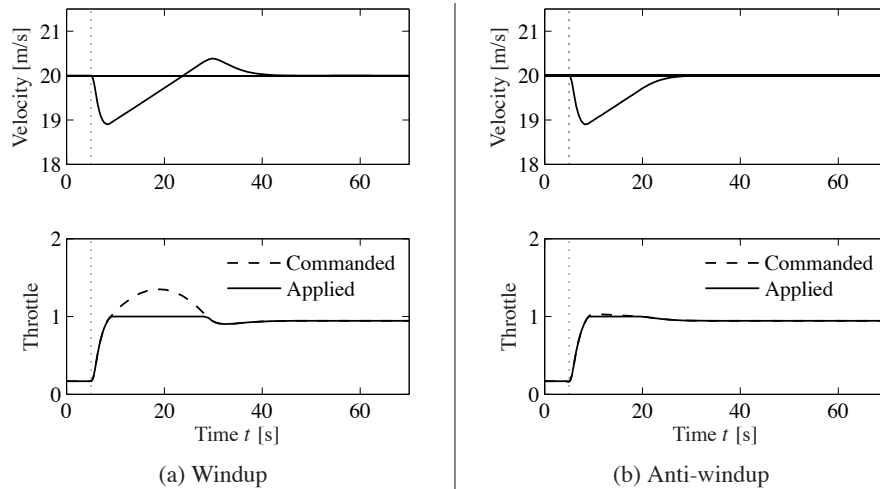
Figure 10.10: Simulation of PI cruise control with windup (a) and anti-windup (b). The figure shows the speed v and the throttle u for a car that encounters a slope that is so steep that the throttle saturates. The controller output is a dashed line. The controller parameters are $k_p = 0.5$ and $k_i = 0.1$. The anti-windup compensator eliminates the overshoot by preventing the error for building up in the integral term of the controller.

actuator, and forming an error signal e_s as the difference between the output of the controller v and the actuator output u. The signal e_s is fed to the input of the integrator through gain k_t. The signal e_s is zero when there is no saturation and the extra feedback loop has no effect on the system. When the actuator saturates, the signal e_s is fed back to the integrator in such a way that e_s goes toward zero. This implies that controller output is kept close to the saturation limit. The controller output will then change as soon as the error changes sign and integral windup is avoided.

The rate at which the controller output is reset is governed by the feedback gain k_t; a large value of k_t gives a short reset time. The parameter k_t cannot be too large because measurement noise can then cause an undesirable reset. A reasonable choice is to choose k_t as a fraction of $1/T_i$. We illustrate how integral windup can be avoided by investigating the cruise control system.

Example 10.6 Cruise control with anti-windup
Figure 10.10b shows what happens when a controller with anti-windup is applied to the system simulated in Figure 10.10a. Because of the feedback from the actuator model, the output of the integrator is quickly reset to a value such that the controller output is at the saturation limit. The behavior is drastically different from that in Figure 10.10a and the large overshoot is avoided. The tracking gain is $k_t = 2$ in the simulation. ∇
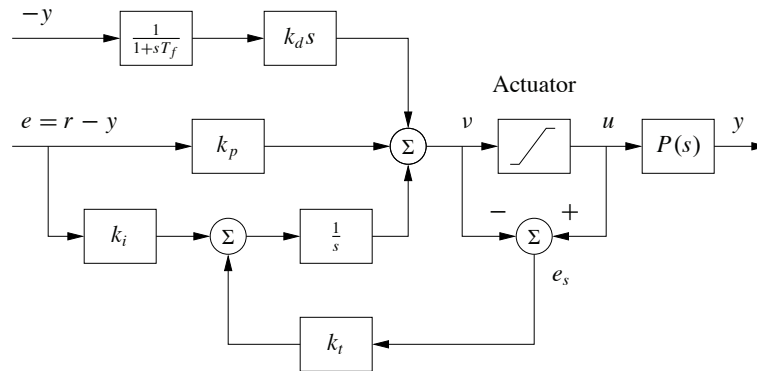
Figure 10.11: PID controller with a filtered derivative and anti-windup. The input to the integrator $(1/s)$ consists of the error term plus a "reset" based on input saturation. If the actuator is not saturated, then $e_s = u - v$, otherwise e_s will decrease the integrator input to prevent windup.

10.5 Implementation

There are many practical issues that have to be considered when implementing PID controllers. They have been developed over time based on practical experience. In this section we consider some of the most common. Similar considerations also apply to other types of controllers.

Filtering the Derivative

A drawback with derivative action is that an ideal derivative has high gain for high-frequency signals. This means that high-frequency measurement noise will generate large variations in the control signal. The effect of measurement noise may be reduced by replacing the term $k_d s$ by $k_d s/(1 + sT_f)$, which can be interpreted as an ideal derivative of a low-pass filtered signal. For small s the transfer function is approximately $k_d s$ and for large s it is equal to k_d/T_f. The approximation acts as a derivative for low-frequency signals and as a constant gain for high-frequency signals. The filtering time is chosen as $T_f = (k_d/k)/N$, with N in the range 2–20. Filtering is obtained automatically if the derivative is implemented by taking the difference between the signal and its filtered version as shown in Figure 10.3b (see equation (10.5)).

Instead of filtering just the derivative, it is also possible to use an ideal controller and filter the measured signal. The transfer function of such a controller with a filter is then

$$C(s) = k_p \left(1 + \frac{1}{sT_i} + sT_d\right) \frac{1}{1 + sT_f + (sT_f)^2/2}, \qquad (10.13)$$

where a second-order filter is used.

(a) Step response (b) Frequency responses
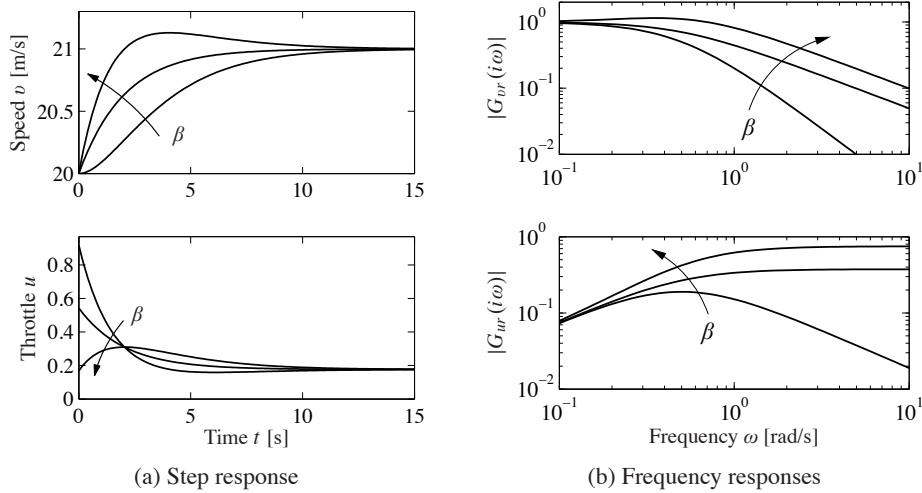
Figure 10.12: Time and frequency responses for PI cruise control with setpoint weighting. Step responses are shown in (a), and the gain curves of the frequency responses in (b). The controller gains are $k_p = 0.74$ and $k_i = 0.19$. The setpoint weights are $\beta = 0, 0.5$ and 1, and $\gamma = 0$.
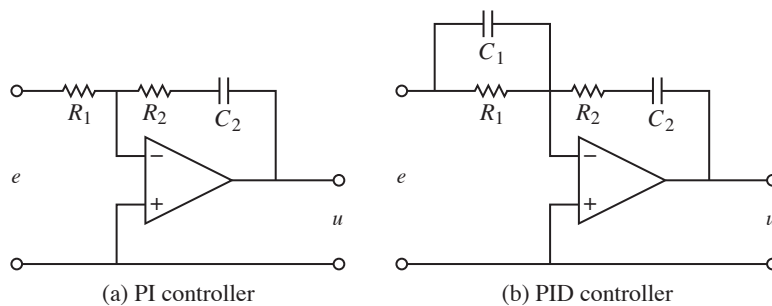
and the output voltage u. The impedances are given by

$$Z_1(s) = \frac{R_1}{1 + R_1 C_1 s}, \qquad Z_2(s) = R_2 + \frac{1}{C_2 s},$$

and we find the following relation between the input voltage e and the output voltage u:

$$u = -\frac{Z_2}{Z_1} e = -\frac{R_2}{R_1} \frac{(1 + R_1 C_1 s)(1 + R_2 C_2 s)}{R_2 C_2 s} e.$$

This is the input/output relation for a PID controller of the form (10.1) with parameters

$$k_p = \frac{R_2}{R_1}, \qquad T_i = R_2 C_1, \qquad T_d = R_1 C_1.$$

(a) PI controller (b) PID controller

Figure 10.13: Schematic diagrams for PI and PID controllers using op amps. The circuit in (a) uses a capacitor in the feedback path to store the integral of the error. The circuit in (b) adds a filter on the input to provide derivative action.

The corresponding results for a PI controller are obtained by setting $C_1 = 0$ (removing the capacitor).

Computer Implementation

In this section we briefly describe how a PID controller may be implemented using a computer. The computer typically operates periodically, with signals from the sensors sampled and converted to digital form by the A/D converter, and the control signal computed and then converted to analog form for the actuators. The sequence of operation is as follows:

1. Wait for clock interrupt   4. Send output to the actuator
2. Read input from sensor   5. Update controller variables
3. Compute control signal   6. Repeat

Notice that an output is sent to the actuators as soon as it is available. The time delay is minimized by making the calculations in step 3 as short as possible and performing all updates after the output is commanded. This simple way of reducing the latency is, unfortunately, seldom used in commercial systems.

As an illustration we consider the PID controller in Figure 10.11, which has a filtered derivative, setpoint weighting and protection against integral windup. The controller is a continuous-time dynamical system. To implement it using a computer, the continuous-time system has to be approximated by a discrete-time system.

A block diagram of a PID controller with anti-windup is shown in Figure 10.11. The signal v is the sum of the proportional, integral and derivative terms, and the controller output is $u = \mathrm{sat}(v)$, where sat is the saturation function that models the actuator. The proportional term $k_p(\beta r - y)$ is implemented simply by replacing the continuous variables with their sampled versions. Hence

$$P(t_k) = k_p\,(\beta r(t_k) - y(t_k))\,, \qquad (10.15)$$

where $\{t_k\}$ denotes the sampling instants, i.e., the times when the computer reads its input. We let h represent the sampling time, so that $t_{k+1} = t_k + h$. The integral term is obtained by approximating the integral with a sum,

$$I(t_{k+1}) = I(t_k) + k_i h\, e(t_k) + \frac{h}{T_t}\big(\mathrm{sat}(v) - v\big), \qquad (10.16)$$

where $T_t = h/k_t$ represents the anti-windup term. The filtered derivative term D is given by the differential equation

$$T_f \frac{dD}{dt} + D = -k_d \dot{y}.$$

Approximating the derivative with a backward difference gives

$$T_f \frac{D(t_k) - D(t_{k-1})}{h} + D(t_k) = -k_d \frac{y(t_k) - y(t_{k-1})}{h},$$

[205] and in the paper [58] cited in the beginning of this chapter. A comprehensive presentation of PID control is given in [16]. Interactive learning tools for PID control can be downloaded from http://www.calerga.com/contrib.

Exercises

10.1 (Ideal PID controllers) Consider the systems represented by the block diagrams in Figure 10.1. Assume that the process has the transfer function $P(s) = b/(s+a)$ and show that the transfer functions from r to y are

$$(a) \quad G_{yr}(s) = \frac{bk_d s^2 + bk_p s + bk_i}{(1 + bk_d)s^2 + (a + bk_p)s + bk_i},$$

$$(b) \quad G_{yr}(s) = \frac{bk_i}{(1 + bk_d)s^2 + (a + bk_p)s + bk_i}.$$

Pick some parameters and compare the step responses of the systems.

10.2 Consider a second-order process with the transfer function

$$P(s) = \frac{b}{s^2 + a_1 s + a_2}.$$

The closed loop system with a PI controller is a third-order system. Show that it is possible to position the closed loop poles as long as the sum of the poles is $-a_1$. Give equations for the parameters that give the closed loop characteristic polynomial

$$(s + \alpha_0)(s^2 + 2\zeta_0\omega_0 s + \omega_0^2).$$

10.3 Consider a system with the transfer function $P(s) = (s + 1)^{-2}$. Find an integral controller that gives a closed loop pole at $s = -a$ and determine the value of a that maximizes the integral gain. Determine the other poles of the system and judge if the pole can be considered dominant. Compare with the value of the integral gain given by equation (10.6).

10.4 (Ziegler–Nichols tuning) Consider a system with transfer function $P(s) = e^{-s}/s$. Determine the parameters of P, PI and PID controllers using Ziegler–Nichols step and frequency response methods. Compare the parameter values obtained by the different rules and discuss the results.

10.5 (Vehicle steering) Design a proportional-integral controller for the vehicle steering system that gives the closed loop characteristic polynomial

$$s^3 + 2\omega_0 s^2 + 2\omega_0 s + \omega_0^3.$$

10.6 (Congestion control) A simplified flow model for TCP transmission is derived in [101, 137]. The linearized dynamics are modeled by the transfer function

$$G_{qp}(s) = \frac{b}{(s + a_1)(s + a_2)} e^{-s\tau_e},$$

which describes the dynamics relating the expected queue length q to the expected packet drop p. The parameters are given by $a_1 = 2N^2/(c\tau_e^2)$, $a_2 = 1/\tau_e$ and $b = c^2/(2N)$. The parameter c is the bottleneck capacity, N is the number of sources feeding the link and τ_e is the round-trip delay time. Use the parameter values $N = 75$ sources, $C = 1250$ packets/s and $\tau_e = 0.15$ and find the parameters of a PI controller using one of the Ziegler–Nichols rules and the corresponding improved rule. Simulate the responses of the closed loop systems obtained with the PI controllers.

10.7 (Motor drive) Consider the model of the motor drive in Exercise 2.10. Develop an approximate second-order model of the system and use it to design an ideal PD controller that gives a closed loop system with eigenvalues in $\zeta\omega_0 \pm i\omega_0\sqrt{1-\zeta^2}$. Add low-pass filtering as shown in equation (10.13) and explore how large ω_0 can be made while maintaining a good stability margin. Simulate the closed loop system with the chosen controller and compare the results with the controller based on state feedback in Exercise 6.11.

10.8 Consider the system in Exercise 10.7 investigate what happens if the second-order filtering of the derivative is replace by a first-order filter.

10.9 (Tuning rules) Apply the Ziegler–Nichols and the modified tuning rules to design PI controllers for systems with the transfer functions

$$P_1 = \frac{e^{-s}}{s}, \qquad P_2 = \frac{e^{-s}}{s+1}, \qquad P_3 = e^{-s}.$$

Compute the stability margins and explore any patterns.

10.10 (Windup and anti-windup) Consider a PI controller of the form $C(s) = 1+1/s$ for a process with input that saturates when $|u| > 1$, and whose linear dynamics are given by the transfer function $P(s) = 1/s$. Simulate the response of the system to step changes in the reference signal of magnitude $1, 2$ and 3. Repeat the simulation when the windup protection scheme in Figure 10.11 is used.

10.11 (Windup protection by conditional integration) Many methods have been proposed to avoid integrator windup. One method called *conditional integration* is to update the integral only when the error is sufficiently small. To illustrate this method we consider a system with PI control described by

$$\frac{dx_1}{dt} = u, \qquad u = \mathrm{sat}_{u_0}(k_p e + k_i x_2), \qquad \frac{dx_2}{dt} = \begin{cases} e & \text{if } |e| < e_0 \\ 0 & \text{if } |e| \geq e_0, \end{cases}$$

where $e = r - x$. Plot the phase portrait of the system for the parameter values $k_p = 1$, $k_i = 1$, $u_0 = 1$ and $e_0 = 1$ and discuss the properties of the system. The example illustrates the difficulties of introducing ad hoc nonlinearities without careful analysis.

Chapter Eleven
Frequency Domain Design

> *Sensitivity improvements in one frequency range must be paid for with sensitivity deteriorations in another frequency range, and the price is higher if the plant is open-loop unstable. This applies to every controller, no matter how it was designed.*
>
> Gunter Stein in the inaugural IEEE Bode Lecture, 1989 [185].

In this chapter we continue to explore the use of frequency domain techniques with a focus on the design of feedback systems. We begin with a more thorough description of the performance specifications for control systems and then introduce the concept of "loop shaping" as a mechanism for designing controllers in the frequency domain. We also introduce some fundamental limitations to performance for systems with time delays and right half-plane poles and zeros.

11.1 Sensitivity Functions

In the previous chapter, we considered the use of proportional-integral-derivative (PID) feedback as a mechanism for designing a feedback controller for a given process. In this chapter we will expand our approach to include a richer repertoire of tools for shaping the frequency response of the closed loop system.

One of the key ideas in this chapter is that we can design the behavior of the closed loop system by focusing on the open loop transfer function. This same approach was used in studying stability using the Nyquist criterion: we plotted the Nyquist plot for the *open* loop transfer function to determine the stability of the *closed* loop system. From a design perspective, the use of loop analysis tools is very powerful: since the loop transfer function is $L = PC$, if we can specify the desired performance in terms of properties of L, we can directly see the impact of changes in the controller C. This is much easier, for example, than trying to reason directly about the tracking response of the closed loop system, whose transfer function is given by $G_{yr} = PC/(1 + PC)$.

We will start by investigating some key properties of the feedback loop. A block diagram of a basic feedback loop is shown in Figure 11.1. The system loop is composed of two components: the process and the controller. The controller itself has two blocks: the feedback block C and the feedforward block F. There are two disturbances acting on the process, the load disturbance d and the measurement noise n. The load disturbance represents disturbances that drive the process away from its desired behavior, while the measurement noise represents disturbances that corrupt information about the process given by the sensors. In the figure, the load
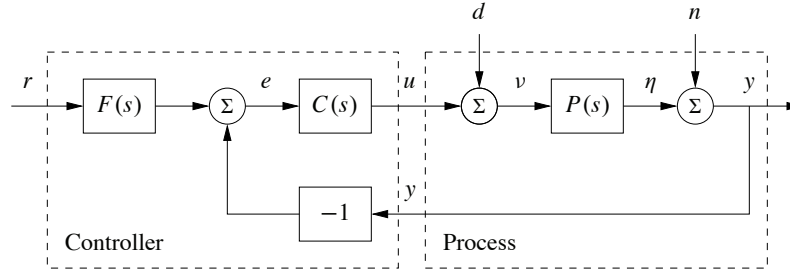
Figure 11.1: Block diagram of a basic feedback loop with two degrees of freedom. The controller has a feedback block C and a feedforward block F. The external signals are the reference signal r, the load disturbance d and the measurement noise n. The process output is η, and the control signal is u.

disturbance is assumed to act on the process input. This is a simplification since disturbances often enter the process in many different ways, but it allows us to streamline the presentation without significant loss of generality.

The process output η is the real variable that we want to control. Control is based on the measured signal y, where the measurements are corrupted by measurement noise n. The process is influenced by the controller via the control variable u. The process is thus a system with three inputs—the control variable u, the load disturbance d and the measurement noise n—and one output—the measured signal y. The controller is a system with two inputs and one output. The inputs are the measured signal y and the reference signal r, and the output is the control signal u. Note that the control signal u is an input to the process and the output of the controller, and that the measured signal y is the output of the process and an input to the controller.

The feedback loop in Figure 11.1 is influenced by three external signals, the reference r, the load disturbance d and the measurement noise n. Any of the remaining signals can be of interest in controller design, depending on the particular application. Since the system is linear, the relations between the inputs and the interesting signals can be expressed in terms of the transfer functions. The following relations are obtained from the block diagram in Figure 11.1:

$$
\begin{bmatrix} y \\ \eta \\ v \\ u \\ e \end{bmatrix} = \begin{bmatrix} \dfrac{PCF}{1+PC} & \dfrac{P}{1+PC} & \dfrac{1}{1+PC} \\[2mm] \dfrac{PCF}{1+PC} & \dfrac{P}{1+PC} & \dfrac{-PC}{1+PC} \\[2mm] \dfrac{CF}{1+PC} & \dfrac{1}{1+PC} & \dfrac{-C}{1+PC} \\[2mm] \dfrac{CF}{1+PC} & \dfrac{-PC}{1+PC} & \dfrac{-C}{1+PC} \\[2mm] \dfrac{F}{1+PC} & \dfrac{-P}{1+PC} & \dfrac{-1}{1+PC} \end{bmatrix} \begin{bmatrix} r \\ d \\ n \end{bmatrix}. \tag{11.1}
$$

In addition, we can write the transfer function for the error between the reference
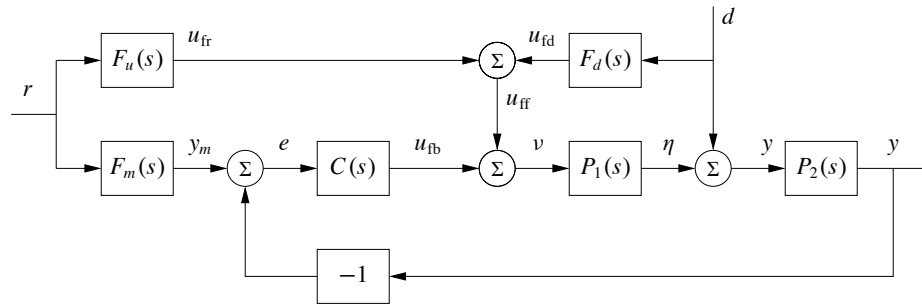
Figure 11.3: Block diagram of a system with feedforward compensation for improved response to reference signals and measured disturbances (2 DOF system). Three feedforward elements are present: $F_m(s)$ sets the desired output value, $F_u(s)$ generates the feedforward command u_{fr} and $F_d(s)$ attempts to cancel disturbances.

Processes with multiple inputs and outputs can also be considered by regarding u and y as vectors. Representations at these higher levels of abstraction are useful for the development of theory because they make it possible to focus on fundamentals and to solve general problems with a wide range of applications. However, care must be exercised to maintain the coupling to the real-world control problems we intend to solve.

11.2 Feedforward Design

Most of our analysis and design tools up to this point have focused on the role of feedback and its effect on the dynamics of the system. Feedforward is a simple and powerful technique that complements feedback. It can be used both to improve the response to reference signals and to reduce the effect of measurable disturbances. Feedforward compensation admits perfect elimination of disturbances, but it is much more sensitive to process variations than feedback compensation. A general scheme for feedforward was discussed in Section 7.5 using Figure 7.10. A simple form of feedforward for PID controllers was discussed in Section 10.5. The controller in Figure 11.1 also has a feedforward block to improve response to command signals. An alternative version of feedforward is shown in Figure 11.3, which we will use in this section to understand some of the trade-offs between feedforward and feedback.

Controllers with two degrees of freedom (feedforward and feedback) have the advantage that the response to reference signals can be designed independently of the design for disturbance attenuation and robustness. We will first consider the response to reference signals, and we will therefore initially assume that the load disturbance d is zero. Let F_m represent the ideal response of the system to reference signals. The feedforward compensator is characterized by the transfer functions F_u and F_m. When the reference is changed, the transfer function F_u generates the signal u_{fr}, which is chosen to give the desired output when applied as input to the process. Under ideal conditions the output y is then equal to y_m, the error signal is zero and

there will be no feedback action. If there are disturbances or modeling errors, the signals y_m and y will differ. The feedback then attempts to bring the error to zero.

To make a formal analysis, we compute the transfer function from reference input to process output:

$$G_{yr}(s) = \frac{P(CF_m + F_u)}{1 + PC} = F_m + \frac{PF_u - F_m}{1 + PC}, \qquad (11.4)$$

where $P = P_2 P_1$. The first term represents the desired transfer function. The second term can be made small in two ways. Feedforward compensation can be used to make $PF_u - F_m$ small, or feedback compensation can be used to make $1 + PC$ large. Perfect feedforward compensation is obtained by choosing

$$F_u = \frac{F_m}{P}. \qquad (11.5)$$

Design of feedforward using transfer functions is thus a very simple task. Notice that the feedforward compensator F_u contains an inverse model of the process dynamics.

Feedback and feedforward have different properties. Feedforward action is obtained by matching two transfer functions, requiring precise knowledge of the process dynamics, while feedback attempts to make the error small by dividing it by a large quantity. For a controller having integral action, the loop gain is large for low frequencies, and it is thus sufficient to make sure that the condition for ideal feedforward holds at higher frequencies. This is easier than trying to satisfy the condition (11.5) for all frequencies.

We will now consider reduction of the effects of the load disturbance d in Figure 11.3 by feedforward control. We assume that the disturbance signal is measured and that the disturbance enters the process dynamics in a known way (captured by P_1 and P_2). The effect of the disturbance can be reduced by feeding the measured signal through a dynamical system with the transfer function F_d. Assuming that the reference r is zero, we can use block diagram algebra to find that the transfer function from the disturbance to the process output is

$$G_{yd} = \frac{P_2(1 + F_d P_1)}{1 + PC}, \qquad (11.6)$$

where $P = P_1 P_2$. The effect of the disturbance can be reduced by making $1 + F_d P_1$ small (feedforward) or by making $1 + PC$ large (feedback). Perfect compensation is obtained by choosing

$$F_d = -P_1^{-1}, \qquad (11.7)$$

requiring inversion of the transfer function P_1.

As in the case of reference tracking, disturbance attenuation can be accomplished by combining feedback and feedforward control. Since low-frequency disturbances can be eliminated by feedback, we require the use of feedforward only for high-frequency disturbances, and the transfer function F_d in equation (11.7) can then be computed using an approximation of P_1 for high frequencies.
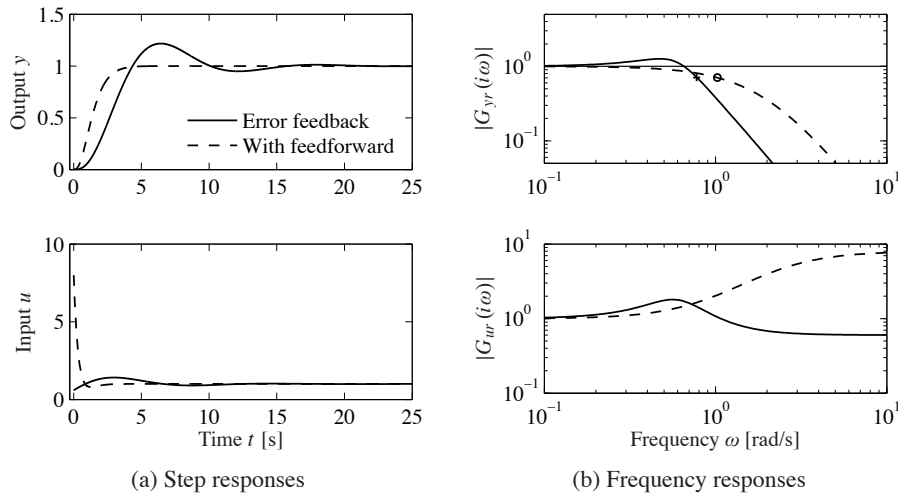
Figure 11.5: Reference signal responses. The responses in process output y and control signal u to a unit step in the reference signal r are shown in (a), and the gain curves of G_{yr} and G_{ur} are shown in (b). Results with PI control with error feedback are shown by solid lines, and the dashed lines show results for a controller with a feedforward compensator.

response with no overshoot. However, much larger control signals are required to obtain the fast response. The largest value of the control signal is 8, compared to 1.2 for the regular PI controller. The controller with feedforward has a larger bandwidth (marked with ○) and no resonant peak. The transfer function G_{ur} also has higher gain at high frequencies.   ∇

Response to Load Disturbances and Measurement Noise

A simple criterion for disturbance attenuation is to compare the output of the closed loop system in Figure 11.1 with the output of the corresponding open loop system obtained by setting $C = 0$. If we let the disturbances for the open and closed loop systems be identical, the output of the closed loop system is then obtained simply by passing the open loop output through a system with the transfer function S. The sensitivity function tells how the variations in the output are influenced by feedback (Exercise 11.7). Disturbances with frequencies such that $|S(i\omega)| < 1$ are attenuated, but disturbances with frequencies such that $|S(i\omega)| > 1$ are amplified by feedback. The maximum sensitivity M_s, which occurs at the frequency ω_{ms}, is thus a measure of the largest amplification of the disturbances. The maximum magnitude of $1/(1 + L)$ is also the minimum of $|1 + L|$, which is precisely the stability margin s_m defined in Section 9.3, so that $M_s = 1/s_m$. The maximum sensitivity is therefore also a robustness measure.

If the sensitivity function is known, the potential improvements by feedback can be evaluated simply by recording a typical output and filtering it through the sensitivity function. A plot of the gain curve of the sensitivity function is a good way to make an assessment of the disturbance attenuation. Since the sensitivity function

(a) Output load response   (b) Input noise response
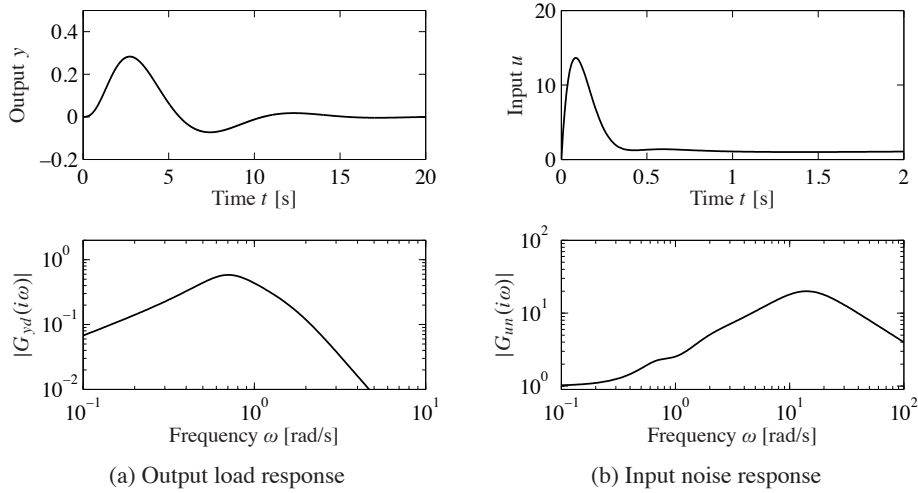
Figure 11.7: Disturbance responses. The time and frequency responses of process output y to load disturbance d are shown in (a) and the responses of control signal u to measurement noise n are shown in (b).

properties of the controller.

The effects of measurement noise are captured by the transfer function from the measurement noise to the control signal,

$$-G_{un} = \frac{C}{1 + PC} = CS = \frac{T}{P}. \tag{11.10}$$

The complementary sensitivity function is close to 1 for low frequencies ($\omega < \omega_{gc}$), and G_{un} can be approximated by $-1/P$. The sensitivity function is close to 1 for high frequencies ($\omega > \omega_{gc}$), and G_{un} can be approximated by $-C$.

Example 11.4 Third-order system

Consider a process with the transfer function $P(s) = (s+1)^{-3}$ and a proportional-integral-derivative (PID) controller with gains $k_p = 0.6$, $k_i = 0.5$ and $k_d = 2.0$. We augment the controller using a second-order noise filter with $T_f = 0.1$, so that its transfer function is

$$C(s) = \frac{k_d s^2 + k_p s + k_i}{s(s^2 T_f^2/2 + s T_f + 1)}.$$

The system responses are illustrated in Figure 11.7. The response of the output to a step in the load disturbance in the top part of Figure 11.7a has a peak of 0.28 at time $t = 2.73$ s. The frequency response in Figure 11.7a shows that the gain has a maximum of 0.58 at $\omega = 0.7$ rad/s.

The response of the control signal to a step in measurement noise is shown in Figure 11.7b. The high-frequency roll-off of the transfer function $G_{un}(i\omega)$ is due to filtering; without it the gain curve in Figure 11.7b would continue to rise after 20 rad/s. The step response has a peak of 13 at $t = 0.08$ s. The frequency

response has its peak 20 at $\omega = 14$ rad/s. Notice that the peak occurs far above the peak of the response to load disturbances and far above the gain crossover frequency $\omega_{gc} = 0.78$ rad/s. An approximation derived in Exercise 11.9 gives $\max |CS(i\omega)| \approx k_d/T_f = 20$, which occurs at $\omega = \sqrt{2}/T_d = 14.1$ rad/s. $\qquad\nabla$

11.4 Feedback Design via Loop Shaping

One advantage of the Nyquist stability theorem is that it is based on the loop transfer function, which is related to the controller transfer function through $L = PC$. It is thus easy to see how the controller influences the loop transfer function. To make an unstable system stable we simply have to bend the Nyquist curve away from the critical point.

This simple idea is the basis of several different design methods collectively called *loop shaping*. These methods are based on choosing a compensator that gives a loop transfer function with a desired shape. One possibility is to determine a loop transfer function that gives a closed loop system with the desired properties and to compute the controller as $C = L/P$. Another is to start with the process transfer function, change its gain and then add poles and zeros until the desired shape is obtained. In this section we will explore different loop-shaping methods for control law design.

Design Considerations

We will first discuss a suitable shape for the loop transfer function that gives good performance and good stability margins. Figure 11.8 shows a typical loop transfer function. Good robustness requires good stability margins (or good gain and phase margins), which imposes requirements on the loop transfer function around the crossover frequencies ω_{pc} and ω_{gc}. The gain of L at low frequencies must be large in order to have good tracking of command signals and good attenuation of low-frequency disturbances. Since $S = 1/(1+L)$, it follows that for frequencies where $|L| > 101$ disturbances will be attenuated by a factor of 100 and the tracking error is less than 1%. It is therefore desirable to have a large crossover frequency and a steep (negative) slope of the gain curve. The gain at low frequencies can be increased by a controller with integral action, which is also called *lag compensation*. To avoid injecting too much measurement noise into the system, the loop transfer function should have low gain at high frequencies, which is called *high-frequency roll-off*. The choice of gain crossover frequency is a compromise among attenuation of load disturbances, injection of measurement noise and robustness.

Bode's relations (see Section 9.4) impose restrictions on the shape of the loop transfer function. Equation (9.8) implies that the slope of the gain curve at gain crossover cannot be too steep. If the gain curve has a constant slope, we have the following relation between slope n_{gc} and phase margin φ_m:

$$n_{gc} = -2 + \frac{2\varphi_m}{\pi} \text{ [rad]}. \qquad (11.11)$$
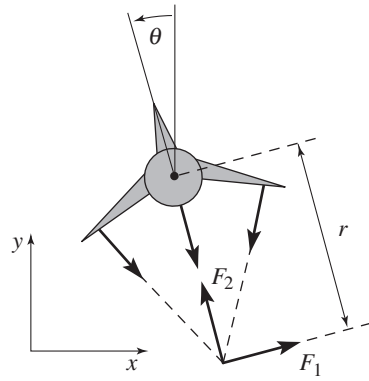
Symbol	Description	Value
m	Vehicle mass	4.0 kg
J	Vehicle inertia, φ_3 axis	0.0475 kg m^2
r	Force moment arm	25.0 cm
c	Damping coefficient	0.05 kg m/s
g	Gravitational constant	9.8 m/s^2

(a) Simplified model   (b) Parameter values

Figure 11.11: Roll control of a vectored thrust aircraft. (a) The roll angle θ is controlled by applying maneuvering thrusters, resulting in a moment generated by F_z. (b) The table lists the parameter values for a laboratory version of the system.

transfer function of the form
$$P(s) = \frac{r}{Js^2},$$

with the parameters given in Figure 11.11b. We take as our performance specification that we would like less than 1% error in steady state and less than 10% tracking error up to 10 rad/s.

The open loop transfer function is shown in Figure 11.12a. To achieve our performance specification, we would like to have a gain of at least 10 at a frequency of 10 rad/s, requiring the gain crossover frequency to be at a higher frequency. We see from the loop shape that in order to achieve the desired performance we cannot simply increase the gain since this would give a very low phase margin. Instead, we must increase the phase at the desired crossover frequency.

To accomplish this, we use a lead compensator (11.12) with $a = 2$ and $b = 50$. We then set the gain of the system to provide a large loop gain up to the desired bandwidth, as shown in Figure 11.12b. We see that this system has a gain of greater than 10 at all frequencies up to 10 rad/s and that it has more than 60° of phase margin.   ∇

The action of a lead compensator is essentially the same as that of the derivative portion of a PID controller. As described in Section 10.5, we often use a filter for the derivative action of a PID controller to limit the high-frequency gain. This same effect is present in a lead compensator through the pole at $s = b$.

Equation (11.12) is a first-order compensator and can provide up to 90° of phase lead. Larger phase lead can be obtained by using a higher-order lead compensator (Exercise 11.11):
$$C(s) = k\frac{(s + a)^n}{(s + b)^n}, \qquad a < b.$$

The system in Example 11.10 is unfortunately an exception. The key feature of the system is that the Nyquist curve of the process is completely contained in the right half-plane. Such systems are called *passive*, and their transfer functions are *positive real*. For typical control systems there are severe constraints on the sensitivity function. The following theorem, due to Bode, provides insights into the limits of performance under feedback.

Theorem 11.1 (Bode's integral formula). *Assume that the loop transfer function* $L(s)$ *of a feedback system goes to zero faster than* $1/s$ *as* $s \to \infty$, *and let* $S(s)$ *be the sensitivity function. If the loop transfer function has poles* p_k *in the right half-plane, then the sensitivity function satisfies the following integral:*

$$\int_0^\infty \log |S(i\omega)| \, d\omega = \int_0^\infty \log \frac{1}{|1 + L(i\omega)|} \, d\omega = \pi \sum p_k. \qquad (11.19)$$

Equation (11.19) implies that there are fundamental limitations to what can be achieved by control and that control design can be viewed as a redistribution of disturbance attenuation over different frequencies. In particular, this equation shows that if the sensitivity function is made smaller for some frequencies, it must increase at other frequencies so that the integral of $\log |S(i\omega)|$ remains constant. This means that if disturbance attenuation is improved in one frequency range, it will be worse in another, a property sometime referred to as the *waterbed effect*. It also follows that systems with open loop poles in the right half-plane have larger overall sensitivity than stable systems.

Equation (11.19) can be regarded as a *conservation law*: if the loop transfer function has no poles in the right half-plane, the equation simplifies to

$$\int_0^\infty \log |S(i\omega)| d\omega = 0.$$

This formula can be given a nice geometric interpretation as illustrated in Figure 11.14, which shows $\log |S(i\omega)|$ as a function of ω. The area over the horizontal axis must be equal to the area under the axis when the frequency is plotted on a *linear* scale. Thus if we wish to make the sensitivity smaller up to some frequency ω_{sc}, we must balance this by increased sensitivity above ω_{sc}. Control system design can be viewed as trading the disturbance attenuation at some frequencies for disturbance amplification at other frequencies. Notice that the system in Example 11.10 violates the condition that $\lim_{s \to \infty} sL(s) = 0$ and hence the integral formula does not apply.

There is result analogous to equation (11.19) for the complementary sensitivity function:

$$\int_0^\infty \frac{\log |T(i\omega)|}{\omega^2} \, d\omega = \pi \sum \frac{1}{z_i}, \qquad (11.20)$$

where the summation is over all right half-plane zeros. Notice that slow right half-plane zeros are worse than fast ones and that fast right half-plane poles are worse than slow ones.

11.7 (Disturbance attenuation) Consider the feedback system shown in Figure 11.1. Assume that the reference signal is constant. Let y_{ol} be the measured output when there is no feedback and y_{cl} be the output with feedback. Show that $Y_{cl}(s) = S(s)Y_{ol}(s)$, where S is the sensitivity function.

11.8 (Disturbance reduction through feedback) Consider a problem in which an output variable has been measured to estimate the potential for disturbance attenuation by feedback. Suppose an analysis shows that it is possible to design a closed loop system with the sensitivity function

$$S(s) = \frac{s}{s^2 + s + 1}.$$

Estimate the possible disturbance reduction when the measured disturbance is

$$y(t) = 5 \sin (0.1\,t) + 3 \sin (0.17\,t) + 0.5 \cos (0.9\,t) + 0.1\,t.$$

11.9 Show that the effect of high frequency measurement noise on the control signal for the system in Example 11.4 can be approximated by

$$CS \approx C = \frac{k_d s}{(sT_f)^2 /2 + sT_f + 1},$$

and that the largest value of $|CS(i\omega)|$ is k_d/T_f which occurs for $\omega = \sqrt{2}/T_f$.

11.10 (Attenuation of low-frequency sinusoidal disturbances) Integral action eliminates constant disturbances and reduces low-frequency disturbances because the controller gain is infinite at zero frequency. A similar idea can be used to reduce the effects of sinusoidal disturbances of known frequency ω_0 by using the controller

$$C(s) = k_p + \frac{k_s s}{s^2 + 2\zeta\omega_0 s + \omega_0^2}.$$

This controller has the gain $C_s(i\omega) = k_p + k_s/(2\zeta)$ for the frequency ω_0, which can be large by choosing a small value of ζ. Assume that the process has the transfer function $P(s) = 1/s$. Determine the Bode plot of the loop transfer function and simulate the system. Compare the results with PI control.
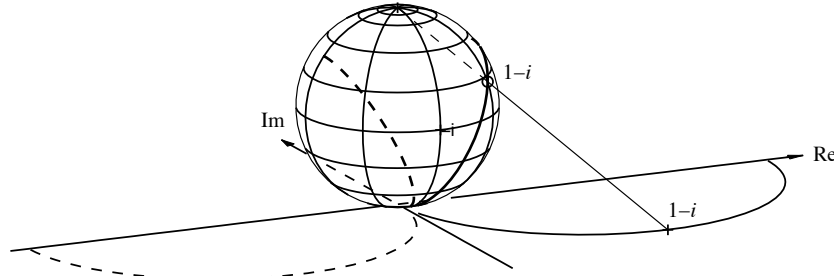
11.11 Consider a lead compensator with the transfer function

$$C_n(s) = \left(\frac{s\sqrt[n]{k} + a}{s + a}\right)^n,$$

which has zero frequency gain $C(0) = 1$ and high-frequency gain $C(\infty) = k$. Show that the gain required to give a given phase lead φ is

$$k = \left(1 + 2\tan^2(\varphi/n) + 2\tan(\varphi/n)\sqrt{1 + \tan^2(\varphi/n)}\right)^n,$$

and that $\lim_{n\to\infty} k = e^{2\varphi}$.

Figure 12.4: Geometric interpretation of $d(P_1, P_2)$. At each frequency, the points on the Nyquist curve for P_1 (solid) and P_2 (dashed) are projected onto a sphere of radius 1 sitting at the origin of the complex plane. The projection of the point $1 - i$ is shown. The distance between the two systems is defined as the maximum distance between the projections of $P_1(i\omega)$ and $P_2(i\omega)$ over all frequencies ω. The figure is plotted for the transfer functions $P_1(s) = 2/(s + 1)$ and $P_2(s) = 2/(s - 1)$. (Diagram courtesy G. Vinnicombe.)

Figure 12.4, where the Nyquist plots of P_1 and P_2 are projected onto a sphere with diameter 1 at the origin of the complex plane (called the *Riemann sphere*). Points in the complex plane are projected onto the sphere by a line through the point and the north pole (Figure 12.4). The distance $d(P_1, P_2)$ is the shortest chordal distance between the projections of $P_1(i\omega)$ and $P_2(i\omega)$. The distance is small when P_1 and P_2 are small or large, but it emphasizes the behavior around the gain crossover frequency.

The distance $d(P_1, P_2)$ has one drawback for the purpose of comparing the behavior of systems under feedback. If P_2 is perturbed continuously from P_1 to P_2, there can be intermediate transfer functions P where $d(P_1, P)$ is 1 even if $d(P_1, P_2)$ is small (see Exercise 12.4). To explore when this could happen, we observe that

$$1 - d^2(P_1, P) = \frac{(1 + P(i\omega)P_1(-i\omega))(1 + P(-i\omega)P_1(i\omega))}{(1 + |P_1(i\omega)|^2)(1 + |P(i\omega)|^2)}.$$

The right-hand side is zero, and hence $d(P_1, P) = 1$ if $1 + P(i\omega)P_1(-i\omega) = 0$ for some ω. To explore when this could occur, we investigate the behavior of the function $1 + P(s)P_1(-s)$ when P is perturbed from P_1 to P_2. If the functions $f_1(s) = 1 + P_1(s)P_1(-s)$ and $f_2(s) = 1 + P_2(s)P_1(-s)$ do not have the same number of zeros in the right half-plane, there is an intermediate P such that $1 + P(i\omega)P_1(-i\omega) = 0$ for some ω. To exclude this case we introduce the set $\mathcal{C}$ as all pairs (P_1, P_2) such that the functions $f_1 = 1 + P_1(s)P_1(-s)$ and $f_2 = 1 + P_2(s)P_1(-s)$ have the same number of zeros in the right half-plane.

The *Vinnicombe metric* or *v-gap metric* is defined as

$$\delta_v(P_1, P_2) = \begin{cases} d(P_1, P_2), & \text{if } (P_1, P_2) \in \mathcal{C} \\ 1, & \text{otherwise.} \end{cases} \tag{12.4}$$

Vinnicombe [196] showed that $\delta_v(P_1, P_2)$ is a metric, he gave strong robustness results based on the metric and he developed the theory for systems with many
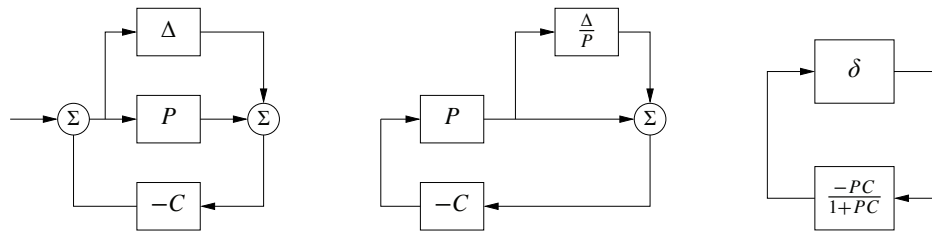
Figure 12.7: Illustration of robustness to process perturbations. A system with additive uncertainty (left) can be manipulated via block diagram algebra to one with multiplicative uncertainty $\delta = \Delta/P$ (center). Additional manipulations isolate the uncertainty in a manner that allows application of the small gain theorem (right)

Example 12.6 Bode's ideal loop transfer function
A major problem in the design of electronic amplifiers is to obtain a closed loop system that is insensitive to changes in the gain of the electronic components. Bode found that the loop transfer function $L(s) = ks^{-n}$, with $1 \leq n \leq 5/3$, was an ideal loop transfer function. The gain curve of the Bode plot is a straight line with slope $-n$ and the phase is constant $\arg L(i\omega) = -n\pi/2$. The phase margin is thus $\varphi_m = 90(2 - n)^\circ$ for all values of the gain k and the stability margin is $s_m = \sin \pi (1 - n/2)$. This exact transfer function cannot be realized with physical components, but it can be approximated over a given frequency range with a rational function (Exercise 12.7). An operational amplifier circuit that has the approximate transfer function $G(s) = k/(s+a)$ is a realization of Bode's ideal transfer function with $n = 1$, as described in Example 8.3. Designers of operational amplifiers go to great efforts to make the approximation valid over a wide frequency range. ∇

Youla Parameterization

Since stability is such an essential property, it is useful to characterize all controllers that stabilize a given process. Such a representation, which is called a *Youla parameterization*, is very useful when solving design problems because it makes it possible to search over all stabilizing controllers without the need to test stability explicitly.

We will first derive Youla's parameterization for a stable process with a rational transfer function P. A system with the complementary sensitivity function T can be obtained by feedforward control with the stable transfer function Q if $T = PQ$.

Table 12.1: Conditions for robust stability for different types of uncertainty

Process	Uncertainty Type	Robust Stability
$P + \Delta$	Additive	$\|CS\Delta\|_\infty < 1$
$P(1 + \delta)$	Multiplicative	$\|T\delta\|_\infty < 1$
$P/(1 + \Delta_{\text{fb}} \cdot P)$	Feedback	$\|PS\Delta_{\text{fb}}\|_\infty < 1$

Nyquist plot indicates that the robustness is poor since the loop transfer function is very close to the critical point -1. The phase margin is $7°$ and the stability margin is $s_m = 0.077$. The poor robustness shows up in the Bode plot, where the gain curve hovers around the value 1 and the phase curve is close to $-180°$ for a wide frequency range. More insight is obtained by analyzing the sensitivity functions, shown by solid lines in Figure 12.12. The maximum sensitivities are $M_s = 13$ and $M_t = 12$, indicating that the system has poor robustness.

At first sight it is surprising that a controller where the nominal closed system has well damped poles and zeros is so sensitive to process variations. We have an indication that something is unusual because the controller has a zero at $s = 3.5$ in the right half-plane. To understand what happens, we will investigate the reason for the peaks of the sensitivity functions.

Let the transfer functions of the process and the controller be

$$P(s) = \frac{n_p(s)}{d_p(s)}, \quad C(s) = \frac{n_c(s)}{d_c(s)},$$

where $n_p(s), n_c(s), d_p(s)$ and $d_c(s)$ are the numerator and denominator polynomials. The complementary sensitivity function is

$$T(s) = \frac{PC}{1 + PC} = \frac{n_p(s)n_c(s)}{d_p(s)d_c(s) + n_p(s)n_p(s)}.$$

The poles of $T(s)$ are the poles of the closed loop system and the zeros are given by the zeros of the process and controller. Sketching the gain curve of the complementary sensitivity function we find that $T(s) = 1$ for low frequencies and that $|T(i\omega)|$ starts to increase at its first zero, which is the process zero at $s = 2$. It increases further at the controller zero at $s = 3.4$, and it does not start to decrease until the closed loop poles appear at $\omega_c = 10$ and $\omega_o = 20$. We can thus conclude that there will be a peak in the complementary sensitivity function. The magnitude of the peak depends on the ratio of the zeros and the poles of the transfer function.

The peak of the complementary sensitivity function can be avoided by assigning a closed loop pole close to the slow process zero. We can achieve this by choosing $\omega_c = 10$ and $\zeta_c = 2.6$, which gives closed loop poles at $s = -2$ and $s = -50$. The controller transfer function then becomes

$$C(s) = \frac{3628s + 40000}{s^2 + 80.28s + 156.56} = 3628 \frac{s + 11.02}{(s + 2)(s + 78.28)}.$$

The sensitivity functions are shown by dashed lines in Figure 12.12. The controller gives the maximum sensitivities $M_s = 1.34$ and $M_t = 1.41$, which give much better robustness. Notice that the controller has a pole at $s = -2$ that cancels the slow process zero. The design can also be done simply by canceling the slow stable process zero and designing the controller for the simplified system. ∇

One lesson from the example is that it is necessary to choose closed loop poles that are equal to or close to slow stable process zeros. Another lesson is that slow unstable process zeros impose limitations on the achievable bandwidth, as already

12.5 Design for Robust Performance

Control design is a rich problem where many factors have to be taken into account. Typical requirements are that load disturbances should be attenuated, the controller should inject only a moderate amount of measurement noise, the output should follow variations in the command signal well and the closed loop system should be insensitive to process variations. For the system in Figure 12.9 these requirements can be captured by specifications on the sensitivity functions S and T and the transfer functions G_{yd}, G_{un}, G_{yr} and G_{ur}. Notice that it is necessary to consider at least six transfer functions, as discussed Section 11.1. The requirements are mutually conflicting, and it is necessary to make trade-offs. The attenuation of load disturbances will be improved if the bandwidth is increased, but so will the noise injection.

It is highly desirable to have design methods that can guarantee robust performance. Such design methods did not appear until the late 1980s. Many of these design methods result in controllers having the same structure as the controller based on state feedback and an observer. In this section we provide a brief review of some of the techniques as a preview for those interested in more specialized study.

Quantitative Feedback Theory

Quantitative feedback theory (QFT) is a graphical design method for robust loop shaping that was developed by I. M. Horowitz [104]. The idea is to first determine a controller that gives a complementary sensitivity that is robust to process variations and then to shape the response to reference signals by feedforward. The idea is illustrated in Figure 12.16a, which shows the level curves of the complementary sensitivity function T on a Nyquist plot. The complementary sensitivity function has unit gain on the line $\operatorname{Re} L(i\omega) = -0.5$. In the neighborhood of this line, significant variations in process dynamics only give moderate changes in the complementary transfer function. The dashed part of the figure corresponds to the region $0.9 < |T(i\omega)| < 1.1$. To use the design method, we represent the uncertainty for each frequency by a region and attempt to shape the loop transfer function so that the variation in T is as small as possible. The design is often performed using the Nichols chart shown in Figure 12.16b.

Linear Quadratic Control

One way to make the trade-off between the attenuation of load disturbances and the injection of measurement noise is to design a controller that minimizes the loss function

$$J = \frac{1}{T} \int_0^T \left(y^2(t) + \rho u^2(t) \right) dt,$$

where ρ is a weighting parameter as discussed in Section 6.3. This loss function gives a compromise between load disturbance attenuation and disturbance injection because it balances control actions against deviations in the output. If all state

(a) Hall chart   (b) Nichols chart
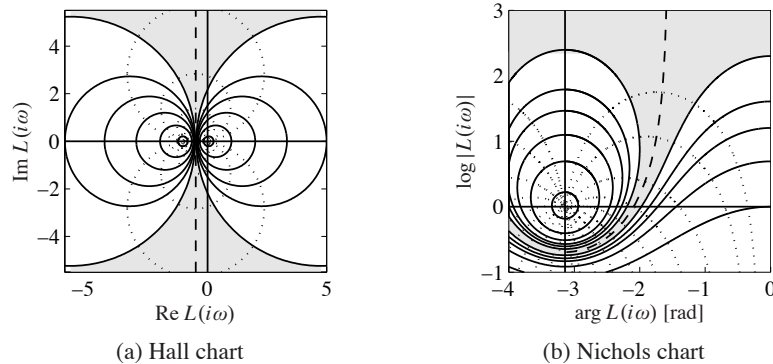
Figure 12.16: Hall and Nichols charts. The Hall chart is a Nyquist plot with curves for constant gain and phase of the complementary sensitivity function T. The Nichols chart is the conformal map of the Hall chart under the transformation $N = \log L$ (with the scale flipped). The dashed curve is the line where $|T(i\omega)| = 1$, and the shaded region corresponding to loop transfer functions whose complementary sensitivity changes by no more than $\pm 10\%$ is shaded.

variables are measured, the controller is a state feedback $u = -Kx$ and it has the same form as the controller obtained by eigenvalue assignment (pole placement) in Section 6.2. However, the controller gain is obtained by solving an optimization problem. It has been shown that this controller is very robust. It has a phase margin of at least $60°$ and an infinite gain margin. The controller is called a *linear quadratic control* or *LQ control* because the process model is linear and the criterion is quadratic.

When all state variables are not measured, the state can be reconstructed using an observer, as discussed in Section 7.3. It is also possible to introduce process disturbances and measurement noise explicitly in the model and to reconstruct the states using a Kalman filter, as discussed briefly in Section 7.4. The Kalman filter has the same structure as the observer designed by eigenvalue assignment in Section 7.3, but the observer gains L are now obtained by solving an optimization problem. The control law obtained by combining linear quadratic control with a Kalman filter is called *linear quadratic Gaussian control* or *LQG control*. The Kalman filter is optimal when the models for load disturbances and measurement noise are Gaussian.

It is interesting that the solution to the optimization problem leads to a controller having the structure of a state feedback and an observer. The state feedback gains depend on the parameter ρ, and the filter gains depend on the parameters in the model that characterize process noise and measurement noise (see Section 7.4). There are efficient programs to compute these feedback and observer gains.

The nice robustness properties of state feedback are unfortunately lost when the observer is added. It is possible to choose parameters that give closed loop systems with poor robustness, similar to Example 12.8. We can thus conclude that there is a

[21] M. Atkinson, M. Savageau, J. Myers, and A. Ninfa. Development of genetic circuitry exhibiting toggle switch or oscillatory behavior in *Escherichia coli*. *Cell*, 113(5):597–607, 2003.

[22] M. B. Barron and W. F. Powers. The role of electronic controls for future automotive mechatronic systems. *IEEE Transactions on Mechatronics*, 1(1):80–89, 1996.

[23] T. Basar (editor). *Control Theory: Twenty-five Seminal Papers (1932–1981)*. IEEE Press, New York, 2001.

[24] T. Basar and P. Bernhard. *H^∞-Optimal Control and Related Minimax Design Problems: A Dynamic Game Approach*. Birkhauser, Boston, 1991.

[25] J. Bechhoefer. Feedback for physicists: A tutorial essay on control. *Reviews of Modern Physics*, 77:783–836, 2005.

[26] R. Bellman and K. J. Åström. On structural identifiability. *Mathematical Biosciences*, 7:329–339, 1970.

[27] R. E. Bellman and R. Kalaba. *Selected Papers on Mathematical Trends in Control Theory*. Dover, New York, 1964.

[28] S. Bennett. *A History of Control Engineering: 1800–1930*. Peter Peregrinus, Stevenage, 1979.

[29] S. Bennett. *A History of Control Engineering: 1930–1955*. Peter Peregrinus, Stevenage, 1993.

[30] L. L. Beranek. *Acoustics*. McGraw-Hill, New York, 1954.

[31] R. N. Bergman. Toward physiological understanding of glucose tolerance: Minimal model approach. *Diabetes*, 38:1512–1527, 1989.

[32] D. Bertsekas and R. Gallager. *Data Networks*. Prentice Hall, Englewood Cliffs, 1987.

[33] B. Bialkowski. Process control sample problems. In N. J. Sell (editor), *Process Control Fundamentals for the Pulp & Paper Industry*. Tappi Press, Norcross, GA, 1995.

[34] G. Binnig and H. Rohrer. Scanning tunneling microscopy. *IBM Journal of Research and Development*, 30(4):355–369, 1986.

[35] H. S. Black. Stabilized feedback amplifiers. *Bell System Technical Journal*, 13:1–2, 1934.

[36] H. S. Black. Inventing the negative feedback amplifier. *IEEE Spectrum*, pp. 55–60, 1977.

[37] J. F. Blackburn, G. Reethof, and J. L. Shearer. *Fluid Power Control*. MIT Press, Cambridge, MA, 1960.

[38] J. H. Blakelock. *Automatic Control of Aircraft and Missiles*, 2nd ed. Addison-Wesley, Cambridge, MA, 1991.

[39] G. Blickley. Modern control started with Ziegler-Nichols tuning. *Control Engineering*, 37:72–75, 1990.

[40] H. W. Bode. *Network Analaysis and Feedback Amplifier Design*. Van Nostrand, New York, 1945.

[41] H. W. Bode. Feedback—The history of an idea. *Symposium on Active Networks and Feedback Systems*. Polytechnic Institute of Brooklyn, New York, 1960. Reprinted in [27].

[42] W. E. Boyce and R. C. DiPrima. *Elementary Differential Equations*. Wiley, New York, 2004.

[43] B. Brawn and F. Gustavson. Program behavior in a paging environment. *Proceedings of the AFIPS Fall Joint Computer Conference*, pp. 1019–1032, 1968.

[44] R. W. Brockett. *Finite Dimensional Linear Systems*. Wiley, New York, 1970.

[45] R. W. Brockett. New issues in the mathematics of control. In B. Engquist and W. Schmid (editors), *Mathematics Unlimited—2001 and Beyond*, pp. 189–220. Springer-Verlag, Berlin, 2000.

[46] G. S. Brown and D. P. Campbell. *Principles of Servomechanims*. Wiley, New York, 1948.